Slovenian Veterinary Research

Slovenski veterinarski zbornik

THE SCIENTIFIC JOURNAL OF THE VETERINARY FACULTY UNIVERSITY OF LJUBLJANA

ISSN 1580-4003
Volume 60, Number 2, Pages 45–114

Slovenian Veterinary Research

Slovenski veterinarski zbornik

THE SCIENTIFIC JOURNAL OF THE VETERINARY FACULTY UNIVERSITY OF LJUBLJANA

Volume 60, Number 2, Pages 45–114

The Scientific Journal of the Veterinary Faculty University of Ljubljana

Slovenian Veterinary Research
Slovenski veterinarski zbornik

Previously: RESEARCH REPORTS OF THE VETERINARY FACULTY UNIVERSITY OF LJUBLJANA
Prej: ZBORNIK VETERINARSKE FAKULTETE UNIVERZA V LJUBLJANI

4 issues per year / Izhaja štirikrat letno
Volume 60, Number 2 / Letnik 60, Številka 2

Published by / Založila	University of Ljubljana Press / Založba Univerze v Ljubljani
For the Publisher / Za založbo	Gregor Majdič, Rector of the University of Ljubljana / Rektor Univerze v Ljubljani
Issued by / Izdala	Veterinary Faculty University of Ljubljana / Veterinarska fakulteta Univerze v Ljubljani
For the Issuer / Za izdajatelja	Breda Jakovac Strajn, Dean of the Veterinary Faculty / Dekanja Veterinarske fakultete
Address	Veterinary Faculty, Gerbičeva 60, 1000 Ljubljana, Slovenia
Naslov	Veterinarska fakulteta, Gerbičeva 60, 1000 Ljubljana, Slovenija
Phone / Telefon	+386 (0)1 4779 100
E-mail	slovetres@vf.uni-lj.si
Sponsored by / Sofinancira	The Slovenian Research Agency / Javna agencija za raziskovalno dejavnost Republike Slovenije
Printed by / Tisk	DZS, d.d., Ljubljana, June 2023
Number of copies printed / Naklada	220
Indexed in / Indeksirano v	Agris, Biomedicina Slovenica, CAB Abstracts, IVSI Urlich's International Periodicals Directory, Science Citation Index Expanded, Journal Citation Reports – Science Edition
	https://www.slovetres.si/
	ISSN 1580-4003

The cover illustration by Pšenica Kovačič, represents the emerald tree boa (*Corallus caninus*).

Table of Content

DOI 10.26873/SVR-1750-2023
UDC 636.09:165.9:164.02:94(38)
Pages: 49–53

Editorial

The Cover and Logo of *Slovenian Veterinary Research* Contains the Rod of Asclepius

Naslovnica in logotip *Slovenskega veterinarskega zbornika* z Asklepijevim simbolom

Vojteh Cestnik

Mirje 2, 1000 Ljubljana, Slovenia

vcestnik@gmail.com

Accepted: 20 June 2023

In the 60th year of continuous publishing, the cover page of *Slovenian Veterinary Research* now features the symbol of veterinary medicine. In other words, the Rod of Asclepius (Greek) or Aesculapius (Latin) is wrapped by a snake, both of which are surrounded by a capital letter V. This symbol originates from Antiquity and was attributed to our profession after this line of work was accepted scientifically based principles and became to be called "veterinary medicine". There are several explanations regarding the origin and source of the symbol. A slightly deeper reflection brings us to the legends and myths of Antiquity.

Some interpretations state that Asclepius actually existed and worked as a very successful physician, who somehow, after the 5th century BC, began to be worshipped throughout ancient Greece as a deity. The greatest cult dedicated to him was cultivated on the island of Kos, and the largest temple in his honour was built in Epidaurus on the Peloponnese peninsula. It was here that also a medical school operated, which was first based on the methods of magic but later grew to develop more scientific and empirically based treatments. Several other temples dedicated to Asclepius are known in antique Greece. Among Asclepius' successors, the most known physician is Hippocrates.

V šestdesetem letu neprekinjenega izhajanja prihaja na naslovnico *Slovenskega veterinarskega zbornika* znak veterinarske medicine, ki smo ga do sedaj pogrešali. To je Asklepijeva (gr.) ali Eskulapova (lat.) palica, ki jo ovija kača, obe pa obdaja velika črka V. Simbol ali atribut Asklepijeve palice s kačo izvira iz Antike in se je v naši stroki pričel uporabljati potem, ko je stroka prevzela znanstveno utemeljena načela dela in se pričela poimenovati veterinarska medicina. O izvoru in nastanku simbola je več razlag. Nekoliko poglobljeno premišljevanje nas popelje v svet simbolike in antičnih mitov.

Nekatere razlage navajajo, da je Asklepij dejansko obstajal in deloval kot zelo uspešen zdravnik, ki so ga nekako od 5. stoletja pr. n. št. dalje pričeli po vsej Grčiji častiti kot božanstvo. Njegov največji kult so gojili na otoku Kos, največje svetišče pa je bilo v Epidavru na Peloponezu. Tu je delovala tudi medicinska šola, ki je najprej temeljila na magičnih postopkih a kasneje prerasla v bolj znanstveno in temeljila svoja zdravljenja predvsem na izkustvih. Poznano pa je še nekaj drugih Asklepijevih svetišč v antični Grčiji. Med Asklepijevimi nasledniki je najbolj znan zdravnik Hipokrat.

Več legend pravi, da je bil Asklepij sin boga Apolona. Po najpogosteje navedeni pripovedi naj bi bila njegova mati tesalska princesa Koronida, ki pa jo je zveza z bogom stala

Several legends claim that Asclepius was the son of the god Apollo. According to the most frequently quoted story, his mother was the Thessalian princess Coronis, who paid with her life for her union with god. A milder version of her death states that she was shot with an arrow by Apollo's sister Artemis, the goddess of hunting. According to a more dreadful version, Coronis was (spiritually) unfaithful to Apollo during her pregnancy, and therefore Apollo killed her, cut their son Asclepius out of her body, and gave him to the centaur Chiron to raise. Another legend states that the mother of Asclepius was the daughter of Peligas, a great thief. She became pregnant by Apollo and secretly gave birth to her son Asclepius in Epidaurus at the foothills of the mountain. The child was nourished by a goat and protected by a dog. The herdsman Arestanas, the owner of the two animals, found the child and was astonished by the light shining on the boy. He did not dare take the boy with him, and the child was left to his fate. Yet another legend states that Asclepius was the son of Arsinoe and brought up by Coronis. Also in this legend, Asclepius was entrusted by his father Apollo to the centaur Chiron.

Chiron stood out from the other half-man, half-horse creatures, who were mostly drunkards and tyrants. Chiron lived by himself in a cave and was clever, kind, and civilised. He also differed from other centaurs by his feet, which were like those of man and not horse. His tutors, Apollon and Artemis, taught him the skills of hunting, medicine, music, and prophecy. In addition to Asclepius, Chiron was also a teacher to some other well-known heroes, including Achilles and Jason. We can see him in the night sky as the Centaur constellation.

Chiron gave Asclepius the knowledge of healing, and thus Asclepius discovered how to awake the dead by the blood of Gorgon, which he received from the goddess Athena. In doing so, he angered Hades, the god of the underworld and the dead, who persuaded Zeus to kill Asclepius with a thunderbolt. After his death, Asclepius is said to have changed into a snake. The constellation Ophiuchus (Serpent Bearer) reminds us of him.

Asclepius had five immortal daughters and two or three mortal sons with his wife Epione. Panacea was the goddess of universal remedy, and the miraculous cure for all diseases is named after her. Iaso was the goddess of healing, Hygieia of health, Aceso of rehabilitation, and Aegle (or Erla) of natural beauty. Their son Podalirius, endowed with many talents, was a famous diagnostician, and his brother Machaon was the founder of surgery. They both took part in the Trojan War in which Machaon fell. In addition to these two sons, some legends also mention a third son, Telesphorus, who was Asclepius' assistant. The fourth son Aratus was illegitimate and born to Aristodema. He is considered the liberator of the decades-long-lasting combats for Sicyon in the 3rd century BC.

življenje. Bolj mila verzija njene smrti navaja, da jo je s puščico ustrelila Apolonova sestra Artemis, boginja lova. Po bolj grozni verziji naj bi bila Koronida med nosečnostjo nezvesta, morda samo duhovno, Apolonu in zato jo je ta ubil, iz njenega telesa izrezal sina Asklepija in ga dal v rejo kentavru Hironu. Druga legenda pripoveduje, da je bila Asklepijeva mati hči Peligasa, tatu velikega kova. Naj bi zanosila z Apolonom, skrivoma rodila sina v Epidavru ob vznožju gore in ga tam pustila. Otroka je hranila koza, varoval pa pes. Pastir Arestanas, lastnik obeh živali, je sicer našel otroka in bil osupel nad svetlobo, ki je sijala na dečka. Zato otroka ni upal vzeti s seboj in je ta bil še naprej prepuščen svoji usodi. Tretja legenda navaja, da je bil Asklepij sin Arsinoe in da ga je vzgojila princesa Koronida. Tudi po tej legendi je Asklepija njegov oče Apolon zaupal v rejo kentavru Hironu.

Hiron je bil posebnež med kentavri, t.j. pol konji in pol ljudje, ki so bili v glavnem pijanci in nasilneži. Hiron pa je živel sam zase v neki votlini in je bil inteligenten, prijazen in civiliziran. Od drugih kentavrov se je razlikoval tudi po tem, da je imel sprednje noge take kot človek in ne kot konj. Njegova vzgojitelja, Apolon in Artemida, sta ga izučila veščin lova, zdravilstva, glasbe in prerokovanja. Poleg Asklepiju je bil Hiron učitelj še nekaterim znanim grškim herojem, med njimi Ahilu in Jazonu. Danes ga na nebu lahko vidimo kot ozvezdje Kentavra.

Hiron je Asklepija izučil zdravljenja, ta pa je odkril kako lahko iz krvi Gorgon, ki jo je dobil od Atene, obudi mrtve. S tem pa je razjezil Hada, boga podzemlja in mrtvih, ki je pregovoril Zevsa, da je s strelo ubil Asklepija. Po smrti naj bi se Asklepij spremenil v kačo, nanj pa nas spominja ozvezdje Kačjenosca (lat. *Ophiuchus*).

Asklepij je imel z ženo Epiono pet nesmrtnih hčera in dva ali tri umrljive sinove. Panakeja je bila boginja zdravljenja, po njej se imenuje magično zdravilo panaceja, ki naj bi ozdravilo vse bolezni. Ias je bila boginja ozdravitve, Higieja varovanja zdravja, Akesa rehabilitacije, Agleja (ali Erla) pa naravne lepote. Sin Podalirij, obdarjen s številnimi naravnimi talenti, je bil diagnostik, njegov brat Mahaon pa utemeljitelj kirurgije. Oba sta se udeležila Trojanske vojne v kateri je Mahaon padel. Poleg teh dveh nekatere legende omenjajo še tretjega sina Telesforja, ki je bil Asklepijev pomočnik. Četrti sin je bil nezakonski Arat, katerega mati naj bi bila Aristodema. Sodeloval naj bi v desetletja trajajočih bojih za Sikion v 3. stoletju pr. n. št. in bil tudi njegov osvoboditelj.

Tudi o izvoru Asklepijeve palice z ovito kačo obstaja več legend. Po eni naj bi si Asklepij naredil palico potem, ko mu je kača zaupala vse skrivnosti medicine. Poleg kače je bil Asklepijev znak še sova, simbol modrosti. Kača je bila tudi sveti simbol njegove hčerke Higieje. Kača, ovita okoli palice, naj bi ponazarjala sposobnost, palica pa moč zdravljenja. Ena od razlag simbola navaja, da naj bi palica predstavljala del drevesa, torej rastlinsko kraljestvo, iz katerega izvirajo zdravila za bolezni. Po drugi legendi naj bi boginja Atena Asklepiju dala kačo, ki jo je odvzela Meduzi. Po tretji, bolj

Furthermore, several legends exist regarding the origin of Asclepius' snake-wrapped rod. According to one, Asclepius made himself a rod after a snake had entrusted him with all the secrets of medicine. In addition to the snake, another sign of Asclepius was an owl, a symbol of wisdom. The snake was also the sacred symbol of his daughter Hygieia. The snake wrapped around the rod is said to represent ability, and the rod the power of healing. One of the interpretations of the symbol states that the rod represents a part of a tree, i.e., the plant kingdom, from which medicines for diseases originate. According to another legend, the snake was given to Asclepius by the goddess Athena, who took it from Medusa. According to a third, more cruel, legend, Asclepius is said to have left his walking stick at the door of a patient's home whilst visiting. The treatment was not successful, and when Asclepius stepped out of the house, he saw a snake wrapped around his rod. He killed it with another stick, but before the snake died, it opened its mouth in which was an unknown plant. Asclepius gave this plant to the patient, who was then cured. After this event, Asclepius placed the head of the snake on the top of his rod. A more practical explanation of the symbol's origin states that the snake wrapped around the rod actually represents the subcutaneous nematode *Dracunculus medinensis*, which is even today removed from subcutaneous tissue by winding it on a stick. In Antiquity, dracunculiasis was quite widespread, and it still exists in some parts of Africa today. However, it will most likely be the third permanently eradicated disease after smallpox and rinderpest.

Since ancient times, the snake had a special mystical or religious status in allegories and symbols and was worshipped as a mysterious creature. There are around 3,400 species of snakes on Earth, of which around 600 are poisonous. For most people, the sight or mere thought of snakes triggers uneasy feelings, even fear, which many believe is somehow implanted in human consciousness. For the ancient Egyptians, the snake was a symbol of life. The pharaohs were worshipped as descendants of snakes and wore the sacred serpent Uraeus on their heads in the form of a crown. The Sumerian god of medicine also originated from a snake. The Celts valued snakes as symbols of wisdom, healing, rebirth, transformation, and fertility because of their ability to shed their skin and live among the roots, deep in the Earth. For the Mayans, the feathered snake Quetzalcoatl was a symbol of fertility. In Norse mythology, the sea snake Jörmungandr represents the endless cycle of life. In India and China, snakes symbolize reincarnation or personify a special inner energy.

It is stated in the Old Testament that before Moses led the Israelites out of Egyptian slavery, he changed his staff into a snake to demonstrate God's help and power, which would convince the pharaoh to free the Israelites. Because the pharaoh refused to do so, ten plagues befell Egypt. After their departure, many troubles fell upon the Israelites, due to which they began to oppose Moses and God himself. God sent poisonous snakes over them, and thus recognizing

okrutni legendi, naj bi Asklepij ob obisku nekega bolnika pustil svojo popotno palico pred vrati bolnikovega doma. Zdravljenje ni bilo uspešno, ko pa je Asklepij stopil iz hiše je videl, da se okoli njegove palice ovija kača. Z drugo palico je kačo ubil, preden pa je ta poginila je odprla usta v kateri je bila neznana rastlina. Asklepij je to rastlino dal bolniku, ki je nato ozdravel. Po tem dogodku je Asklepij namestil glavo te kače na vrh svoje palice. Bolj praktična razlaga izvora simbola pa navaja, da naj bi na palici ovita kača dejansko predstavljala podkožnega nematoda *Dracunculus medinensis*, ki ga še danes odstranjujejo iz podkožja z navijanjem na paličko. V antiki je bila drakunkulóza precej razširjena, medtem ko je danes le še v nekaterih področjih v Afriki. Vse pa kaže, da bo to tretja stalno izkoreninjena bolezen, za kozami in govejo kugo.

Sicer pa je kača od pradavnih kultur dalje imela posebno mistično ali religiozno mesto v prispodobah in simbolih in bila čaščena kot skrivnostno bitje. Na Zemlji živi okoli 3400 vrst kač, od katerih jih je okoli 600 strupenih. Pri večini ljudi pogled ali zgolj razmišljanje o kačah sproži nelagodne občutke ali celo strah za katerega mnogi menijo, da je nekako vsajen v človekovo zavest. Pri starih Egipčanih je bila kača simbol življenja. Faraone so častili kot potomce kač in ti so sveto kačo Ureus nosili na glavi v obliki krone. Tudi Sumerski bog medicine je izviral iz kače. Kelti so kače, zaradi njihove sposobnosti levitve in življenja med koreninami globoko v zemlji, cenili kot simbole modrosti, ozdravitve, ponovnega rojstva, preobrazbe in plodnosti. Pri Majih je bila pernata kača Quetzalcoatl simbol plodnosti. V nordijski mitologiji nastopa morska kača Jörmungandr, ki predstavlja neskončni življenjski krog. Tudi v Indiji in na Kitajskem so kače simbolizirale reinkarnacijo ali poosebljale posebno notranjo energijo.

V Stari zavezi je navedeno, da preden je Mojzes povedel Izraelce iz egipčanske sužnosti, je svojo palico spremenil v kačo, s čimer naj bi pokazal božjo pomoč in moč, zaradi katere naj bi faraon osvobodil Izraelce. Ker faraon tega ni naredil, je Egipt zadelo deset nesreč. Po odhodu iz sužnosti so se pričele različne težave, zaradi katerih so Izraelci pričeli nasprotovati Mojzesu in Bogu samemu. Ta je nad njih poslal strupene kače, zaradi česar so uvideli svojo zmoto, se pokesali in z molitvami prosili Boga za pomoč. Mojzes je po božjem ukazu naredil bronasto kačo in jo namestil na palico ali križ. Vsi, ki so jih kače pičile, so ob pogledu nanjo ozdraveli. Kače so omenjene tudi v Novi zavezi. Jezus svetuje, da naj bodo ljudje modri kot kače, kar pomeni, da je potrebno razvijati sposobnosti uma in razuma. Alkemisti so prevzeli egipčansko-grški simbol Ouroboros, t.j., kačo ki grize svoj rep in predstavlja naravo, življenjsko moč in božansko, neprestano, ciklično obnovljivo silo. O kačah sta razmišljala tudi slovita psihologa Sigmund Freud in Karl Gustav Jung. Za Freuda je bila kača simbol seksualnosti, ki je ob prikazovanju v sanjah pri ženskah vzbujala strah pred spolnostjo ali asociacijo na privlačnega moškega. Junga je levitev kače spominjala na človekovo preobrazbo.

their mistake, they repented and prayed to God for help. At God's command, Moses made a bronze serpent and placed it on top of a rod or cross. All who were bitten by snakes were healed at the sight of it. Snakes are also mentioned in the New Testament. Jesus advised that people should be as wise as serpents, which means that one must develop the ability of intellect and reason. Alchemists adopted the Egyptian-Greek symbol Ouroboros, a serpent biting its own tail, representing nature, the life force, the divine, and the never-ending, cyclical, renewing force. The famous psychologists Sigmund Freud and Karl Gustav Jung also considered the meaning of snakes. For Freud, the snake was a symbol of sexuality, which, when appearing in dreams, evoked in women a fear of sexuality or an association with an attractive man. For Jung, the shedding of snakes was reminiscent of human transformation.

In the Middle Ages, Asclepius and his sign were abandoned. Only in the Renaissance, with the rediscovery of the ancient heritage and its values, did the forgotten symbol start to gain ground again. In 1593, the author Cesare Ripa published the book Iconologia, in which he presented various ancient figures. The symbol of the snake and rod began to appear on the cover pages of medical discussions and pharmacopoeias. It became generally accepted in the 17th century.

In addition to the Rod of Asclepius, we can, not rarely, find another symbol in medicine, the so-called caduceus (lat. caduceus) or kerykeion (gr. kērukeion, κηρύκειον). Some even use the same expression for both symbols. However, there are considerable differences in the appearances, meanings, and origins of the two signs. The caduceus is represented by two snakes coiling around a rod topped by two wings. A similar symbol appears on the Mesopotamian seals dating from 4000 to 3000 BC and is most probably connected with their deity. According to one of the Greek myths about the origin of the kerykeion, the prophet Tiresias found two snakes mating and killed the female with his staff. He was immediately turned into a woman and remained in this form for 7 years until he killed a male snake in a similar event. The staff with its power of transformation was later passed into the possession of the god Hermes. Another story states that Hermes was appointed a divine herald by Apollo after he had played the lyre for him. On this occasion, he presented him with a kerykeion as a symbol of his service. The Greek name of the symbol means herald's staff and derives from the word keruks (κήρυξ), which means herald. Yet a third story says that Hermes saw two snakes entwined in mortal combat. He separated them with his staff and calmed them down. Such an origin of the rod with two entwined snakes supposedly represents a sign of peace.

Hermes was the god of roads, passages, borders, and herds; herald of the gods; intercessor between mortals and gods; and companion of souls to the afterlife who moved freely between the worlds of mortals and gods. He was

V srednjem veku sta bila Asklepij in njegov znak opuščena. Šele v renesansi, ob ponovnem odkrivanju antične zapuščine in njenih vrednot, se je pozabljeni simbol spet pričel uveljavljati. Leta 1593 je avtor Cesare Ripa izdal knjigo *Iconologia*, v kateri je predstavil različne antične figure. Simbol kače in palice se je začel pojavljati na naslovnih straneh medicinskih razprav in farmakopej ter se v 17. stoletju dokončno uveljavil.

Poleg Asklepijevega lahko v medicini neredko zasledimo še en znak, kaducej (lat. caduceus) ali kerikej (gr. kērukeion, κηρύκειον). Nekateri tako poimenujejo kar Asklepijev simbol. Vendar so med videzom, pomenom in izvorom obeh znakov precejšnje razlike. Kaducej predstavljata dve kači, ki se ovijata okoli palice, na vrhu katere sta dve krili. Podoben znak se pojavlja na mezopotamskih pečatnikih 4000 do 3000 let pr. n. št. in je najverjetneje povezan z njihovim božanstvom. Po enem od grških mitov, ki govori o izvoru kerikeja, je prerok Tirezij našel dve kači med parjenjem in s svojo palico ubil samico. Takoj se je spremenil v žensko in v tej podobi ostal sedem let, dokler ob podobnem dogodku ni ubil kačjega samca. Palica s svojo močjo pretvorbe je kasneje prešla v last boga Hermesa. Druga zgodba pripoveduje, da je Hermesa postavil za božjega glasnika Apolon, potem, ko mu je ta igral na liro. Ob tem mu je podaril kerikej kot simbol njegove službe. Grško poimenovanje znaka pomeni glasnikova palica in izvira iz besede keruks (κήρυξ), ki pomeni glasnik. Spet tretja zgodba pravi, da je Hermes zagledal dve kači prepleteni v smrtnem boju. S svojo palico ju je razdvojil in pomiril. Tako je nastala palica z dvema prepletenima kačama, ki naj bi predstavljala mir.

Hermes je bil bog cest, prehodov, mej in čred, glasnik bogov, priprošnjik med smrtniki in bogovi in spremljevalec duš v posmrtno življenje; brez ovir se je gibal med svetom smrtnikov in nesmrtnih bogov. Bil je tudi zaščitnik in pokrovitelj pastirjev, trgovcev, trgovine, tatov, popotnikov, govorništva, duhovitosti, izumov, literature, poezije, športnikov in športa. Z medicino in zdravljenjem ni imel nobenega opravka. Poleg kerikeja kot najpomembnejšega simbola, so bili njegovi prepoznavni znaki še petelin, želva, torbica oziroma denarnica, krilati sandali in krilati klobuk. V rimskem panteonu je dobil ime Merkur.

Prva znana uporaba kaduceja v medicini je bila vinjeta, ki jo je pri tisku medicinskih besedil uporabil švicarski tiskar Johann Frobenius (1460–1527). Znak je, kot vse kaže, uporabljal tudi William Butts (1486–1545), zdravnik kralja Henrika VIII. Armada Združenih držav Amerike je pričela uporabljati kaducej pri oznakah vojaških bolničarjev okoli leta 1856 in tudi pri sanitetnih oficirjih leta 1902, ker je tega leta znak sprejela medicinska služba vojske ZDA. Leta 1901 je pričel v Franciji izhajati vojni medicinski mesečnik *La Caducée*. V ZDA so znak uporabljali tudi po prvi svetovni vojni in ga lahko srečamo marsikje še danes. Kaducej uporabljajo tudi nekatera komercialna podjetja ali združenja, saj je bil Hermes bog trgovine. Nekaj časa je znak uporabljalo Ameriško zdravniško združenje, vendar ga je po burni

also the protector and patron of shepherds, merchants, commerce, thieves, travellers, oratory, wit, inventions, literature, poetry, athletes, and sports. He had nothing to do with medicine and treatment. In addition to the caduceus, his identification signs were a rooster, turtle, purse or wallet, winged sandals, and winged hat. He was named Mercury in the Roman pantheon.

The first known use of the caduceus in medicine was a vignette used by the Swiss printer Johann Frobenius (1460–1527) when printing medical texts. Apparently, the symbol was also used by William Butts (1486–1545), the physician of King Henry VIII. The United States Army began to use the caduceus in the insignia of military male nurses around 1856 and sanitary officers in 1902, which was also the year the sign was adopted by the US Army Medical Service. In 1901, the wartime medical monthly magazine *La Caducée* began to be published in France. In the USA, the symbol was also used after World War I and can still be found used today. The caduceus is also used by some commercial companies or associations, as Hermes was the god of trade. The American Veterinary Medical Association initially used the image of the centaur Chiron, which was replaced by the caduceus in 1920 and in 1971 replaced by the Rod of Asclepius with a snake, which is still used today. The use of the caduceus as a symbol of medical associations is in decline but is occasionally still used today. However, the caduceus is more appropriately associated with banks and other businesses of commerce because of the connection to Hermes. Veterinary medicine and human medicine, however, will use the rod of Asclepius, who was the Greek god of healing.

We greet with great pleasure the decision of the editors to introduce the Rod of Asclepius to the cover page of the only Slovenian scientific veterinary medicine journal. We wish the editors, editorial board members, and all co-workers much success and many high-quality scientific papers.

Prof. Vojteh Cestnik, professor emeritus of Veterinary Medicine, UL

razpravi opustilo že leta 1912. Ameriško združenje veterinarjev je v začetku uporabljalo podobo kentavra Hirona, ki jo je leta 1920 zamenjala podoba kaducej, od leta 1971 do sedaj pa uporabljajo Asklepijevo palico s kačo. Čeprav vse manj, nekatera medicinska združenja še vedno uporabljajo simbol kaduceja. Vendar lahko rečemo, da je uporaba tega znaka napačna, nepravilna in nestrokovna, saj je glede na mitološko povezanost kaduceja s Hermesom bolj primerna za poslovna in trgovska podjetja, medtem ko se v veterinarski in humani medicini uporablja simbol Asklepija, ki je bil bog zdravljenja.

Z veseljem lahko pozdravimo odločitev urednic za uvedbo Asklepijevega simbola na naslovnici znanstvenega časopisa, ki ga izdaja naša Veterinarska fakulteta. Uredniškemu odboru in vsem drugim sodelujočim pa želimo uspešno delo in čim več kvalitetnih znanstvenih člankov.

Prof. dr. Vojteh Cestnik, zaslužni profesor UL

DOI 10.26873/SVR-1519-2023
UDC 616.13-004.6:612.874.2:616.153:636.028
Pages: 55–66

Original Research Article

Female Gonadal Hormones are a Risk Factor for Developing Atherosclerotic Changes in C57BL/6J Mice on Atherogenic Diet

Key words

atherosclerosis;
Paigen diet;
sex;
gonadal hormones;
mouse models;
lipids and cholesterol

Malan Štrbenc, Katja Kozinc Klenovšek, Gregor Majdič*

Institute of Preclinical sciences, Veterinary Faculty, University of Ljubljana, Gerbičeva 60, 1000 Ljubljana, Slovenia

***Corresponding author:** gregor.majdic@vf.uni-lj.si

Abstract: In humans, estrogens are considered protective factor against atherosclerosis because the risk increases in postmenopausal women. However, it is not clear whether estrogens are the only factor, whether sex chromosomes also have an influence, and whether estrogens play the same role in all mammals. The mouse line C57BL/6J is prone to develop atherosclerotic changes in the largest arteries after prolonged feeding of a highfat diet containing cholesterol and cholate (Paigen diet). We aimed to examine effect of sex hormones and sex chromosome complement on the development of atherosclerotic plaques using agonadal SF-1 knockout mouse on C57BL/6J background. Gonadally intact and prepubertally gonadectomized WT and agonadal SF-1 knockout C57BL/6J mice of both sexes were exposed to a Paigen diet and a control diet for 20 weeks. We monitored their body weight, food intake, and serum lipid profile. The aortas were examined by the en face method, and the cross sections of the aortic bulbs were stained for lipid content. In all groups of mice, atherosclerotic changes were small and confined to the aortic bulb. The formation of atherosclerotic plaques was sex- and hormone-dependent, as female animals with functioning ovaries developed the most prominent atherosclerotic plaques. Gonadally intact females were also the only group that gained weight comparably on control or atherogenic diet. Diet affected blood biochemistry, but there were almost no significant differences between groups in serum lipid levels. Results indicated main mechanism causing sex-dependent differences in atherosclerosis depends on sex hormones rather than sex chromosomes. Our results also suggest that a mouse model of dietary induced atherosclerosis is of limited use to study the mechanisms of atherosclerosis in humans because the presence of estrogens impairs lipid metabolism and contributes to the formation of atherosclerotic plaques.

Abbrevations: SF-1 KO: steroidogenic factor 1 (*Nr5a1* gene) knockout mice; WT: wild-type mice; CAS: castrated males; OVX: ovarectomised females; HDL: high-density lipoprotein; LDL: low-density liporotein; FFA: free fatty acids; PBS: phosphate buffered saline; FGF: fibroblast growth factor

Received: 3 August 2022
Accepted: 16 March 2023

Introduction

Atherosclerosis is a progressive disease characterised by the accumulation of lipids and fibrous elements in large arteries and presents a serious health problem for humans in western societies with limited treatment options. Although it is wildly studied, there is no ideal animal model since other mammals are relatively resistant to the atherosclerosis and mechanisms of development of atherosclerotic lesions differ between species (1, 2). Apolipoprotein E-deficient (ApoE

KO) mouse model is probably the most commonly used rodent model, followed by LDL receptor knock-out (3–5). These mice exhibit significant hypercholesterolemia that cannot be induced by diet alone. In general, however, mice are relatively resistant to atherosclerotic changes, although there are differences between strains and each genetically modified model has some limitations for extrapolation to human disease (5–7). Mild atherogenic changes can be induced with Paigen diet containing 1.25 % cholesterol, 0.5 % cholate and polyunsaturated to saturated ratio of 0.7 in wild type C57BL/6 mice (8, 9) and combination with high-fat diet is usually preferred or even needed in testing potential therapies in other rodent models (2). The complexity of atherosclerosis as a disease arises from many genetic loci that contribute to lipoprotein levels, body fat, and other risk factors, as well as the interactions among these factors. In humans, male sex and menopause in women are considered important risk factors, although the mechanisms of this sex difference remain poorly understood and hormone-based therapies haven't produced the desired results (10–13). In animal models, the correlation is even less clear. Standard paper on methodology of atherosclerotic assessment from Paigen et al (9) already reported atherosclerotic changes more numerous or larger in female mice in comparison to male mice. Because most of the experiments in this study were performed in female mice, the sex effect was not emphasized and was usually overlooked in subsequent studies. In most other studies, only one sex was used-usually the male-to avoid variation due to the estrous cycle in females, and until recently, sex was not emphasized in basic research, including cardiovascular topics (14–16). Studies using *ApoE* knockout mice yielded equivocal results, as in some studies atherosclerotic changes were more pronounced in males (16–20) and in others in females (21–24). Possible explanations for these discrepancies are the different genetic background of the genetically modified mice and the duration of the study. In older mice, the males are more susceptible than at younger ages (reviewed in (25)).

In order to elucidate sex differences and the effects of sex hormones and sex chromosomes, we studied wild-type (WT), gonadectomized WT (OVX and CAS), and agonadal SF-1 knockout mice exposed to an atherogenic diet for 20 weeks. Steroidogenic factor 1 (SF-1) is a gene with an important function in gonadal and adrenal development. Mice lacking the *Sf-1* (*Nr5a1*) gene (abbreviated as SF-1 KO mice) are born without gonads and adrenal glands (26). Newborns die within 24 hours but can be rescued by adrenal hormone replacement and adrenal gland transplantation and are used as an agonadal adult mouse model to study possible effects of sex chromosomes on various sex-specific traits (27, 28).

Materials and methods

Animals

Heterozygous mice with a disrupted SF-1 (*Nr5a1*) allele (SF1+/-) (originally produced by dr. Keith L. Parker at DUKE University, North Carolina, USA) were backcrossed to a C57BL/6J mouse line for more than 10 generations to generate a congenic line. All mice were housed in dedicated facilities at the Faculty of Veterinary Medicine, University of Ljubljana, providing a controlled environment with relative humidity of 45-60%, temperature between 21 and 24 °C, and a 12:12 light-dark cycle. Every 2 years, the in-house breeding colony is refreshed with males of strain C57BL/6JOlaHsd (Envigo Italy). Entry and all safety measures at the animal facility are in accordance with SFP standards. Incoming animals are examined for the absence of the most common pathogens in accordance with FELASA recommendations, and internal monitoring of sentinel animals and waste bedding is conducted once a year. Animals were housed in pairs in conventional cages (Eurostandard type II or II L) on irradiated bedding (Lignocel, Rosenberg, Germany) with phytoestrogen-free feed (#2916, Harlan Teklad, Milano, Italy) and acidified water (HCl, Sigma Aldrich, Steinheim, Germany, to pH 3) ad libitum. All animal procedures were performed in accordance with the EU Directive (2010/63/EU) and approved by the Slovenian Veterinary Commission (Decision U34401-22/2015/13). SF-1 +/- mice were mated to produce homozygous SF-1 knockout (SF-1 KO) and control wild-type progeny (WT). To ensure survival of SF-1 KO mice, all newborn pups were subcutaneously injected daily with 50 µl of a corticosteroid cocktail in corn oil (400 ng/ml hydrocortisone, 40 ng/ml dexamethasone, and 25 ng/ml fludrocortisone acetate; all from Sigma Aldrich, Steinheim, Germany). Mice were genotyped between days 4 and 6 postnatal by PCR analysis of skin DNA. The primers used were *Nr5a1* F 5'-ACAAGCATTACACGTGCACC-3' and *Nr5a1* R 5'-TGACTAGCAACCACCTTG CC-3' for SF-1 WT, *Nr5a1-neo* R 5'- AGGTGA GATGACAGGAGATC-3' for disrupted SF-1 allele, and F 5'-AGGCGCCCCATGAATGCA TT-3' plus R 5'-TCCATGAGGCTGATA TTTA TAG-3' for *Sry* gene. Female WT littermates or female pups from other C57BL/6J litters born within 3 days as KO pups were used as the source of adrenal transplants. The technique was previously published (27), we omitted keeping adrenals from donors in PBS and FGF, but rather transplanted them immediately after collection. After adrenal gland transplantation on postnatal day 7, SF-1 KO mice received corticosteroid injections and then three more - on days 9, 12 and 16, weaning took place on postnatal day 21. WT mice used in the study were subjected to the same corticosteroid treatment protocol as SF-1 KO mice. After weaning, mice of the same experimental group with the same age and sex were housed in pairs until sacrifice. Half of the WT mice were gonadectomized before puberty (P23-28) to represent groups without sex hormones in adulthood: ovarectomized females – designated WT F OVX and castrated males - WT M CAS. For gonadectomies, WT mice were anaesthetized

with a mixture of ketamine (Vetoquinol Biowet 100 mg/ml, Gorzowie, Poland; 100 µg/g bw), xylazine (Xylased 20 mg/ml, Bioveta; Czech Republic; 10 µg/g bw), and acepromazine (Calmivet 5 mg/ml, Vetoquinol, France; 2 µg/g bw). The ovaries were removed trough flank incisions and the testes through bilateral inguinal incisions. Any bleeding was stopped with a battery-powered cautery, and the wound was closed with absorbable polyfilament PGA in two layers. After gonadectomy, mice received a subcutaneous injection of the analgesic butorphanol (Fort Dodge Animal Health; 1.7 µg/g body weight), followed by another injection in 4-5 hours and 100-200 µl saline subcutaneously if some blood loss occurred. SF-1 KO and intact wild-type mice (WT F and WT M) were sham-operated at P23-28 with the same anaesthetic protocol, incision and suture, according to their genetic sex. The decision of which animals were gonadectomized and which were left intact (sham operations) was made randomly by the animal caretaker, with the operator receiving the daily sequence.

Inclusion criteria were at least 7 g body mass at weaning for SF -1 KO mice, and the total number of available KO females and males was the limiting factor for the randomization strategy. The minimisation principle was applied: all WT mice were littermates or closely related young born at the same time (+/- 3 days) as KO, housed in pairs, and assigned to the diet regime on the appropriate days. Exclusion criteria included complications during surgery or prolonged recovery time after surgery, and general health problems such as persistent loss of body mass. 4 animals met the criteria for a humane end point during the diet regime, and body mass measurement and consumption data from these animals were excluded from the final analysis. Because some losses, especially in SF -1 KO mice, were expected, additional pairs were initially included in the study, in the end each experimental group consisted of 8 animals. Because of the different coloration of the diets, the researcher could not be blinded during animal and food weighing, but the order of the animals at the time of killing was randomised, and complete blinding was possible in the analysis of blood serum and tissue.

Table 1: Composition of both diets used in the study as per manufacturer's declarations (Sniff Spezi-aldiäten, Soest, Germany).

	High fat – Paigen (ssniff S1102-E124)	**Low fat – Control** (ssniff S1102-E122)
Energy ME MJ/kg	18	16
diet specific	15% cocoa butter 1.25% cholesterol 0.5% Na cholate	n.a.
crude protein %	17.6	17.6
crude fat %	16.1	7.1
crude fibre %	5.0	5.0
crude ash %	3.6	3.6
starch %	19.2	32.7
sugar %	21.0	11.0
Vitamin A (IU)	15, 000	15, 000
Vitamin D3 (IU)	1, 500	1, 500
Vitamin E (mg)	150	150
Vitamin K3 (mg)	20	20
Vitamin C (mg)	30	30
Copper (mg)	11	11
other	without phytoestrogens, sterilized 25 kGy, 10 mm round pellet	

Diets, food intake, and body mass measurement

Mice were housed in pairs and fed Paigen diet (S1102-E124) or control diet (S1102-E122, both produced on order by Sniff Spezialdiäten, Soest, Germany) for 20 weeks after reaching the second month of life - between postnatal day 65 and 75. Animals were remained on the diet until time of sacrifice, up to 22nd week. The diets were free of phytoestrogens to exclude external hormonal influences. The atherogenic diet was prepared according to the Paigen recipe with 15% cocoa oil, 1.25% cholesterol, and 0.5% sodium cholate. The control feed contained the same amount of protein, fibre, and vitamin supplements but differed in crude oils and fats. The food declaration is presented in Table 1. The stock feed was stored in the freezer and added to the animal cages in small amounts to avoid rancidity: the needed weekly amount was thawed, cages racks filled up to one tird and the remaining pelletes vacuum sealed and stored in refrigerator to be added during if needed. Every week during cages changing food was renewed from the stock.

Feed consumption was measured every month during the treatment for 1 week: Feed was weighed every other day, divided by two to determine average consumption per animal, and further divided by two to determine daily consumption. Measurements were taken at the first, fourth, 8th, 12th, 16th, and 20th weeks. Body mass was measured individually each week.

Tissue collection

The animals were euthanized at 220 to 230 days of age. The killing took place between 10 am and 2 pm, when the animals were in the second half of the light cycle and are semi-fasted by their natural behaviour (mostly sleeping). The thoracic cavity was exposed under surgical anaesthesia, a blood sample was taken from the left ventricle, followed by complete exsanguination. The incision was made in the right atrium, and the cannula was inserted in left ventricle from apex in cranial direction. The blood vessels were washed with saline (B. Braun Medical) and gentle manual pressure. Micro-scissors were used to excise the heart and the entire aorta. The *en face* aorta was prepared as previously described (29) and the entire protocol can also

be found complemented with video (30). In brief, the aorta was separated from the heart under a stereomicroscope, placed in 4% paraformaldehyde (Sigma Aldrich) in 0.05 M PBS, pH = 7.4, for 24-48 hours, washed in PBS, cleared of adventitia, pinned to a black wax support, and visualised under a stereomicroscope with 20× magnification. To quantify atherosclerotic plaques in the aortic bulb (31), the heart was sectioned transversely on a plane connecting the tips of the two atria with the line perpendicular to the aortic outlet. The lower two-thirds of the heart were discarded, and the upper portion, including the aortic bulb, was placed in a Corning microcentrifuge, covered with tissue freezing medium (Leica Biosystems, Nussloch, Germany), frozen in liquid nitrogen, and stored at -80 °C. Serial 10-µm cryosections of the heart perpendicular to the aortic bulb were cut at -20 °C with the Leica CM1850 cryotome, collected on charged glass slides (Thermo Scientific Superfrost Plus, Menzel-Glaser) and stored at -20 °C until staining. Before staining, they were air dried and fixed with 4% paraformaldehyde for staining with Oil Red O (0.3%, Sigma-Aldrich, Steinheim; Germany) and a light hematoxylin counterstain. For labelling mast cells with toluidine blue stain, they were air dried only. We excluded samples of aortic bulb if sections were too distorted due to freezing storage or not cut at appropriate angle.

Measurement of blood plasma parameters

A blood sample (200µl) was taken from the left cardiac ventricle of each animal with a 21-gauge needle washed with heparin (5000 i.e./ml Braun, Melsungen, Germany). The blood was transferred to a microcentrifuge (Eppendorf® 5415R) and spun at 3000 rpm for 10 minutes at 4 °C. Plasma was transferred to another microcentrifuge and stored at -20 °C until analysis. All analyses were performed using the Olympus AU400 analyzer (Mishima Olympus co., LTD, Japan). Cholesterol was measured using an enzymatic colour assay with chromophore detection at a wavelength of 540/600 nm (Beckman Coulter, Inc, USA). For HDL cholesterol, an enzymatic colour assay with product detection at 600/700 nm (Beckman Coulter. Inc., USA) was used. LDL cholesterol was determined using an enzymatic colour assay with cholesterol oxidase/ PAP system with detection at 600/700 nm (Beckman Coulter, Inc., USA). Triglyceride concentration was measured using an enzymatic colour assay with product detection at 660/800 nm (Beckman Coulter, Inc., USA). Non-esterified fatty acids were determined by enzymatic colorimetric method with product detection at 550 nm (Randox Laboratories Ltd, United Kingdom). Total bile acid concentration was measured indirectly by measuring the rate of thio-NADH formation in the presence of the enzyme 3-a-hydroxysteroid dehydrogenase (Diazyme Laboratories, USA).

Morphometric and Statistical Analysis

En-face aorta preparations were photographed under a stereomicroscope (Olympus SZ40, Japan), Canon 500D digital camera, and Quick-PHOTO CAMERA 3.1 software (Microscope Imaging Software 2014, Promicra, Prague, Czech Republic) and visually examined for the presence of opaque plaques. Cryosections stained with Oil red-O and hematoxylin were photographed under 100× magnification using a Nikon microscope (Nikon Microphot FXA Eclipse 80i, Japan) in conjunction with a 3CCD camera (Nikon DS -Fi1, Japan) and NIS -Elements software (F 2.20, Laboratory Imaging s.r.o. for Nikon Corporation, Praha, Czech Republic). Only sections in which all three cusps of the aortic valve were visible (2-3 per slide) were included. The area of positive staining was measured as a percentage of the total visible area using the Image J polygonal tool (v. 1.51n, NIH, Bethesda, Maryland, USA). To minimise polygonal errors, three consecutive measurements were taken at each cross-section and the mean values per animal were calculated.

Data are reported as mean ± SEM. Statistical analysis was performed using IBM SPSS Statistics v 24.00. Normality tests (Kolmogorov-Smirnov and Shapiro Wilk) rejected the null hypothesis based on median. Body weight beasurements and food consumption were analysed with repeated measurements ANOVA and Bonferroni post hoc test. For total body mass gain, cumulative calorical intake and plaque area multifactorial analysis of variance (MANOVA) with the independent variables of diet, sex, and hormones (genotype) followed by the Tukey post hoc test was used for multiple comparisons of variables between groups. For plasma parameters, a one-way ANOVA and LSD post hoc test was performed. $P < 0.05$ was considered significant.

Results

Food consumption and weight gain

The increase in body mass and estimated cumulative consumption during the experiment are shown in Fig. 1, separately for female and male animals. Intact animals (WT M and WT F) consumed more of both diets. Animals without gonads (SF-1 KO and OVX/CAS) became obese on the control diet, but on the atherogenic diet, despite its high fat content, body mass increased slowly and even stopped in some animals - the curves begin to differ between weeks 9 and 10. Gonadally intact mice continued to gain weight until the time of sacrifice. Repeated measurements ANOVA showed that the type of diet affected both body mass gain and food consumption ($p < 0.001$). The presence of sex hormones affected body mass and the interaction between hormones and diet was significant $F(1, 84)=9.8$, $p=0.002$. For food consumption also sex had an effect and the interaction between hormones and sex was significant $F(1.1, 86.6)=6.7$, $p=0.009$.

Animals that developed without hormones (SF-1 KO) significantly increased their body mass on a normal diet (as expected from previous studies(27, 32)) but on atherogenic diet the obesity was less evident. In general, most animals

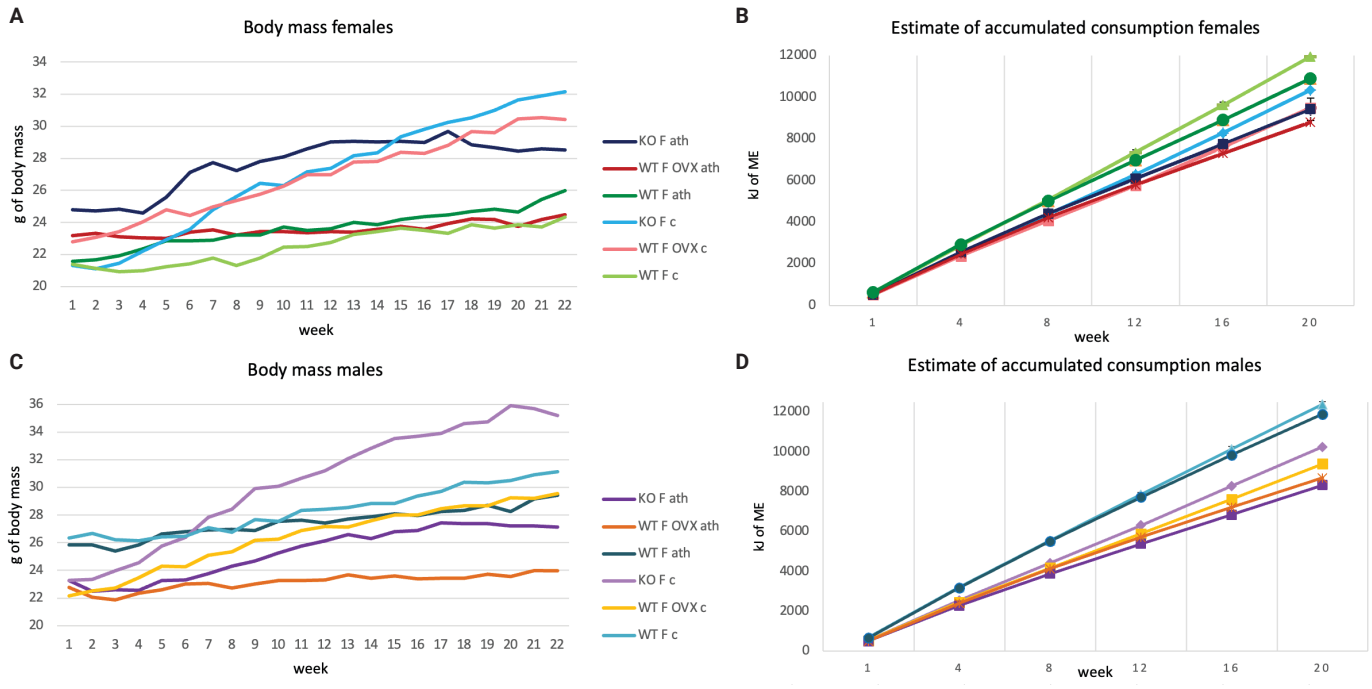

Figure 1: Graphical representation of weekly increase in body mass, separated for clarity into female (A) and male groups (C), and estimated cumulative consumption on two different diets (B, D). The colors for the groups are matched between left and right panels

gained significantly less weight in association with the reduced consumption of the atherogenic diet, except for the intact females, whose body mass increased on the atherogenic diet despite unchanged consumption.

Correlation between body mass gain and cumulative consumption was analyzed on the end-point measurements, which are also presented as bars in Figure 2. Correlation was only weak to moderate in most groups, as represented with Pearson's r in Table 2. Intact females and castrated males stand out as correlation was high on control food but Paigen diet disrupted the expected weight gain.

All groups gained significantly less body weight on the atherogenic diet, except for gonadally intact males and females (WT), in which the difference was not significant; in fact, females (WT F) appeared to utilise more energy from the high fat diet. Food consumption was significantly higher in the gonadally intact male and female groups than in the groups without sex hormones. Although consumption of atherogenic food was lower when weighted in grammes of pallets, the difference in energy value was not significant except in SF -1 KO males, whose body mass gain was also much lower on atherogenic food.

Table 2: Correlation of weight gain from the beginning to the end of the experiment with estimated cumulative consumption within groups

	Pearson Correlation body mass gain - total consumed food	
r	Paigen diet	Control diet
KO F	0, 28	0, 32
OVX	0, 45	0, 16
WT F	0, 32	0, 82
KO M	0, 49	0, 22
CAS	0, 10	0, 86
WT M	0, 17	0, 51

Atherosclerotic plaques

None of the animals had conspicuous changes in the aortic wall or visible fatty streaks on the thoracic or abdominal aorta visible as en face preparations under 20× magnification (Fig. 3). Therefore, further staining and analysis were not performed.

Oil-red-O staining revealed minimal fatty deposits on the cross-sections of the aortic bulbs of mice receiving a control diet: in couple of the SF-1 KO female group, in one ovariectomized female, and none in males without gonads (KO M, CAS), while most intact females and males on control diets exhibited minimal deposits.

On the other hand, in all groups fed an atherogenic diet histologically visible aortic root lesions in the tunica intima of the aortic wall were found (Figure 4A). Significant effect of factors sex, diet and hormones was found ($p < 0.001$) and also interaction between all three $F(1, 61)=11.13$; $p= 0.002$). The lesions were most pronounced in the intact females

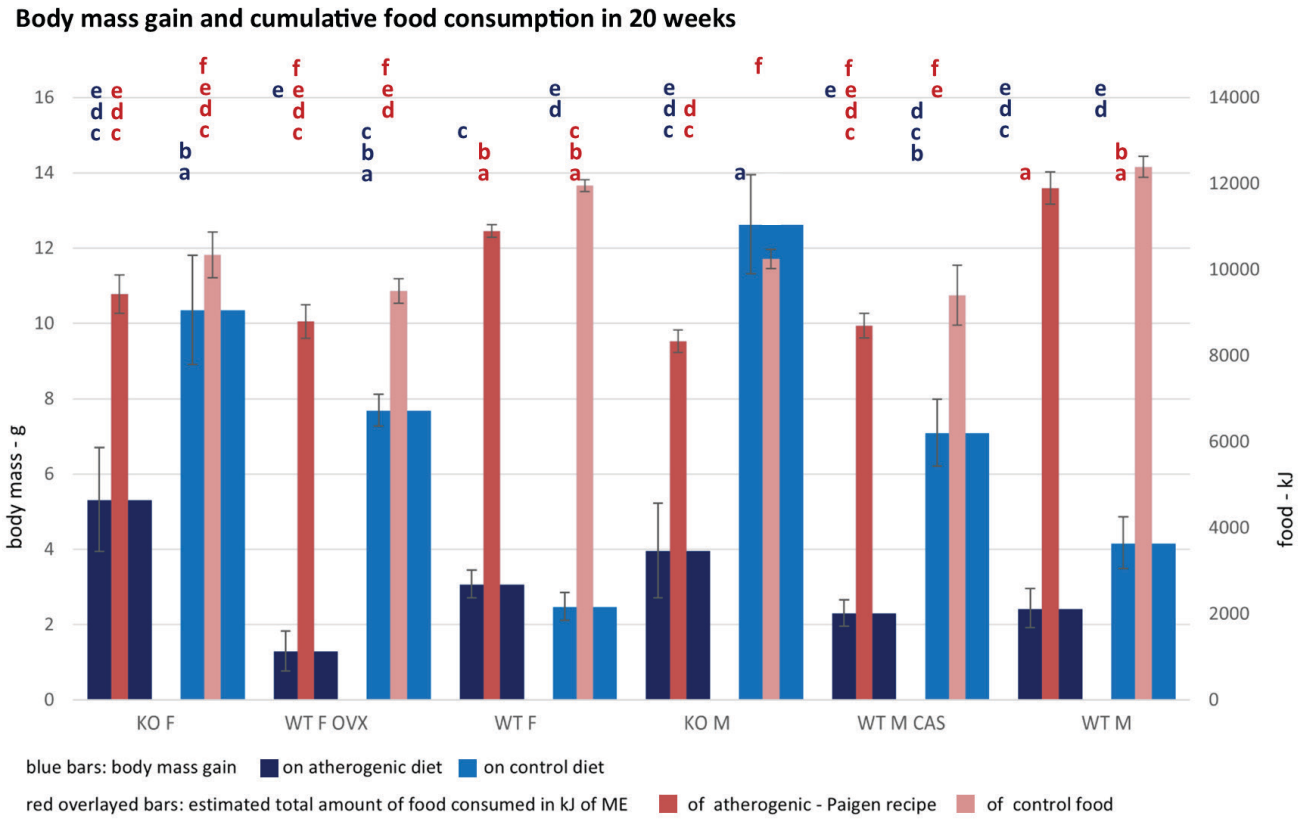

Figure 2: Direct comparison of total body mass gain (blue bars) and estimated total consumption (red overlayed bars, secondary Y axis) on atherogenic (dark red or blue) and control food (light red or blue). Different lowercase letters indicate significant differences at $p < 0.05$ probability level determined with MANOVA and Tukey's HSD test for multiple comparisons, color matched with corresponding bars. N=8 in most groups, WT F on control diet n=7, WT F OVX on atherogenic diet n=6

and measured plaque areas were significantly different from all other groups ($p < 0.001$), whereas the other groups were not significantly different from each other (Fig. 4B).

Lesions were confined to the tunica intima and rarely extended into the aortic lumen or onto the valve cusps. Most of the oil-red-O positive droplets were debris, foam cells were few (Fig. 5A) and small acellular regions were present. Necrotic cores or calcifications were not observed. Scattered mast cells, as determined by metachromatic staining with toluidine blue, were present in all samples (Fig. 5B). Their location and number were not clearly related to plaque extent, but in 50% of sections belonging to females on atherogenic diet, metachromasia was observed on the aortic valves themselves as a sign of mast cell degranulation and inflammation of the tunica intima (Fig. 5C).

Serum lipids

Measurements of total cholesterol, low-density lipoprotein (LDL), high-density lipoprotein (HDL), tryglicerides, free fatty acids, and serum bile acids in serum are shown in Fig. 6. Some differences in baseline values (animals on control diet) were observed: Total triglyceride level was higher in intact males (Fig. 6B) and HDL level was significantly lower in intact females than in intact males, SF-1 knock-out males

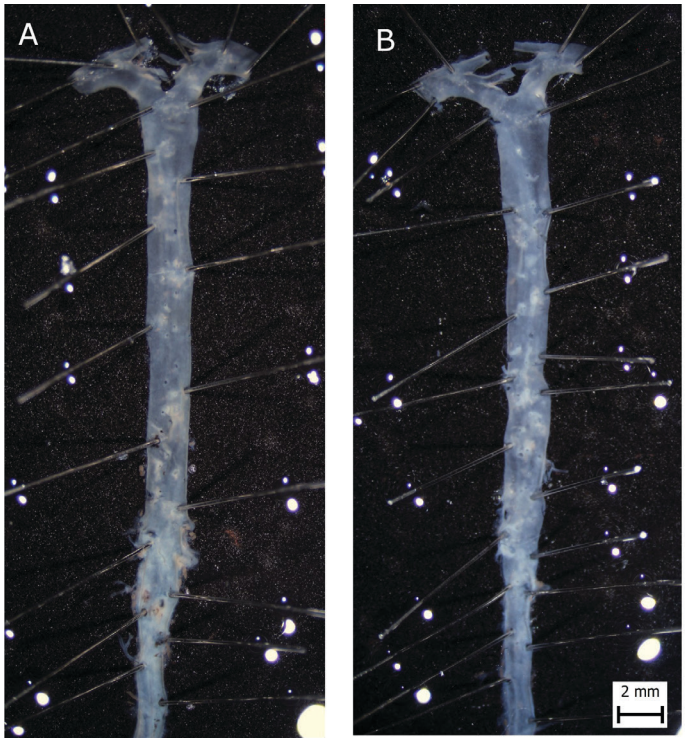

Figure 3: Photomicrograph of thoracic aorta with clear transparent wall of an intact female fed atherogenic diet (A) or control diet (B). No fatty streaks are seen, and this was similar in all groups (not shown)

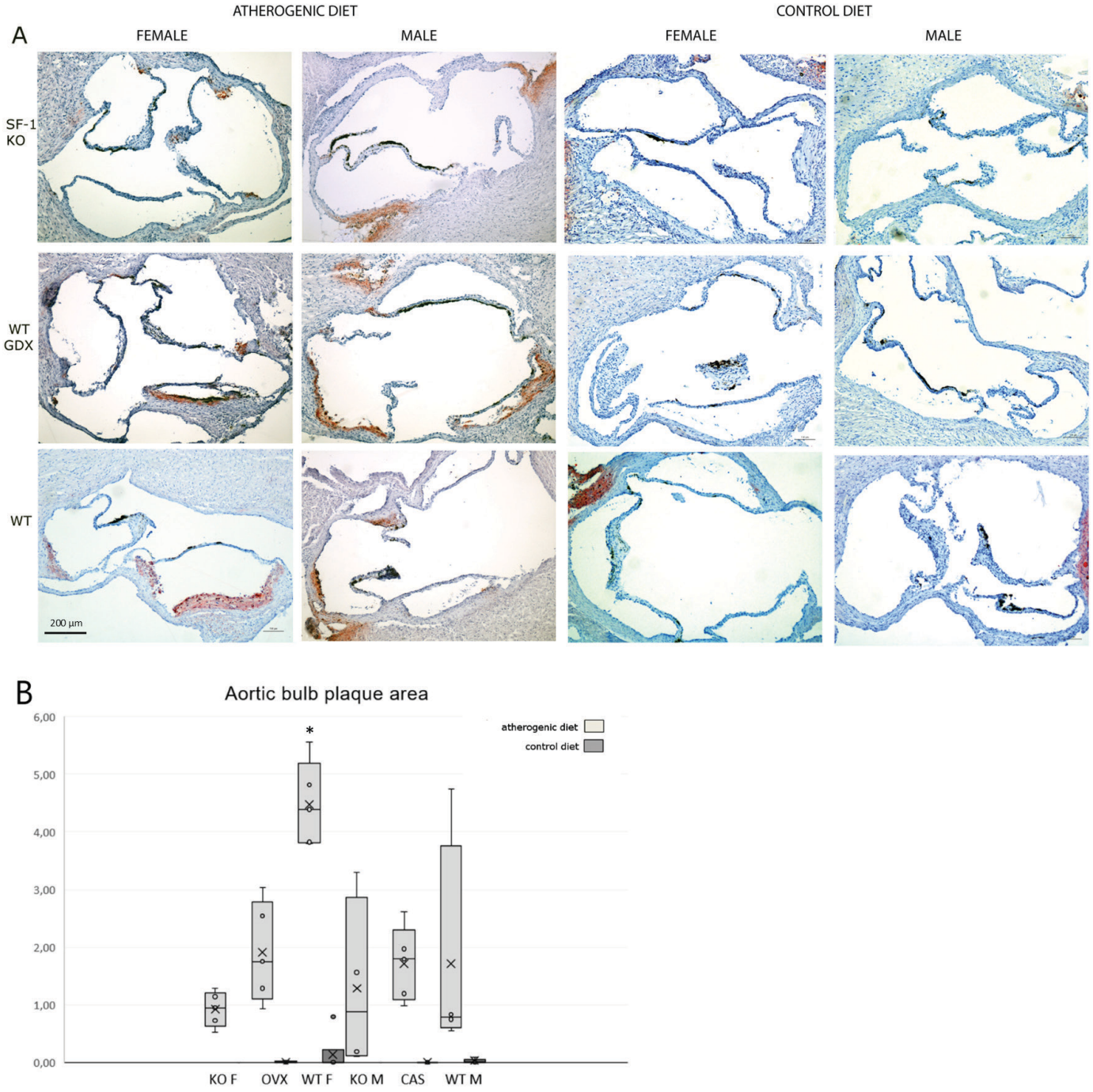

Figure 4: Atherosclerotic plaques form in the aortic root of wild-type C57BL/6J and SF-1 KO mice fed Paigen diet for 20 weeks. A) Representative photomicrographs of atherosclerotic plaques in the aortic root stained with Oil-red-O and hematoxilyn in all 6 groups fed atherogenic (two left columns) or con-trol diet (right columns). B) Quantification of plaques area as percentage of visual field with region-of-interest (aortic bulb) shows that they were most prevalent in intact female wild-type mice fed an ather-ogenic diet (* $p < 0.001$). Some minimal plaques were found in individuals from WT F and WT M (intact males and females) on control diet. (n=6 on control diet and n=5 on atherogenic diet, except for KO M and WT M on atherogenic diet n=4)

and ovariectomized females (6D, $p < 0.05$). Atherogenic diet significantly increased (nonfasting) total plasma cholesterol, LDL cholesterol, and total bile acids (Fig.6A, C, E; $p < 0.05$). No significant change in total triglycerides was observed. Free fatty acids were significantly decreased (6F) but less so in intact and castrated males, which were significantly different from all females and SF-1 KO males ($p < 0.001$). No other significant changes were observed between the atherogenic diet groups.

Discussion

The present study shows that gonadally intact female C57BL/6J mice develop more marked atherosclerotic plaques on atherogenic diet than gonadally intact males

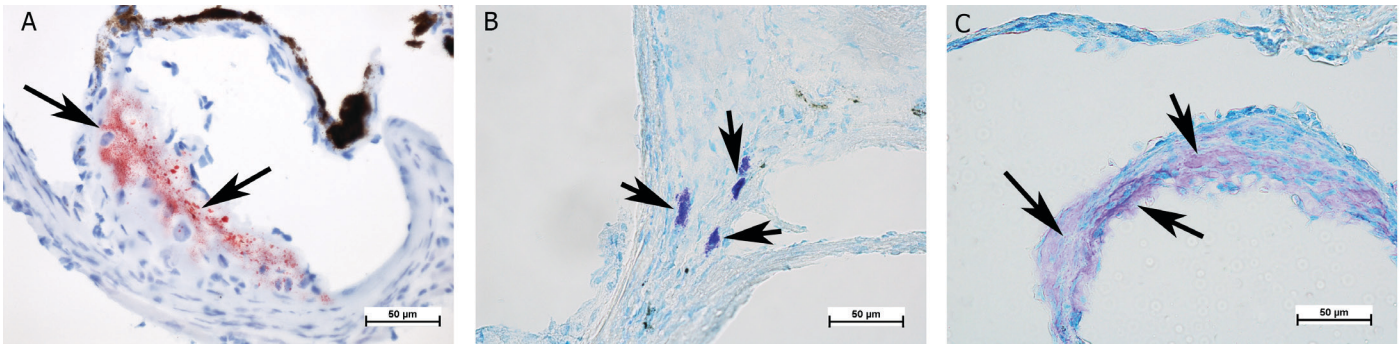

Figure 5: A) Oil- red-O stain shows lipid droplets in few foam cells (arrows) - early plaque formation in the space behind the aortic valve, dark brown are pigment cells in the valves; B) Migration of mast cells (arrows) to the aortic bulb wall, metachromatic granules (purple) in the citoplasm with toluidine blue staining, not related to extensive plaques C) mast cell degranulation (touluidine blue metachromatic reaction, arrows) in the intima of the aortic valve, found in WT females on atherogenic diet only

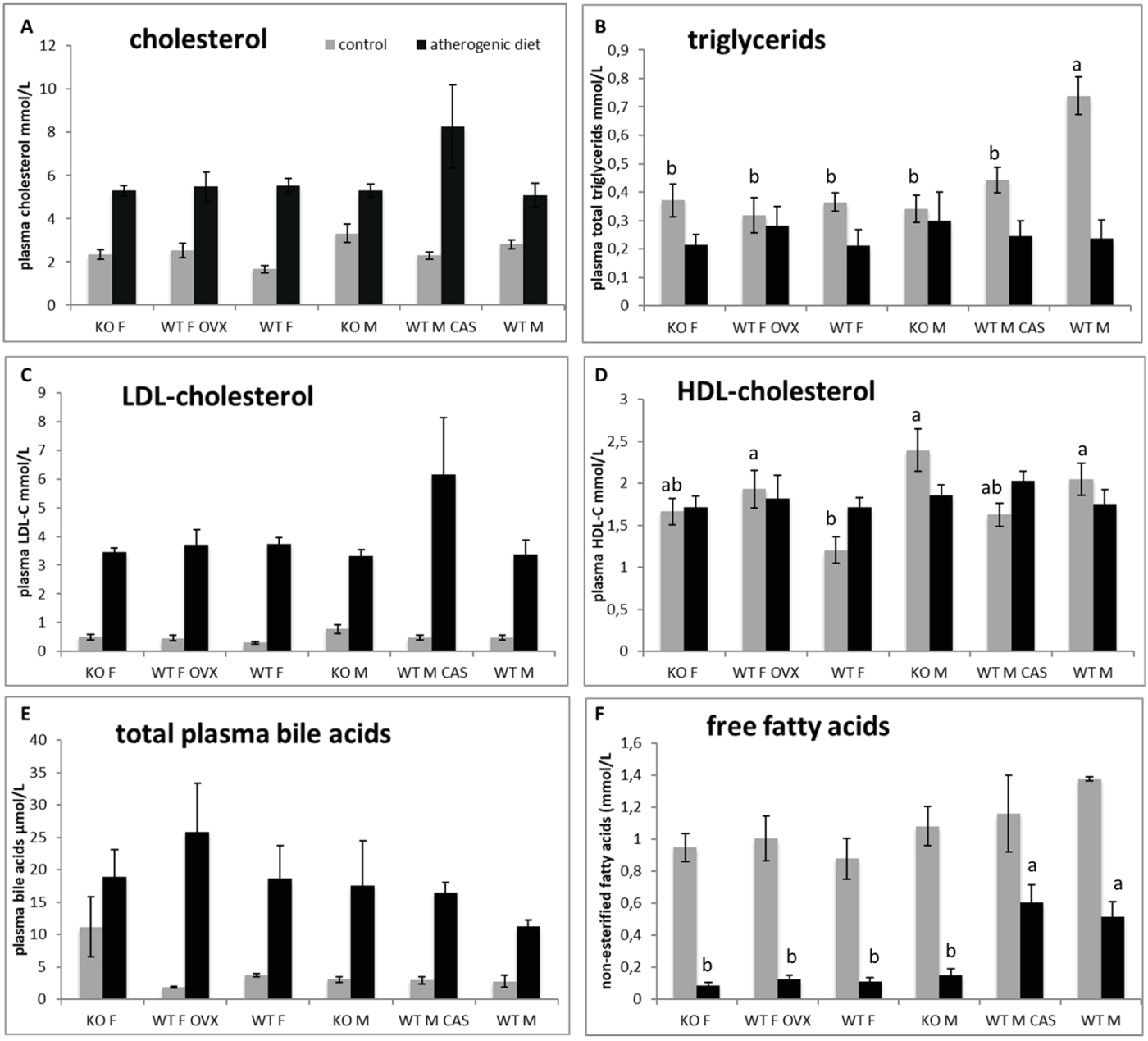

Figure 6: Effects of atherogenic diet on plasma lipid levels measured by enzymatic color assays, n=8 per group. Data are expressed as mean± SEM. Atherogenic diet significantly increased total and LDL cholesterol and total bile acids and decreased free fatty acids (significant differences between black and grey bars; $p < 0.05$). Differences between groups either on atherogenic or control diet were few and are indicated by lowercase letters at probability level $p < 0.05$

or male and female mice with suppressed sex hormones. Serum lipid profiles could not explain the increased atherosclerosis in females because there was almost no difference between the groups on atherogenic diet. Interestingly, intact females appeared to metabolise the high fat content of the diet better, as only this group consistently gained weight while fed the Paigen diet, although they didn't reach the obesity level of the agonadal mice during duration of experiment. In agonadal SF-1 knockout mice, there were no sex differences in any of the parameters studied, suggesting that the main mechanism causing sex-dependent differences in atherosclerosis depends on sex hormones rather than sex chromosomes.

In the present study, all animals fed the atherogenic diet consumed slightly less food than animals fed the control diet. When converted to estimated total consumption in caloric value of metabolic energy, the differences were not statistically significant, except for SF -1 KO males. These males also gained weight poorly on the atherogenic diet with the greatest difference from the animals on the normal diet - likely due in part to reduced consumption. Daily consumption did not change significantly over the course of the experiment and correlation between final weight gain and total amount of food consumed was only moderate. It should be noted that the Paigen diet is hepatotoxic. High cholesterol diets might not be sufficient to induce atherosclerosis, but it does lead to steatohepatitis characterised by oxidative stress and expression of inflammatory genes. The addition of cholate to induce atheroclerotic plaques also makes the diet lithogenic and specifically affects the expression of extracellular matrix deposition genes thus exacerbating liver injury (33, 34). All animals on the atherogenic diet in our study had hepatosteatosis as macroscopicaly observed at necropsy, in some individuals also large gallbladder stones and/or jaundice was observed. 4 animals reached humane endpoint between week 17 and 18 as their health detoriated with evident body mass loss. Also noted control SF-1 KO animals did not reach the usual extreme body weights observed in previous studies (27), probably due to the lower fat content of the control diet in this study, but were still heavier than gonadectomized mice. Some studies assume that only prolonged feeding of the atherogenic diet (up to a year) causes the obvious atherosclerotic changes (31), but we found that it seriously affected the general health our mouse strain already in 20 weeks, at least in SF-1 KO and gonadectomized mice. Since the animals without gonads gained significantly more weight on the control diet, we suspect that the gonadal hormones prevented the (early) deleterious effects of the Paigen diet. The average increase in body mass was slightly higher in intact females on the atherogenic diet than on the low-fat diet, although the ratio of consumation was not changed. It is known that X chromosome effects pose a risk for obesity and estrogens are generally protective against obesity (reviewed in (35)). Still the effect can be strain-dependent like it was demonstrated by Surra et al. (36) where female ApoE KO mice gained significantly more weight when on C57BL/6 background than other strains. In our study, the combination of dietary fats and normal oestrogen levels appears to have contributed to the observed sustained weight gain, but the experiment ended too early to see the long-term effect, neither total body fat content was analyzed.

In the original work by Paigen et al (9) it was reported that atherosclerotic changes were more numerous or/and extensive in female mice compared with male mice. This study was primarily a methodological study, and most experiments were performed with female mice only, so sex differences in atherosclerosis were not further emphasised. Most subsequent studies examined only one sex, and studies using ApoE-deficient mice yielded conflicting results, with some reporting atherosclerotic changes were more pronounced in male (17, 18, 20) and others in female mice (21, 22, 37). The explanation for the discrepancies may be due to the different genetic background of the modified mice (36, 38) and the duration of the study or the age of the mice. Some evidence suggests female sex hormones sensitize inflammation in atherogenesis (7) but as males get older, they are more prone to plaque formation (25). Mapping mouse atherosclerosis modifier genes in some congenic mouse strains yielded replicating results in females and males but the extent of atherosclerosis plaques appears to be slightly higher in females where the data were normally distributed but was skewed in males (39), somewhat comparable to our results. In our study, we found significant differences in atherosclerotic lesions between groups, with gonadally intact WT females having two to three times bigger atherosclerotic lesions than all other groups: gonadally intact males, prepubertally gonadectomized males and females, and agonadal SF-1 KO mice. It should be noted that the overall extent of plaques was small in the aortic bulb, not (yet) apparent in the aortic arch, and only a few foam cells (macrophage uptake of LDL) and degranulation of mast cells were observed (Fig. 5). This suggests an early inflammatory process - plaque initiation of the aortic wall (40, 41), again more pronounced in intact females. We can speculate that longer exposure to the atherogenic diet or starting the diet in much older mice would result in larger plaques and associated signs of atherosclerosis. The observation of more pronounced atherosclerotic changes in gonadally intact females is consistent with the previously reported findings of Caligiuri et al. (37) and Marek et al. (22) both of which showed more severe lesions in females compared with males and both of which used the C57BL/6 background for the ApoE mouse model. It is also consistent with some data on LDLr-deficient mice (7, 24), although these studies used only gonadally intact mice and therefore it is not possible to speculate whether testosterone plays a protective role in WT males or whether estrogens increase risk in female mice. Therefore, in our study, we used prepubertal gonadectomized WT males and females and agonadal SF-1 KO males and females for comparison and no significant difference were found among those groups. This strongly suggests that estrogens are a

risk factor for the development of diet- induced atherosclerotic plaques in mice, unlike in humans.

In general, early atherosclerotic plaque formation in all animals receiving an atherogenic diet but not in those receiving a control diet is in accordance with an overall increase in total cholesterol and LDL cholesterol in all groups. The sexual dimorphism in plasma lipid levels was associated with XX chromosome complement in four core mouse model (42) and to some extent we observed a similar effect of male sex (increased levels of tryglicerides and FFA on normal diet). However, there was no evidence that the extent of plaques can be predicted from serum cholesterol levels, because no significant differences were found between groups; in particular, gonadally intact females didn't have different LDL or HDL cholesterol levels compared with other groups on atherogenic diets. To some extent also intact males (individuals) were gaining weight and had more pronounced aortic plaques on both, atherogenic and control diet compared to males without testosterone and would possiby gain statistic significance if kept on the diet for prolonged period. Obesity has long been recognised as an important atherogenic risk factor associated with unhealthy diet, but the mouse and diet model in our study could not directly demonstrate this effect.

In humans, estrogens appear to play a protective role in the development of cardiovascular disease and the formation of atherosclerotic plaques, as both are more common in men than in women, although the risk increases in menopausal women (35). Thus, the possibility of hormone treatment (estrogens) for atherosclerosis has attracted considerable interest in medicine but has had mixed success (13). Interestingly, most studies using estrogens to treat the progression of atherosclerosis report a reduction in lesion size, although many studies show that atherosclerosis in mice is more severe in female animals (in contrast to humans). Direct comparison is complicated by the choice of mouse models, ApoE- or LDL receptor-deficient mice have been used mostly for treatments with 17beta-estradiol (5, 43)). The effects of endogenous and exogenous hormones may also differ, and whereas in some studies ovariectomy increased atherosclerosis in mice (44) other studies reported that ovariectomy did not cause vascular senescence in female C57BL/6 mice and did not exacerbate it in female ApoE KO (20). Lack of alteration in plasma cholesterol and trygliceride levels in mice is rather common observation in atherosclerosis induction or treatment (20, 44–46).

Not only ovariectomy but also complete ovarian agenesis had no effect in our SF-1 knock-out mouse model. In humans, there is some evidence that declining testosterone levels also contribute to the progression of atherosclerosis, but testosterone replacement therapies remain controversial (35). This suggests that the hormonal contribution to the development of atherosclerosis is complex, and interestingly, a study using the *ApoE-/-:Ins2+/Akita* model of accelerated atherosclerosis in mice reported that testosterone had both atheroprotective and proatherogenic effects depending on the glycemic status of the mouse. Castration accelerated atherosclerosis in normoglycemic mice but ameliorated it in diabetic mice (19). In our study, neither castration nor gonadal agenesis had significant effect on the extent of atherosclerotic plaques that developed after mice were fed a Paigen diet.

An important risk factor for atherosclerosis in humans and in mouse models is age. In C57BL/6 mice fed normal chow, vascular lipid deposits can develop spontaneously and become more prominent with age, probably because of increased oxidative stress, but only in very old animals (47). Another group also found lipid deposition on aortic valves and aortic regurgitation in old C57BL/6 mice fed normal chow, with more pronounced effects in male mice (38). In our study, individual control animals had minimal lipid deposition in the aortic root, especially intact females and males. The mice were less than 8 months old at euthanasia and thus not truly geriatric. Furthermore, no serum marker used in our study is likely to predict spontaneous/geriatric atherosclerotic changes in mice. Atherogenic diet generally affected serum lipids, but there was no difference between sexes or correlation with sex hormones. This is consistent with other studies (17, 18, 48) with the exception of study with Apo-E KO mice by Smith et al., (21) which found a similar higher incidence of atherosclerosis in females but reported a reversed lipid profile of serum lipids, as total cholesterol, tryglicerides, HDL, LDL, and VLDL were elevated in males.

The primary goal of animal studies is to determine whether drugs can evoke the regression of atherosclerotic plaques. However, many of the drugs tested have shown limited effects on plaque regression in animal studies. Quite often they have been studied in animals of only one sex, making extrapolation difficult when sexual difference in humans is long known. But at least one promising diagnostic and therapeutic agent - interleukin 19 (IL - 19) - had the same effect in male and female LDLR-deficient mice (46)

In conclusion, our study shows that atherosclerotic plaques in C57BL/6J mice on Paigen diet are exacerbated by female gonadal hormones, that female gonadal hormones also cause higher weight gain on atherogenic diet, and that serum lipid levels correspond poorly with atherosclerotic changes in mice. This suggests that estrogens are a risk factor for the development of atherosclerotic lesions and thus calls into question the validity of mouse models for the study of cardiovascular disease in humans, because in humans the situation is generally reversed and estrogens play a protective role in the development of cardiovascular disease.

Acknowledgements

We would like to thank Nina Šterman for animal husbandry and technical assistance.

Sources of Funding: This study was supported by ARRS (Slovenian Research Agency) grants P4-0053 and J7-7226. Katja Kozinc Klenovšek was supported by a doctoral fellowship from ARRS.

Disclosures: Authors have nothing to disclose.

References

1. Lusis A. Atherosclerosis. Nature. 2000; 407(6801): 233–41.
2. Leong XF, Ng CY, Jaarin K. Animal models in cardiovascular research: hypertension and atherosclerosis. Biomed Res Int 2015; 2015: e528757, 11 pages. doi:10.1155/2015/528757.
3. Getz GS, Reardon CA. Diet and murine atherosclerosis. Arterioscler Thromb Vasc Biol 2006; 26(2): 242–9.
4. Lee YT, Lin HY, Chan YWF, et al. Mouse models of atherosclerosis: a historical perspective and recent advances. Lipids Health Dis 2017; 16(1): 12.
5. Veseli BE, Perrota P, De Meyer GRA, et al. Animal models of atherosclerosis. Eur J Pharmacol. 2017; 816(April): 3–13.
6. Zou MH, Shen YH, Zhang X, et al. Dare to Compare. Development of atherosclerotic lesions in human, mouse, and zebrafish. Front Cardiovasc Med 2020; 7: e109. doi: 10.3389/fcvm.2020.00109
7. Chen S, Markman JL, Shimada K, et al. Sex-specific effects of the Nlrp3 inflammasome on atherogenesis in LDL receptor-deficient mice. JACC Basic Transl Sci 2020; 5(6): 582–98.
8. Ishida BY, Blanche PJ, Nichols A V, Yashar M, Paigen B. Effects of atherogenic diet consumption on lipoproteins in mouse strains C57BL/6 and C3H. J Lipid Res 1991; 32(4): 559–68.
9. Paigen B, Morrow A, Holmes PA, Mitchell D WR. Quantitative assessment of atherosclerotic lesions in mice. Atherosclerosis. 1987; 68(3): 231–40.
10. TS M, TB C. Estrogen replacement therapy, atherosclerosis, and vascular function. Cardiovasc Res 2002; 53(3): 605–19.
11. Vlachopoulos C, Ioakeimidis N, Miner M, et al. Testosterone deficiency: a determinant of aortic stiffness in men. Atherosclerosis. 2014; 233(1): 278–83.
12. Fairweather D. Sex differences in inflammation during atherosclerosis. Clin Med Insights Cardiol 2015; 8(Suppl 3): 49–59.
13. Dos Santos RL, Da Silva FB, Ribeiro RF, Stefanon I. Sex hormones in the cardiovascular system. Horm Mol Biol Clin Investig 2014; 18(2): 89–103.
14. Ventura-Clapier R, Dworatzek E, Seeland U, et al. Sex in basic research: concepts in the cardiovascular field. Cardiovasc Res 2017; 113(7): 711–24.
15. Man JJ, Beckman JA, Jaffe IZ. Sex as a biological variable in atherosclerosis. Circ Res 2020; 126(9): 1297–319.
16. Bywaters BC, Pedraza G, Trache A, Rivera GM. Endothelial NCK2 promotes atherosclerosis progression in male but not female Nck1-null atheroprone mice. Front Cardiovasc Med 2022; 9: e955027. doi: 10.3389/fcvm.2022.955027.
17. Bourassa P, Milos PM, Gaynor BJ, Breslow JL, Aiello RJ. Estrogen reduces atherosclerotic lesion development in apolipoprotein E-deficient mice. Proc Natl Acad Sci U S A 1996; 93(19): 10022–7.
18. McRobb L, Handelsman DJ, Heather AK. Androgen-induced progression of arterial calcification in apolipoprotein E-null mice is uncoupled from plaque growth and lipid levels. Endocrinology 2009; 150(2): 841–8.
19. Venegas-Pino DE, Wang PW, Stoute HK, et al. Sex-specific differences in an ApoE-/-:Ins2+/Akita mouse model of accelerated atherosclerosis. Am J Pathol 2016; 186(1): 67–77.
20. Pereira TMC, Nogueira B v., Lima LCF, et al. Cardiac and vascular changes in elderly atherosclerotic mice: the influence of gender. Lipids Health Dis 2010; 9: e87. doi: 10.1186/1476-511X-9-87
21. Smith DD, Tan X, Tawfik O, Milne G, Stechschulte DJ, Dileepan KN. Increased aortic atherosclerotic plaque development in female apolipoprotein E-null mice is associated with elevated thromboxane A2 and decreased prostacyclin production. J Physiol Pharmacol 2010; 61(3): 309–16.
22. Marek I, Canu M, Cordasic N, et al. Sex differences in the development of vascular and renal lesions in mice with a simultaneous deficiency of Apoe and the integrin chain Itga8. Biol Sex Differ 2017; 8(19): 1–13.
23. Maeda N, Johnson L, Kim S, Hagaman J, Friedman M, Reddick R. Anatomical differences and atherosclerosis in apolipoprotein E - deficient mice with 129/SvEv and C57BL/6 genetic backgrounds. Atherosclerosis 2007; 195(1): 75–82.
24. Petrovan RJ, Kaplan CD, Reisfeld RA, Curtiss LK. DNA vaccination against VEGF receptor 2 reduces atherosclerosis in LDL receptor-deficient mice. Arterioscler Thromb Vasc Biol 2007; 27(5): 1095–100.
25. Man JJ, Beckman JA, Jaffe IZ. Sex as a biological variable in atherosclerosis. Circ Res 2020; 126(9): 1297–319.
26. Luo X, Ikeda Y, Lala D, Baity L, Meade J, Parker K. A cell-specific nuclear receptor plays essential roles in adrenal and gonadal development. Endocr Res 1995; 21(1/2): 517–24.
27. Majdic G, Young M, Gomez-Sanchez E, et al. Knockout mice lacking steroidogenic factor 1 are a novel genetic model of hypothalamic obesity. Endocrinology 2013; 143(3): 607–14.
28. Büdefeld T, Tobet SA, Majdic G. Steroidogenic factor 1 and the central nervous system. J Neuroendocrinol 2012; 24(1): 225–35.
29. Palinski W, Ord VA, Plump AS, Breslow JL, Steinberg D, Witzrum JL. ApoE-deficient mice are a model of lipoprotein oxidation in atherogenesis. Arterioscler Thromb Vasc Biol. 1994; 14(4): 605–16.
30. Centa M, Ketelhuth DFJ, Malin S, Gisterå A. Quantification of atherosclerosis in mice. J Vis Exp 2019; 148: e1–9. doi: 10.3791/59828.
31. Venegas-Pino DE, Banko N, Khan MI, Shi Y, Werstuck GH. Quantitative analysis and characterization of atherosclerotic lesions in the murine aortic sinus. J Vis Exp 2013 Dec 7; (82): e50933. doi: 10.3791/50933..
32. Büdefeld T, Grgurevic N, Tobet SA, Majdic G. Sex differences in brain developing in the presence or absence of gonads. Dev Neurobiol 2008; 68(7): 981–95.
33. Liu Y, Meyer C, Xu C, et al. Animal models of chronic liver diseases. Am J Physiol Gastrointest Liver Physiol 2013; 304: 449–68.
34. Vinué Á, Herrero-Cervera A, González-Navarro H. Understanding the impact of dietary cholesterol on chronic metabolic diseases through studies in rodent models. Nutrients 2018; 10(7): e939. doi: 10.3390/nu10070939

35. Arnold AP, Cassis LA, Eghbali M, Reue K, Sandberg K. Sex hormones and sex chromosomes cause sex differences in the development of cardiovascular diseases. Arterioscler Thromb Vasc Biol 2017; 37(5): 746–56.

36. Surra JC, Guillén N, Arbonés-Mainar JM, et al. Sex as a profound modifier of atherosclerotic lesion development in apolipoprotein E-deficient mice with different genetic backgrounds. J Atheroscler Thromb 2010; 17(7): 712–21.

37. Caligiuri G, Nicoletti A, Zhou X, Törnberg I, Hansson GK. Effects of sex and age on atherosclerosis and autoimmunity in apoE-deficient mice. Atherosclerosis 1999; 145(2): 301–8.

38. Paigen B, Morrow A, Brandon C, Mitchell D HP. Variation in susceptibility to atherosclerosis among inbred strains of mice. Atherosclerosis 1985; 57(1): 65–73.

39. Han J, Ritchey B, Opoku E, Smith JD. Fine mapping of the mouse Ath28 locus yields three atherosclerosis modifying sub-regions. Genes 2022; 13(1): e70. doi: 10.3390/genes13010070.

40. Libby P. Inflammation during the life cycle of the atherosclerotic plaque. Cardiovasc Res 2021; 117(13): 2525–36.

41. Kovanen PT, Bot I. Mast cells in atherosclerotic cardiovascular disease: activators and actions. Eur J Pharmacol 2017; 816(Sept): 37–46.

42. Link JC, Chen X, Prien C, et al. Increased high-density lipoprotein cholesterol levels in mice with XX versus XY sex chromosomes. Arterioscler Thromb Vasc Biol 2015; 35(8): 1778–86.

43. Shelton KA, Cline JM, Cann JA. 17-β Estradiol reduces atherosclerosis without exacerbating lupus in ovariectomized systemic lupus erythematosus-susceptible LDLr-/- mice. Atherosclerosis 2013; 227(2): 228–35.

44. Marsh MM, Walker VR, Curtiss LK, Banka CL. Protection against atherosclerosis by estrogen is independent of plasma cholesterol levels in LDL receptor-deficient mice. J Lipid Res1999; 40(5): 893-900.

45. Clark M, Centner AM, Ukhanov V, Nagpal R, Salazar G. Gallic acid ameliorates atherosclerosis and vascular senescence and remodels the microbiome in a sex-dependent manner in Ap-oE−/− mice. J Nutr Biochem. 2022; 110: e109132. doi: 10.1016/j.jnutbio.2022.109132

46. Chen W, Xing J, Liu X, Wang S, Xing D. The role and transformative potential of IL-19 in atherosclerosis. Cytokine Growth Factor Rev 2021; 62: 70–82. doi: 10.1016/j.cytogfr.2021.09.001

47. Merat S, Fruebis J, Sutphin M, Silvestre M, Reaven P. Effect of aging on aortic expression of the vascular cell adhesion molecule-1 and atherosclerosis in murine models of atherosclerosis. J Gerontol A Biol Sci Med Sci 2000; 55(2): B85–94.

48. Villablanca A, Lubahn D, Shelby L, Lloyd K, Barthold S. Susceptibility to early atherosclerosis in male mice is mediated by estrogen receptor alpha. Arterioscler Thromb Vasc Biol 2004; 24(6): 1055–61.

Ženski spolni hormoni predstavljajo dejavnik tveganja za nastanek ateroskleroznih sprememb pri miših linije C57BL/6J na aterogeni dieti

M. Štrbenc, K. Kozinc Klenovšek, G. Majdič

Izvleček: Pri ženskah se v postmenopavznem obdobju poveča tveganje za razvoj ateroskleroze, zato je splošno sprejeto, da estrogeni hormoni varujejo ožilje pred razvojem tega žilnega obolenja. Ni pa še popolnoma raziskano, ali so estrogeni poglavitni dejavnik, ali imajo vpliv tudi spolni kromosomi in ali je vpliv spolnih hormonov enak med sesalci. Živalski modeli za proučevanje ateroskleroznega obolenja so redki, eden izmed njih so miši linije C57BL/6J, ki lahko spontano razvijejo aterosklerotične spremembe v večjih telesnih arterijah, če se jih dlje časa hrani s hrano z visoko vsebnostjo maščob, z dodatkom holesterola in holata - s t.i. aterogeno dieto po Paigenu. V raziskavi smo želeli proučiti vpliv spolnih hormonov in spolnih kromosomov na razvoj aterosklerotičnih plakov v žilah s pomočjo modela miši z izbitim genom SF-1, ki se razvijejo brez spolnih organov. 20 tednov smo mišim dajali hrano po receptu Paigen oziroma kontrolno hrano z nižjo vsebnostjo maščob. Miši obeh spolov so bile bodisi brez spolnih organov zaradi izbitega gena SF-1 (na ozadju C57BL/6J), bodisi smo jim gonade operativno odstranili pred puberteto. Tretjino samcev in samic smo pustili intaktne z gonadami. Spremljali smo telesno težo živali, povprečno porabo hrane in opravili analizo serumskih lipidov. Pregledali smo preparirane aorte po metodi *en-face* ter ocenili obseg plakov in maščob na prečnih rezih aortnega korena na nivoju aortnih zaklopk s histološkim barvanjem in analizo mikroskopske slike. Pri vseh skupinah miši, ki so bile hranjene z aterogeno dieto, so bile aterosklerotične spremembe relativno majhne in omejene na aortni koren. Obseg plakov je bil odvisen od kromosomskega spola in prisotnosti hormonov, plaki so bili najbolj očitni pri samicah z jajčniki. Istočasno so bile intaktne samice edina skupina živali, ki so podobno pridobivale na teži tako na aterogeni kot kontrolni hrani, pri ostalih skupinah so živali na aterogeni dieti priraščale bistveno manj. Vrsta hrane je imela vpliv na serumski lipidni profil, vendar praktično ni bilo statistično značilnih razlik med različnimi skupinami živali in analize krvnega seruma nismo mogli povezati z drugimi ugotovljenimi odstopanji pri samicah. Rezultati raziskave kažejo, da so glavni povod za spolne razlike pri razvoju aterosklerotičnih sprememb spolni hormoni in ne spolni kromosom. Hkrati pa rezultati postavljajo pod vprašaj uporabnost mišjih modelov za proučevanje ateroskleroze, ki jo induciramo s prehrano, saj prisotnost estrogenov - obratno kot pri ljudeh - pri miših negativno vpliva na presnovo lipidov in doprinese k izoblikovanju aterosklerotičnih plakov.

Ključne besede: ateroskleroza; dieta po Paigenu; spol; spolni hormoni; miš, lipidi in holesterol

DOI 10.26873/SVR-1525-2023
UDC 636.5:536.7:611.013.9:636.033
Pages: 67–73

Original Research Article

Effects of Thermal Manipulation of Japanese Quail Embryo on Post-hatch Carcass Traits, Weight of Internal Organs, and Breast Meat Quality

Key words

Coturnix japonica;
meat-type quail;
breast traits;
thermal biology

Saad N. El-Shater[1], Karim M. Khalil[1,5]*, Hamdy Rizk[1], Hamdy M.B.A. Zaki[2], Hisham A. Abdelrahman[3], Hassanein H. Abozeid[4], Elsayed F. Khalifa[1]

[1]Anatomy and Embryology Department, [2]Department of Food Hygiene and Control, [3]Department of Veterinary Hygiene and Management, [4]Department of Poultry Diseases, Faculty of Veterinary Medicine, Cairo University, Giza, 12211, Egypt, [5]Department of Veterinary Medicine, College of Applied & Health Sciences, A`Sharqiyah University, 400 Ibra, Sultanate of Oman

***Corresponding author:** karim.khalil@asu.edu.om

Abstract: Embryonic thermal manipulation was known as an effective protocol for improving post-hatch growth performance and thermotolerance acquisition among avian species. Previously, we evaluated the impact of embryonic thermal manipulation of Japanese quail on embryonic development, hatchability, and post-hatch performance. We conducted the current study to furtherly elucidate the effects of thermal manipulations of Japanese quail embryos on internal organ weights, carcass traits, and meat quality parameters at post-hatch day 35. Quail eggs of control group were incubated at 37.7 °C and relative humidity (RH) 55%. Three thermally manipulated groups of quail eggs were incubated intermittently at 41°C and 65% RH intermittently (3 hours/day): the early embryonic group (TM_1) was thermally challenged at embryonic day (ED6) to ED8, the late embryonic group (TM_2) was thermally challenged at ED12-14, and early/late embryonic group (TM_3) was thermally challenged in both time windows. Quail meat quality parameters, carcass traits, and internal organ weights were evaluated at post-hatch day 35. The results revealed that early embryonic thermal manipulation (TM_1 group) is an effective protocol for decreasing fat pad accumulation. The pH value of breast meat in all TM treatments revealed significant ($P < 0.05$) decreases by 5% in comparison with that of control without any negative effects on breast meat composition or sensory criteria. Early embryonic thermal manipulation would be recommended as an enhanced protocol that can be used to reach the favored lucrative effects of the thermal treatment in meat-type quail.

Received: 17 August 2022
Accepted: 3 April 2023

Introduction

Several countries depend on Japanese quail (*Coturnix japonica*) as a source of meat and eggs. Japanese quail is a migratory bird that is characterized by short generation intervals besides its distinctive physical, physiological, and behavioral features, that's why, it is a very important animal model in scientific research and lab experiments (1, 2). Embryonic thermal manipulation (TM) was identified as a beneficial technique that improves muscle development and growth in avian species, in which the embryos are challenged with high or low incubation temperatures during a critical time window in their embryonic life (3, 4). Adaptation for thermotolerance and breast muscle yield were enhanced

without any significant alterations in the characteristics of breast meat quality (5). The intermittent embryonic TM of Japanese quail at ED 6 - 8 improved final body weight at post-hatch day 35 which was manifested by significant breast muscle hypertrophy (6, 7). The reduction of the abdominal fat pad relative weight is one of the goals of broiler management. Embryonic TM had been identified as an effective technique to decrease abdominal fat accumulation (4). To date, there are no studies on quail that have indicated whether TM has a beneficial effect on meat quality, internal organ weights, and carcass traits or not. Therefore, the current study aimed to elucidate the effects of embryonic TM on quail breast meat quality, carcass traits, and internal organs weights at post-hatch day 35.

Materials and methods

Egg incubation and hatching management

The study was conducted at the Faculty of Veterinary Medicine, Cairo University, Egypt (FVMCU). All experimental procedures and management conditions used in this study were approved by the Institutional Animal Care and Use Committee (IACUC; Reference No. Vet CU16072020190).

One thousand eggs were obtained from a quail maternal flock of 13 weeks old from the experimental farm, Faculty of Agriculture, Cairo University, Egypt. After egg selection, individually weighted and disinfected, a final number of 816 quail eggs were randomly assigned into four groups (204 eggs per group), incubated in four homologous incubators (PTO- Italy) with continuous turning system, and fully digital programmable temperature and humidity. Incubation conditions for the control group (Ctrl) were 37.7°C and 55% relative humidity (RH) from embryonic day 0 (ED0) to ED17 (8). Three thermally treated egg groups: incubation temperature was increased to 41°C and 65% RH - intermittently (3 hours/day) during early embryogenesis (ED6-8) in the TM1 group and during late embryogenesis (ED12-14) in the TM2 group. The last group (TM3) was thermally treated in both time windows. Immediately after the thermal manipulation techniques were terminated, incubation conditions were restored to the standard conditions (37.7°C and 55% RH). During the incubation period, the eggs in all incubators were automatically turned through 270° every hour. The eggs were transferred to hatching trays on the 15th day of incubation and RH% was increased to 60-65%.

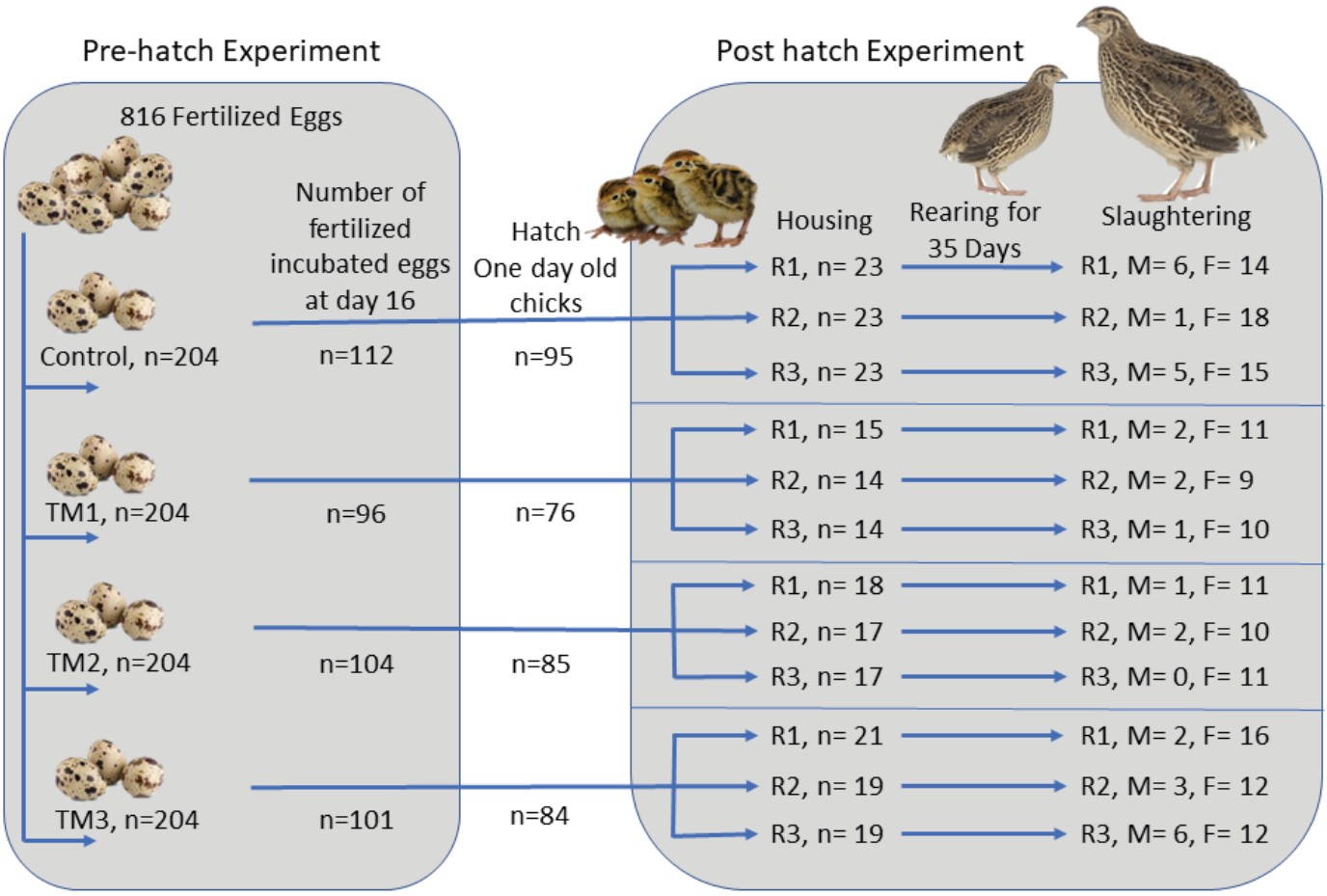

Figure 1: Experimental design for the post-hatch experiment. 12 pens were created from the total hatched chicks (R1,R2,R3; three replicate pens per group, M; Male, F; Female).

Housing and rearing

The chicks were randomly housed on a deep litter system in 12 separate pens (three replicate pens per group) under the same managemental conditions with ad libitum feeding and free access to water. The experimental design is shown in figure 1. The starting room temperature was 35°C in the first week of age and then decreased by 1.5 °C per week until the 5th week of age. Quail chicks were exposed to 23 h light and 1h darkness. During the first 20 days of age, quail chicks were fed with crumbled starter feed (Leader-Egypt ™) containing 3.000 kcal/kg metabolic energy and 23% crude protein. The grower feed (Leader-Egypt ™) containing 2.900 kcal/kg metabolic energy and 21% crude protein was introduced from day 20 till the end of the experiment.

Slaughtering and carcass traits

At 35 days old, after 4 hours of feed deprivation, three birds per replicate were weighed and slaughtered following the halal slaughter procedures according to ethical approval by the Institutional Animal Care and Use Committee (IACUC; Reference No. Vet CU16072020190). Weights of the carcass, abdominal fat, breast, breast muscle, and internal organs (heart, liver, spleen, gizzard, and intestine) were determined for each bird and expressed as a percentage of live body weight. The lengths of the intestines and caeca were measured and recorded. All measurements were taken immediately after slaughtering. Then the carcasses were chilled at 4 °C for 24 hours then examined.

Breast meat quality Parameters

Nine birds from each group (3 birds/replicate) were slaughtered and examined for breast meat quality parameters (proximate compositional analysis and Physico-chemical characteristics). Boneless breasts without skin on both sides of the sternum were separated.

Proximate composition analysis. The proximate chemical analysis was conducted for raw quail meat. Moisture, protein, fat, and ash contents of quail meat were determined for each group after the processing according to the method of the Association of Official Analytical Chemists (9). For determination of moisture contents (g/100g or %), 3 g of sample were dried at 100°C until a constant weight was obtained. Protein content (g% sample) was determined using the Kjeldahl method of analysis. For the conversion of nitrogen into crude protein, a factor of 6.25 was used. Fat (g/100g or %) was determined by 6-cycle extraction with petroleum ether in a Soxhlet apparatus and the weight loss was calculated. Ash was determined by ignition at 500 °C for 5 hours (g% sample).

Physico-chemical characteristics

Shear force. The quail meat was cooked in a convection oven (Heraeus, D-63450 Hanau, Germany). The oven was adjusted at 150 °C for an internal temperature of 75 °C (average cooking time 20 min). The cooking temperature was monitored by a needle thermocouple probe attached to a previously calibrated hand-held thermometer (Hanna HI 9850911; Pasadena, Texas, USA). The cooked meat was cooled to room temperature. Six core samples (each of 1.27 cm diameter) were collected parallel to the surface using a hand-held coring device. Each core sample was sheared once with a Warner-Bratzler shear force (WBSF) device attached to an Instron Universal Testing Machine (Model 2519 105; Instron Corp., Canton, Massachusetts, USA) with a 55-kg tension/compression load cell and a crosshead speed of 200 mm/min. The average shear force value was calculated and recorded for each sample (10).

Color evaluation. The surface color of freshly cut raw quail meat was measured using a Croma meter (Konica Minolta, model CR 410, Japan) calibrated with a white plate and light trap supplied by the manufacturer. The L (lightness), a (redness), and b (yellowness) values were obtained using Commission International de l'Eclairage (CIE) standard illuminant D65 light source. The color was expressed using CIE (11).

Cooking loss (CL%). The cooking was performed in a convection oven (Heraeus, D-63450 Hanau, Germany) adjusted at 150 °C for an internal temperature of 75 °C (average cooking time 20 min). Cooking loss was calculated as outlined by Neel et al. (12). Due to the small size of quail carcass, the whole dressed, eviscerated, and cleaned bird carcass (approximately 70.9 g) was cooked. To obtain more accurate results, the readings were taken from different locations of the cooked quail carcass so the reported results will be representative of the whole cooked quail sample. The meat samples were blotted with blotting paper and weighed accurately just before cooking. After cooking, the samples were cooled, wiped with blotting paper, and weighed immediately. The cooking loss as a percentage was determined as the difference in the weights of the sample before and after cooking.

$$CL\% = \frac{(W1-W2)}{W1} \times 100$$

pH value analysis. A meat/muscle homogenate was prepared from a 5 g sample and 20 mL of distilled water. Measurement of pH using a digital pH meter (Lovibond Senso Direct) previously calibrated with 7.0 and 4.0 buffers using a probe-type electrode (Senso Direct Type 330). Three pH readings for each replicate were recorded and the average was calculated according to Abdel-Naeem et al. (13).

Sensory analysis

Sensory analysis was carried out by panelists (25 experienced panelists were selected based on their previous

experience in consuming quail meat) from the members of the Food Hygiene and Control Department, Faculty of Veterinary medicine, Cairo University, Egypt. Different cooked quail samples were randomly coded, and the panelists were asked to score the samples using a five-point hedonic scale for tenderness (five denotes extremely tender and one denotes very tough), flavor (five denotes extremely strong flavor and one denotes extremely bland flavor) and juiciness (five denotes very juicy and one denotes very dry) according to the guidelines provided by the American Meat Science Association (14).

Statistical analyses

To compare carcass`s traits, weights of internal organs, and breast meat quality parameters among treatment groups, a one-way analysis of variance test (ANOVA) was used. Levene's test was used to evaluate the homogeneity of variances (homoscedasticity), and the Shapiro–Wilk test was utilized for normality analysis of the variables. The data that were not normally distributed or violated the homogeneity of variance assumption were analyzed with the Kruskal-Wallis test (Meat tenderness, flavor, and juiciness). Tukey's Studentized Range (HSD) test was used for post-hoc analysis. All P values less than 0.05 were considered statistically significant. Analyses were performed with SAS® version 9.4 (15). All data were presented as the mean ± standard error of the mean (SEM).

Results and Discussion

Carcass traits and internal organ weights

Analysis of the results revealed that the means final body weights of TM1 were numerically higher but there were no significant differences in final body weights among TM1, TM3, and control. Table 1 shows the effects of embryonic thermal manipulation on carcass traits and internal organs weight of 35-day-old Japanese quails. Thermal manipulation at both early and late embryogenesis (TM3) resulted in a significant reduction in the relative weights of carcass, breast, and breast muscle when compared to the control ($P < 0.05$). Abdominal fat weights in TM1 groups were significantly lower ($t(28) = 2.79$, $P = .0441$) than those in the control group.

Embryonic TM had no significant effect ($P > 0.05$) on the weights of the internal organs (liver, spleen, heart, and intestine) as well as the length of the intestine and caeca. Regardless of treatments, the relative weight of the heart is significantly larger ($t(28) = 3.03$, $P = 0.0052$) in males (0.92 ± 0.02 g) than in females (0.84 ± 0.01 g).

Table 1: Influence of embryonic thermal manipulation on carcass traits and weights of internal organs of 35-day-old meat-type Japanese quails[1]

Parameters[3]	Treatments[2]				Comparisons	
	Ctrl	TM1	TM2	TM3	F-statistics (df_1, df_2)	P value
Live Body weight (g)	197.89 ± 6.52^{a}	205.61 ± 4.56^{a}	175.80 ± 6.06^{b}	192.33 ± 7.63^{ab}	5.09 (3, 171)	.0021
Carcass weight % (Without blood, feather, Head, and shank)	85.28 ± 0.63^{a}	83.99 ± 0.42^{a}	83.36 ± 0.82^{ab}	81.08 ± 0.44^{b}	6.88 (3, 28)	.0013
Carcass weight % (Without viscera)	72.00 ± 0.35^{a}	71.52 ± 0.36^{ab}	70.71 ± 0.32^{ab}	69.48 ± 0.87^{b}	4.15 (3, 28)	0.0149
Breast weight %	35.90 ± 0.54^{a}	35.81 ± 0.20^{ab}	34.87 ± 0.42^{ab}	34.12 ± 0.83^{b}	3.64 (3, 28)	0.0248
Breast muscle weight %	20.54 ± 0.22^{ab}	21.80 ± 0.42^{a}	20.01 ± 0.61^{b}	19.56 ± 0.45^{b}	6.15 (3, 28)	0.0024
Abdominal fat weight %	1.81 ± 0.18^{a}	1.10 ± 0.09^{b}	1.21 ± 0.16^{ab}	1.22 ± 0.25^{ab}	3.09 (3, 28)	0.0429
Heart weight %	0.87 ± 0.03	0.89 ± 0.02	0.86 ± 0.03	0.85 ± 0.02	0.51 (3, 28)	0.6776
Spleen weight %	0.06 ± 0.00	0.07 ± 0.01	0.07 ± 0.01	0.07 ± 0.01	0.56 (3, 28)	0.6450
Liver weight %	2.02 ± 0.12	2.44 ± 0.12	2.30 ± 0.18	2.05 ± 0.18	1.34 (3, 28)	0.2821
Intestine weight %	4.12 ± 0.30	4.30 ± 0.10	4.55 ± 0.25	4.30 ± 0.21	0.51 (3, 28)	0.6783
Gizzard weight %	2.09 ± 0.08^{ab}	2.26 ± 0.11^{a}	2.30 ± 0.06^{a}	1.84 ± 0.05^{b}	6.89 (3, 28)	0.0013
Intestine length (cm)	60.33 ± 2.22	62.78 ± 2.36	58.67 ± 2.30	58.67 ± 2.22	0.46 (3, 28)	0.7138
Length of ceca (cm)	7.67 ± 0.36	8.33 ± 0.29	7.89 ± 0.27	8.06 ± 0.26	0.89 (3, 28)	0.4604

[1]All data are presented as the mean ± standard error of the mean (SEM). Within the same row, means followed by different superscript letters are significantly different at $P < 0.05$. [2]Treatments (Ctrl: control, TM1: early embryogenesis, TM2: late embryogenesis, TM3: early/late embryogenesis). [3]The relative weights of carcass, breast, muscles, abdominal fat, and internal organs were expressed as a percentage of live body weight.

Earlier studies revealed varied and sometimes contradictory results, Collin et al. (16) reported that no effects of thermal manipulation on gross weight were detected during the entire growth period, however, breast yield was higher in late-term TM chickens than in controls at 43 days old. Al-Zghoul and El-Bahr (17) reported that chicken embryo TM induced a significant increase in broiler carcass weight, breast muscle weight, and breast weight/carcass weight percentage if compared with control at post-hatch days 28 and 35. We suggest that the difference in body weight between the TM chicks and the control disappeared after day 35 of age due to the phenomenon of compensatory growth in broilers (18, 19). It is also worth considering the method of measuring and recording temperatures when comparing the results of thermal treatments. It has previously been shown that there can be a significant difference between incubator air temperature and eggshell temperature (EST) (20). Previous studies in quail and chicken revealed that TM chicks had a larger relative breast muscle weight (4, 5, 7, and 19). These results are attributable to a higher percentage of larger diameter (hypertrophy) muscle fibers than the control group (7, 19).

Our results indicated that the relative weight of the abdominal fat pad was markedly decreased in the early-term TM1 group. We suggest that early TM in quail embryos may interfere with adipocyte development and reduce the fat pad in the long term as suggested by Hammond et al. (21) in broiler chicken embryo TM. The reduction of the abdominal fat pad relative weight is one of the aims of broiler management, and TM had been identified as an effective way to decrease abdominal fat accumulation (4, 19).

Concerning liver weight, our results disagree with Al-Zghoul and El-Bahr (17) who reported that embryonic TM caused a significant increase in liver weight of broiler chickens when compared to control chicks on post-hatch day 35. Massimino et al. (22) documented that embryonic TM in mule ducks resulted in the heavier liver (foie grass production). These significant increases in the liver weight in both species were obtained after long thermal treatment which extends to more than 16 hours/day, so the duration of thermal manipulation is one of the major aspects that should be taken into consideration. The increased liver weight in the TM chicken and duck may be attributed to the increase in glycogen or fat accumulation in the liver (liver steatosis). Our findings agree with Al-Zghoul and El-Bahr (17) who illustrated that broiler embryo TM caused no changes in the spleen, intestine weights as well as intestine and cecum lengths in all TM groups compared to controls.

Breast meat quality

The Physico-chemical characteristics of breast meat are illustrated in Table 2.

The pH values of all TM treatments revealed significant ($P < 0.05$) decreases in comparison with that of the control. The pH value is considered one of the shelf life-determining factors and lower pH values "more acidic" means longer product shelf life (23).

Table 2: Influence of embryonic thermal manipulation on breast meat quality parameters of Japanese quails at 35-day-old[1]

Parameters[3]	Treatments[2]				Comparisons	
	Ctrl	TM1	TM2	TM3	Test statistics	P value
Moisture %	72.30 ± 0.13	72.26 ± 0.16	72.94 ± 0.43	72.39 ± 0.10	$F_{3,8} = 1.88$	0.2118
Fat %	2.37 ± 0.22	2.73 ± 0.04	2.51 ± 0.25	2.98 ± 0.21	$F_{3,8} = 1.86$	0.2141
Protein %	23.30 ± 0.53	23.38 ± 0.18	22.88 ± 1.04	22.99 ± 0.45	$F_{3,8} = 0.14$	0.9311
Ash %	1.46 ± 0.03	1.57± 0.05	1.50 ± 0.05	1.53 ± 0.06	$F_{3,8} = 1.07$	0.4155
pH	6.17 ± 0.09[a]	5.80 ± 0.06[b]	5.77 ± 0.03[b]	5.90 ± 0.00[b]	$F_{3,8} = 10.76$	0.0035
Cooking loss %	23.12 ± 0.49	22.81 ± 0.17	22.65 ± 0.51	23.66 ± 0.46	$F_{3,8} = 0.26$	0.8521
Shear force (N)	1.68 ± 0.07	1.76 ± 0.03	1.77 ± 0.04	1.80 ± 0.07	$F_{3,8} = 0.74$	0.5551
L (Lightness)	41.32 ± 1.04	42.67 ± 0.42	42.45 ± 0.53	43.96 ± 0.36	$F_{3,8} = 2.85$	0.1052
a (Redness)	13.33 ± 0.70	12.94 ± 0.08	13.66 ± 0.59	12.14 ± 0.30	$F_{3,8} = 1.81$	0.2225
B (Yellowness)	3.32 ± 0.86	3.46 ± 0.19	4.49 ± 0.19	4.27 ± 0.32	$F_{3,8} = 2.08$	0.1820
Tenderness	4.00 ± 0.00	4.00 ± 0.21	4.00 ± 0.11	4.00 ± 0.08	$x^2(3) < 0.001$	> 0.999
Flavor	5.00 ± 0.00	5.00 ± 0.00	5.00 ± 0.00	5.00 ± 0.00	$x^2(3) < 0.001$	> 0.999
Juiciness	4.00 ± 0.00	4.00 ± 0.00	4.00 ± 0.00	4.00 ± 0.00	$x^2(3) < 0.001$	> 0.999

[1]All data are presented as the mean ± standard error of the mean (SEM). Within the same row, means followed by different superscript letters are significantly different at $P < 0.05$. [2]Treatments (Ctrl: control, TM1: early embryogenesis, TM2: late embryogenesis, TM3: early/late embryogenesis).

Meat composition (fat%, protein %, ash %, moisture %) and sensory quality (cooking loss %, juiciness, flavor, tenderness) showed no significant differences among treatments. Our results are in agreement with Loyau et al. (5) and Collin et al. (16) who revealed that the embryonic TM favored breast muscle growth without significant alterations in breast meat characteristics. The cooking loss, moisture %, and fat % represent important parameters that reflect the quality of processed meat and are important for the juiciness and mouth feel of cooked meat. The current study revealed no significant difference between the control and TM groups in the sensory examination of breast meat, which could explain why TM did not alter the sensory criteria.

Importantly for the poultry industry, embryonic TM modifies the physiology and body composition of broilers without negatively affecting the processing quality of breast meat at slaughter age. For instance, TM chickens were 1.4% lighter and had 8% less relative abdominal fat pad than controls while consistently having larger myofiber and 4.6% heavier relative breast muscle at 35 days compared to the controls (24). Loyau et al. (5) also reported that breast muscle yield was enhanced by TM, especially in females, without significant change in breast meat characteristics (pH, color, drip loss). These studies highlight the possibility that embryonic TM can promote breast muscle yield without lowering the quality of the muscle.

Conclusions

The quail early embryonic TM is an effective protocol in decreasing fat pad accumulation and pH value of breast meat without any negative effects on breast meat composition or sensory criteria. Intermittent early embryonic TM could be used to reach the favored lucrative effects of the thermal treatment in quail broilers.

Acknowledgments

This work was supported by the general scientific research department of Cairo University, Egypt.

The authors declare no conflicts of interest.

References

1. Ozcelik M, Ozbey O. The effect of the high environmental temperature on some blood parameters and the laying performance of Japanese quails with different body weights. Arch Anim Breed 2004; 47: 93–8. doi:10.5194/AAB-47-93-2004

2. Seker I, Kul S, Bayraktar M. Effects of storage period and egg weight of Japanese quail eggs on hatching results. Arch Anim Breed 2005; 48: 518–26. doi:10.5194/AAB-48-518-2005

3. Yalcin S, Siegel P. Exposure to cold or heat during incubation on developmental stability of broiler embryos. Poult Sci 2003; 82: 1388–92. doi:10.1093/ps/82.9.1388.

4. Piestun Y, Halevy O, Shinder D, Ruzal M, Druyan S, Yahav S. Thermal manipulations during broiler embryogenesis improves post-hatch performance under hot conditions. J Therm Biol 2001; 36: 469–74. doi:10.1016/j.jtherbio.2011.08.003

5. Loyau T, Berri C, Bedrani L, et al. Thermal manipulation of the embryo modifies the physiology and body composition of broiler chickens reared in floor pens without affecting breast meat processing quality. J Anim Sci 2013; 91: 3674–85. doi:10.2527/jas.2013-6445

6. Alkan S, Karslı T, Karabağ K, Galic A, Balcıoğlu M. The effects of thermal manipulation during early and late embryogenesis on hatchability, hatching weight and body weight in Japanese quails (Coturnix japonica). Arc Tierz 2013; 18: 789–96.

7. El-Shater S, Rizk H, Abdelrahman H, Awad M,Khalifa E,K. Khalil K. Embryonic thermal manipulation of Japanese quail: effects on embryonic development, hatchability, and post-hatch performance. Trop Anim Health Prod 2021; e263. doi: 10.1007/s11250-021-02726-y

8. Alkan S, Narinç D, Karslı T, Karabag K, Balcıoglu M. Effects of thermal manipulations during early and late embryogenesis on growth characteristics in Japanese quails (Coturnix japonica). Eur Poult Sci 2012; 76: 184–90.

9. AOAC. Association of Official Analytical Chemists International. Official Methods of Analysis, 21st ed. Arlington, Virginia,U.S.A., 2019.

10. Shackelford S, Wheeler T, Koohmaraie M. Evaluation of sampling, cookery, and shear force protocols for objective evaluation of lamb longissimus tenderness. J Anim Sci 2004; 82: 802–7. doi:10.2527/2004.823802X

11. Shin H, Choi Y, Kim H, Ryu Y, Lee S, Kim B. Tenderization and fragmentation of myofibrillar proteins in bovine longissimus dorsi muscle using proteolytic extract from Sarcodon aspratus. LWT-Food Sci Tech 2008; 41: 1389–95. doi:10.1016/j.lwt.2007.08.019

12. Neel S, Reagan J, Mabry J. Effects of rapid chilling and accelerated processing on the physical and sensory characteristics of fresh pork loins. J Anim Sci 1987; 64: 765–73. doi:10.2527/jas1987.643765x

13. Abdel-Naeem H, Sallam K, Zaki H. Effect of different cooking methods of rabbit meat on topographical changes, physicochemical characteristics, fatty acids profile, microbial quality and sensory attributes. Meat Sci 2021; 181: e108612. doi:10.1016/j.meatsci.2021.108612

14. AMSA. American Meat Science Association (AMSA) & National Livestock and Meat Board. Research guidelines for cookery, sensory evaluation, and instrumental tenderness measurements of fresh meat. Chicago, IL, U.S.A., 1995.

15. SAS Institute. Statistical user's guide' statistical analysis system. INT., Cary, NC. U.S.A., 2014.

16. Collin A, Berri C, Tesseraud S, et al. Effects of thermal manipulation during early and late embryogenesis on thermotolerance and breast muscle characteristics in broiler chickens. Poult Sci 2007; 86: 795–800. doi:10.1093/ps/86.5.795

17. Al-Zghoul M, El-Bahr S. Thermal manipulation of the broilers embryos: expression of muscle markers genes and weights of body and internal organs during embryonic and post-hatch days. BMC Vet Res 2019; 15: e166. doi:10.1186/s12917-019-1917-6

18. Zubair A, Leeson S. Compensatory growth in the broiler chicken: a review. Worlds Poult Sci J 1996; 52: 189-201. doi:10.1079/WPS19960015

19. Piestun Y, Yahav S, Halevy O. "Thermal manipulation during embryogenesis affects myoblast proliferation and skeletal muscle growth in meat-type chickens. Poult Sci 2015; 94: 2528–36. doi:10.3382/ps/pev245

20. Lourens A, Van Den Brand H, Meijerhof R, Kemp B. Effect of eggshell temperature during incubation on embryo development, hatchability, and posthatch development. Poult Sci 2005; 84: 914–20. doi: 10.1093/ps/84.6.914

21. Hammond C, Simbi B, Stickland N. In ovo temperature manipulation influences embryonic motility and growth of limb tissues in the chick (Gallus gallus). J Exp Biol 2007; 210: 2667–75. doi: 10.1242/jeb.005751

22. Massimino W, Bernadet M, Pioche T, et al. Positive impact of thermal manipulation during embryogenesis on foie gras production in mule ducks. Front Physiol 2019; 10: e1495. doi: 10.3389/fphys.2019.01495

23. Wapi C, Nkukwana T, Hoffman L, et al. Physico-chemical shelf-life indicators of meat from broilers given Moringa oleifera leaf meal. S Afr J Anim Sci 2013; 43: S43–7. doi: 10.4314/sajas.v43i5.8

24. Piestun Y, Halevy O, Shinder D, Ruzal M, Druyan S, Yahav S. Thermal manipulations during broiler embryogenesis improves post-hatch performance under hot conditions. J Therm Biol 2011; 36: 469–74. doi:10.1016/j.jtherbio.2011.08.003

Učinki toplotne manipulacije zarodkov japonskih prepelic na lastnosti trupa po izvalitvi, težo notranjih organov in kakovost prsnega mesa

S. N. El-Shater, K. M. Khalil, H. Rizk, H. M.B.A. Zaki, H. A. Abdelrahman, H. H. Abozeid, E. F. Khalifa

Izvleček: Toplotna manipulacija zarodka različnih vrst ptic je znana kot učinkovit protokol za izboljšanje rasti po izvalitvi in pridobivanje odpornosti na povišano temperaturo. Predhodno smo ocenili vpliv embrionalne toplotne manipulacije zarodkov japonskih prepelic na embrionalni razvoj, valilnost in uspešnost po izvalitvi. V tej študiji smo natančneje pojasnili učinke toplotne manipulacije zarodkov japonskih prepelic na težo notranjih organov, lastnosti trupa in parametre kakovosti mesa na 35. dan po izvalitvi. Jajca prepelic kontrolne skupine so bila inkubirana pri 37,7 °C in 55-odstotni relativni vlažnosti. Tri preiskovane skupine prepeličjih jajc so bile občasno izpostavljene temperaturi 41 °C in relativni vlagi 65 % (3 ure/dan): zgodnja embrionalna skupina (TM1) je bila izpostavljena toploti 6.– 8. embrionalni dan (ED), pozna embrionalna skupina (TM2) 12.–14. ED, zgodnja/pozna embrionalna skupina (TM3) pa v obeh časovnih intervalih. Parametre kakovosti mesa prepelic, lastnosti trupa in težo notranjih organov smo ocenili na 35. dan po izvalitvi. Rezultati so pokazali, da je toplotna manipulacija v zgodnjem embrionalnem obdobju (skupina TM1) učinkovit protokol za zmanjšanje kopičenja maščobnih blazinic. Vrednost pH prsnega mesa pri vseh toplotno manipuliranih skupinah se je znatno ($P < 0,05$) znižala za 5 % v primerjavi s kontrolno skupino, brez negativnih učinkov na sestavo prsnega mesa ali senzorične kriterije. Zgodnjo embrionalno toplotno manipulacijo bi bilo priporočljivo uporabiti kot izboljšan protokol, s katerim bi bilo mogoče doseči prednostne donosne učinke pri mesnih prepelicah.

Ključne besede: *Coturnix japonica*; mesna prepelica; lastnosti prsnega mesa; toplotna biologija

DOI 10.26873/SVR-1672-2023
UDC 599.32:61.341:577.352.4:620.3
Pages: 75–93

Original Research Article

Pathomorphological Changes in the Duodenum of Rats in Case of Subchronic Peroral Administration of Gadolinium Orthovanadate Nanoparticles Against the Background of Food Stress

Key words

rare earth metals;
gadolinium orthovanadate nanoparticles;
pathomorphological changes, duodenum;
white rats;
feed stress

Alla Masliuk[1], Olena Lozhkina[2], Oleksandr Orobchenko[1]*, Volodymyr Klochkov[3], Svitlana Yefimova[3], Nataliya Kavok[3]

[1]Laboratory for toxicological monitoring, National Scientific Center Institute of Experimental and Clinical Veterinary Medicine, Pushkinska St., 83, 61023, Kharkiv, [2]Research pathomorphology department, State Scientific Research Institute of Laboratory Diagnostics and Veterinary and Sanitary Expertise, Donetska St., 30, 03151, Kyiv, [3]Nanostructured materials department, Institute for Scintillation Materials National Academy of Sciences of Ukraine, Nauky Ave., 60, 61072, Kharkiv, Ukraine

***Corresponding author:** toxy-lab@ukr.net

Abstract: In our research, we were interested in the actual presence of adaptive or negative reactions in the wall of the small intestine of white rats under the influence of gadolinium orthovanadate nanoparticles in the range of doses (≈0.03-0.3 mg/kg of body weight) under conditions of food stress (due to an excess of fiber and lack of protein in the diet) and their degree of manifestation, since this type of ration disproportion occurs quite often in Ukraine. Nanoparticles of gadolinium orthovanadate have a significant potential for use in animal husbandry and poultry farming, as in the range of doses of 0.03-0.15 mg/kg of body weight, they prevent negative effects on the intestinal mucosa, even in conditions of feed stress. It has been established that administration of gadolinium orthovanadate nanoparticles in doses of 0.03 and 0.15 mg/kg of body weight to white rats with drinking water for 56 and 28 days, respectively, leads to activation of the mechanical and immunological barrier of the mucous membrane, as indicated by an increase goblet cells, hyperplasia of enterocytes of some crypts, thickening of villi and infiltration by lymphocytes of the own plate, which reach the control level 14 days after stopping their administration. However, increasing the dose of gadolinium orthovanadate nanoparticles to 0.3 mg/kg of body weight in conditions of food stress leads to the depletion of the adaptive capabilities of the intestinal mucosa and excessive activation of the immunological barrier, which were manifested by dystrophic changes from the 14th day of administration, which deepened to the 56th day and do not level off after 14 days after stopping administration.

Received: 11 July 2022
Accepted: 6 February 2023

Introduction

Rare earth metals (rare earth elements, REM) are a group of 17 elements that includes Lanthanum, Scandium, Yttrium, Gadolinium and lanthanides. All these elements are silvery-white metals, and they all have similar chemical properties (the most characteristic oxidation state is +3). The name "rare earth elements" was historically formed at the end of the 18th – beginning of the 19th century, when it was mistakenly believed that the mineral-containing elements of two

subfamilies: cerium (light – Sc, La, Ce, Pr, Nd, Pm, Sm, Eu) and yttrium (heavy – Y, Gd, Tb, Dy, Ho, Er, Tm, Yb, Lu) are rarely found in the Earth's crust (1, 2, 3).

Currently, elements of the yttrium subgroup are used for the production of nanoparticles with good biocompatibility. These are, for example, nanoparticles based on Gd (such as gadolinium orthovanadate), which can be modified with Eu, Lu, Dy (to obtain fluorescent radiation, which is useful for the latest methods of magnetic resonance imaging), as well as a shell of silica to increase biocompatibility or various ligands for targeted delivery of nanoparticles (4, 5, 6).

Nanoparticles of gadolinium orthovanadate exhibit enzyme-like properties: inhibition of superoxide anion formation (similar to the action of superoxide dismutase) and acceleration of decomposition of hydrogen peroxide (similar to the action of catalase) were observed in aqueous solutions (7). The antioxidant properties of gadolinium orthovanadate nanoparticles were also observed during X-ray irradiation of aqueous solutions, despite the fact that the nanoparticles absorb the soft X-ray used in the experiment. In aqueous solutions, in the presence of nanoparticles, a decrease in the concentration of hydroxyl radicals was found as the main product of water radiolysis (8), and therefore, $GdVO_4:Eu^{3+}$ nanoparticles have radioprotective properties.

Significant progress in the study of this type of nanoparticles has been achieved in reproductive science. It was established that NP $GdVO_4:Eu^{3+}$ is a practically non-toxic compound (LD_{50} per os is more than 5000.0 mg/kg), and their effect, including on spermatogenesis, depends on the clinical condition of the animals, dose and duration of administration. Thus, in 6-month-old intact rats, when NP was used for 30 days in doses of 0.03, 0.3 and 3.0 mg/kg, only the proportion of pathological forms of spermatozoa increased statistically in the spermogram. After receiving 70 days of NP $GdVO_4:Eu^{3+}$ in minimum or maximum doses, no significant effect on spermatogenesis of intact rats was detected. The use of gadolinium orthovanadate NPs at a dose of 0.3 mg/kg led to a statistically significant decrease in the total concentration of sperm (by 47%), the concentration of morphologically normal gametes (by 50%), their motility (by 35%) and an increase in the percentage of pathological forms (by 50%) compared to the indicators of the control group. Whereas, in 10-month-old male rats with model hypofertility (in whose spermogram there is a lower total sperm concentration, a concentration of morphologically normal gametes and reduced fertility), administration of NP $GdVO_4:Eu^{3+}$ at a dose of 0.3 mg/kg for 70 days normalized all the studied spermogram indicators excluding cell motility, which decreased, and contributed to the normalization of fertility (9, 10, 11, 12, 13).

Due to a good bioavailability and antioxidant properties, one of the promising areas of application of REM nanoparticles is their use in agriculture, in particular, in poultry farming, since cerium dioxide nanoparticles have been proven to have a positive effect on the body of poultry through the intensification of egg production, their mass, and the fertilization of hatching eggs, and antioxidant action (14, 15, 16).

The assimilation and positive effect of minerals (including rare earth elements) depends on the quality of the diet: for example, fiber and some related substances have a strong ability to bind minerals or form complexes, so there is a suspicion that fiber impairs the assimilation of minerals (17). With an optimal amount of protein in the diet, protein components – amino acids and oligopeptides facilitate the absorption of trace elements, which confirms the greater availability of organic forms of trace elements (18, 19).

Disproportions of nutrients in feed can lead to so-called "feed stress" (by the way, this fact was described almost 65 years ago (20). Feed stress has a negative effect on the animal body (21), in particular, the first the digestive tract suffers (22). Along with this (23), a therapeutic dose of $GdVO_4:Eu^{3+}$ nanoparticles was established for induced mild intestinal inflammation – 0.02 mg/kg of body weight: administration of nanoparticles improved the morphology of small intestine, reduced the rate of infiltration of immune cells without affecting the intensity of apoptosis.

Studying the impact of stress on the poultry organism, three main stages were identified, which to some extent coincide with the stages of stress in the animal body according to H. Selye: the stage of stress detection (short-term stress regulation), the stage of development of resistance to stress and adaptation, the stage of exhaustion and the appearance of negative consequences (24, 25). In our research, we were interested in the actual presence of adaptive or negative reactions in the wall of the small intestine of white rats under the influence of $GdVO_4:Eu^{3+}$ nanoparticles in the range of doses (≈0.03-0.3 mg/kg of body weight) under conditions of food stress (due to an excess of fiber and lack of protein in the diet) and their degree of manifestation, since this type of ration disproportion occurs quite often in Ukraine (26, 27).

Therefore, the work aimed to determine the pathomorphological changes in the duodenum of rats in case ofsubchronic oral administration of gadolinium orthovanadate nanoparticles against the background of food stress.

Materials and methods

The experiments have been conducted in the laboratory for toxicological monitoring of the National Scientific Center "Institute of Experimental and Clinical Veterinary Medicine"

(NSC "IECVM"), Kharkiv, Ukraine, and the research pathomorphology department of the State Scientific Research Institute of Laboratory Diagnostics and Veterinary and Sanitary Expertise (SSRILDVSE) Kyiv, Ukraine.

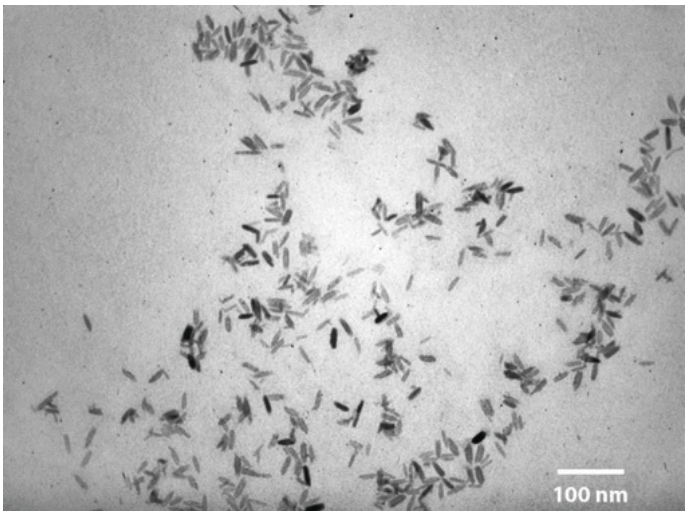

Figure 1: Photograph (transmission electron microscopy) of NP $GdVO_4:Eu^{3+}$ nanoparticles (30)

Experimental samples of gadolinium orthovanadate nanoparticles (NP $GdVO_4:Eu^{3+}$) (spindle-like geometry, size 8×25 nm) (Fig. 1) with an initial concentration of 1.0 g/dm^3 were used in the work.

Experimental samples of nanoparticles were synthesized and standardized by stability and size in the department of nanostructured materials named after Yu.V. Malyukin of the Institute of Scintillation Materials of the National Academy of Sciences of Ukraine (28, 29).

Experiments on rats were conducted in the vivarium of the National Scientific Center "IECVM", 140 sexually mature male *Wistar* rats with an initial weight of 180.0-200.0 g were used as the object of research. Four groups of animals with 28 rats in each group were formed by the principle of analogs.

During the experiment, animals of the control group received drinking water without additives, rats of the first experimental group received a solution of gadolinium orthovanadate nanoparticles 0.2 mg/dm^3 (≈0.03 mg/kg of body weight); experimental group II – 1.0 mg/dm^3 (≈0.15 mg/kg body weight), and experimental group III – 2.0 mg/dm^3 (≈0.3 mg/kg body weight). Rats had received water or water with additives for 56 days, then the rats had been observed for another 14 days. Laboratory animals had free access to water and food.

A granulated grain mixture (with a disproportional content of nutrients) was used as a monofeed for rats to create food stress (Table 1). The content of nutrients in the diet was determined by the following normative documents.

Determination of crude protein content was carried out following the Kjeldahl method in accordance with DSTU ISO 5983:2003, crude fiber – in accordance with DSTU ISO 6865:2004, crude fat – in accordance with DSTU ISO 6492:2003, Calcium – in accordance with DSTU ISO 6490-1: 2004, Phosphorus – according to DSTU ISO 6491:2004. The content of vitamins – in accordance with DSTU 4687:2006, trace elements – in accordance with DSTU EN 14082:2019. The results of the experiment are summarized in Table 1.

Before the administration of nanoparticles, the rats were kept on the above diet for 14 days. An indicator of the presence of food stress was considered to be the failure of all groups of rats to gain conditioned mass during the experiment.

During the experiment, the clinical condition of animals of all groups was observed: attention was paid to behavior, reaction to external stimuli, presence of appetite, skin condition, color of mucous membranes, frequency of breathing

Table 1: Qualitative composition of the diet of rats (granulated grain mixture)

Indicator	Value	Norm *	± to the norm
Carbohydrates, g/100 g	64,57	59,30	+ 5,27
Energy value, MJ	14,07	14,00	+ 0,07
Mass fraction of fat, %	3,12	4,40	– 1,28
Mass fraction of crude protein, %	12,50	19,60	– 7,1
Mass fraction of crude fiber, %	11,90	4,60	+ 7,3
Vitamin B_2, mg/kg	14,00	30,00	– 16,0
Vitamin A, IU/kg	4400,00	10000,0	– 5600,0
Vitamin E, mg/kg	137,50	100,00	+ 37,5
Selenium, mg/kg	0,46	0,10	+ 0,36
Copper, mg/kg	5,39	16,00	– 10,61
Zinc, mg/kg	42,26	60,00	– 17,74

Note * According to (Diet Meat Free Rat and Mouse Diet (SF00-100)) (31)

Table 2: Algorithm of tissue processing in the machine for histological processing of tissues of the carousel-type STP – 120

The name of the reagent	Concentration, %	Processing time, min.	Temperature, °C
Formalin	10, neutral	60	20-25
Tap water	-	60	20-25
Ethanol	70	90	20-25
Ethanol	80	90	20-25
Ethanol	90	90	20-25
Ethanol	96	60	20-25
Ethanol	96	60	20-25
Ethanol	96	60	20-25
Xylene	-	90	20-25
Xylene	-	90	20-25
Histological paraffin	-	120	62
Histological paraffin	-	120	62

Table 3: Algorithm of deparaffinization and staining of sections in a linear tissue staining machine

Reagent name	Concentration, %	Processing time, min.
Xylene	-	5
Xylene	-	5
Ethanol	96	5
Ethanol	96	5
Tap water	-	5
Hematoxylin	-	10
Tap water	-	5
Alcoholic eosin	0,3	1
Tap water	-	5
Ethanol	70	5
Ethanol	96	5
Ethanol	96	5
Carbol-xylene	3:1	5
Xylene	-	5

and defecation, changes in color and consistency of feces, etc. (32). 14, 28, 42 and 56 days after the start of the administration of nanoparticle solutions and 14 days after its termination, using CO_2 anesthesia 7 rats from each group were decapitated and samples of the small intestine (segment of the duodenum) were taken for histomorphological studies.

Experiments were conducted on the basis of specialized laboratories of the National Scientific Center "Institute of Experimental and Clinical Veterinary Medicine" (protocol № 321). The research program was reviewed and approved by the Bioethics Commission of the National Scientific Center "Institute of Experimental and Clinical Veterinary Medicine" in the current order. Animal experiments do not contradict the current legislation of EU (Directive 2010/63/EU of the European Parliament and of the Council on the protection of animals used for scientific purposes, 22 September 2010).

Histomorphological studies were carried out following generally accepted methods in the research pathomorphological department of the SSRILDVSE.

Fixation and cutting of pieces of patmaterial

Pieces were cut from different parts of the organ. In the presence of visible pathomorphological changes in the organs (tissues), pieces were cut on the border of the area with visible pathomorphological changes and without visible changes.

To preserve the tissue and cellular structure, pieces of organs were fixed. For this, a 10% aqueous solution of neutral formalin was used, the volume of which should be (20-40) times greater than the volume of the sampled material. Laboratory ware was tightly closed and left in a fume cupboard at room temperature. After a day, the fixing liquid was changed. After (5-7) days, pieces (2-3) mm thick were cut through the entire thickness of the organ (tissue) and placed in plastic cassettes. The latter were labeled and placed in a fixing liquid (10% aqueous solution of neutral formalin) for another day.

The rest of the organs (tissues) were packed, labeled (indicating the number of the work protocol, the date of receipt of the sample) and stored in a 10% formalin solution until the results of the research were obtained.

The algorithm for histological processing of the selected samples is given in Table 2.

Formation of paraffin blocks

Paraffin blocks were formed using a paraffin pouring station, using special molds and cassettes. The forms were transferred to the filling platform of the dosing unit, the piece was placed in the desired position with tweezers, covered with a cassette and filled with paraffin. The form was transferred to a cooling platform until the paraffin solidifies completely. The formed paraffin block was removed.

Microtoming

Before microtoming, slides were prepared. They were degreased in a mixture of equal volumes of ethanol and ether, followed by flaming in the flame of spirit lamp.

Table 4: Algorithm for Van-Gieson staining of sections

Reagent name	Concentration, %	Processing time, min.
Xylene	-	5
Xylene	-	5
Ethanol	96	5
Ethanol	96	5
Tap water	-	5
Weigert hematoxylin	-	3-5
Tap water	-	5
Tap water	-	5
Picrofuchsin	10:1	2-3
Tap water	-	10-15 сек.
Ethanol	96	2-3
Ethanol	96	2-3
Carbol-xylene	3:1	5
Xylene	-	5

The glass was marked, indicating the number of the work protocol, the date of receipt of the samples and the index of the piece.

Sections with a thickness of (5-7) μm were made using a rotary microtome, a section transfer system and a water bath.

The obtained sections were smoothed out on the surface of water (temperature +45 °C), then they were transferred to a prepared glass slide and left to dry overnight.

Hematoxylin and eosin staining of preparations

Directly before staining, paraffin was removed from the sections pasted on the glass. Deparaffinization was performed with a paraffin solvent (xylene, an organic solvent). To remove solvent residues, the sections were transferred to alcohol, after which they were ready for staining (the procedure was carried out in the HMS 70 staining apparatus, which is installed in the fume hood). The program is designed for 1 hour 10 min (Table 3).

Differential staining was also used in the work (Table 4).

Administration of histopreparations

The stained section was placed in the final medium, covered with a cover glass and left to dry overnight.

Light microscopy of drugs

Stained preparations were examined under a light microscope at low (ob. ×5, 10, 20) and high (ob. ×40) magnification using an Axioskop 40 microscope ("Carl Zeiss", Germany) and software for making photos.

Statistical analysis

The results were processed by variation statistics using the analysis of variance software package (ANOVA) StatPlus 5 (6.7.0.3) (AnalystSoft Inc., USA). The reliability of the obtained results was evaluated by Tukey's test (HSD mean difference) at a reliability level of 95.0% ($p < 0.05$).

Results

Clinical observations of the rats of both the control and experimental groups I and II showed that the general condition of the animal bodies during the 56-day administration of gadolinium orthovanadate nanoparticles was satisfactory: the rats were mobile and responded adequately to external stimuli.

No violations of appetite, breathing, urination, defecation and appearance (fur was shiny, smooth, clean) were observed in rats. While after the administration of gadolinium orthovanadate nanoparticles at a dose of 2.0 mg/dm^3, starting from the 28th day of administration, a decrease in the body weight of animals was observed, on the 42nd and 56th days along with this a violation of defecation was noted – the dilution of feces in 71.4 and 23.8% of animals, respectively, the rats were not active enough, the fur was dull and disheveled, and on the 14th day after the cessation of the administration of nanoparticles, the weight of the rats did not differ from the control, the appearance also came to the level of the control group. It should be noted that no animal deaths were recorded during the entire observation period in all experimental groups.

Fig. 2 shows the dynamics of the post-slaughter weight of rats during the experiment. Thus, in case of the administration of gadolinium orthovanadate nanoparticles at a dose of 0.2 mg/dm^3 of drinking water during the entire experiment, no reliable deviations of the post- slaughter weight of rats from the control group were observed. In case of administration of nanoparticles at a dose of 1.0 mg/dm^3 of drinking water from the 14th to the 56th day, no changes were noted in the post- slaughter weight of rats, while after stopping the administration of gadolinium orthovanadate nanoparticles, the post-slaughter weight of rats exceeded the control by 7.4% ($p<0.05$).

Dynamics of the post-slaughter weight of rats in the experimental group III that received gadolinium orthovanadate nanoparticles at a dose of 2.0 mg/dm^3 of drinking water was as follows: on the 14th day, no changes were noted in the post-slaughter weight of rats from the control, on the

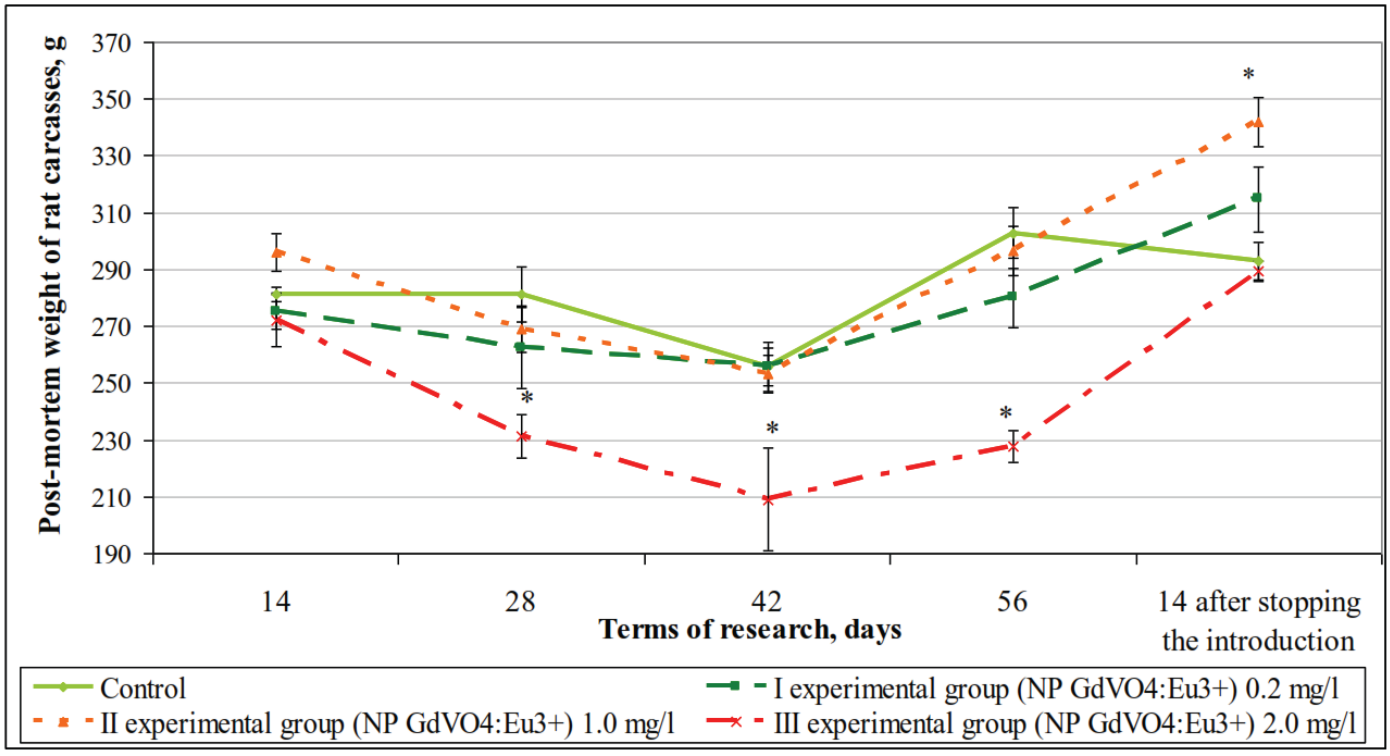

Figure 2: Dynamics of the post-slaughter weight of rats under conditions of administration of different doses of gadolinium orthovanadate nanoparticles with water (M±m, n=7, *– p<0.05 – relative to the control)

28th and 42nd days its decrease (p<0.05) was noted – by 17.8 and 18.3%, while on the 56th day the decrease was 24.8% (p<0.05), and after stopping the administration of gadolinium orthovanadate nanoparticles, the post-mortem weight of rats did not differ reliably from the control.

No organic changes were recorded during the post-mortem examination in the experimental groups I and II at all periods of the experiment. The appearance of the bodies of laboratory animals before dissection: the color of the coat was white, shiny; changes in visible mucous membranes, discharge from the oral (nasal) cavity and anus were not noted.

At the autopsy (relative to the control group), there were no changes in the mucous membranes of the oral cavity, trachea, pharynx, and esophagus; food remains were observed in the stomach; hyperemia of the subcutaneous tissue was not noted; the heart was not enlarged in volume, cone-shaped, the consistency of the myocardium was elastic; the liver was brown, elastic; consistency, not increased in volume; spleen and pancreas – unchanged; kidneys of brown color, not increased in volume; the vessels of the mesentery of the small intestine were not filled with blood, signs of inflammation in the stomach, small and large intestines were not detected.

The exception was the large intestine dilatation in rats of the experimental group II on the 56th day of the experiment. Whereas in the rats of the experimental group III (received gadolinium orthovanadate nanoparticles at a dose of 2.0 mg/dm^3 of drinking water), starting from the 42nd day of the experiment, signs of inflammation were observed in the small intestine, and on the 56th day of the experiment, in addition to this, the liver was light color, slightly increased in volume, flabby consistency, intestinal distention was also noted.

It should be noted that these organic changes disappeared 14 days after stopping the administration of the nanoparticle solution (Fig. 3).

The morphological characteristics of the intestinal samples of the control and experimental groups are given below. Thus, on the 14th day of the experiment, histological studies of the fragments of the duodenum of the control group of rats it was found that the demarcation of the layers was well expressed, the villi were intact, and the epithelium covered the surface evenly. Nuclei of enterocytes were moderately basophilic, rounded, equal in size, located at the basal pole of the cells. Goblet cells were contoured, vacuoles were transparent, rounded. Acidophilic cells were well defined. The crypt lumen was free. Lymphocytes, plasma cells and fibroblasts of the lamina propria were evenly distributed and had a contoured, basophilic nucleus. Lacteal lumen was moderate. The muscle plate was intact, the cytoplasm of the cells was oxyphilic, the nuclei were contoured, basophilic. The vessels of the submucosal base were moderately filled with blood. Reticular fibers were oxyphilic, evenly stained. The number of fibrocytes and lymphocytes in the submucosal base was moderate. The muscle layers were intact, structured, the cell nuclei ere well

contoured, basophilic, the cytoplasm was oxyphilic, and the layer between the fibers was defined. The color of the preparation was even. Slight fuchsinophilia was observed in the structures of the submucosal base and muscle layers. The nuclei of epithelial cells, lymphocytes, and fibroblasts were stained brown-black, the intercellular substance was light brown. Connective tissue structures were painted in red (Fig. 4).

In the experimental group I on the 14th day of administration of gadolinium orthovanadate nanoparticles at a dose of 0.2 mg/l of drinking water, it was established that the demarcation of the layers was good, the villi were intact, and evenly covered with a layer of epithelium. Some villi were thickened due to to an increase in lymphocytes and plasma cells of the main plate.

The goblet cells of the crypts were enlarged. Enterocytes of individual crypts had signs of hyperplasia: the nuclei were hyperchromic, closely adjacent to each other, and their number was significantly increased. The lacteals were narrowed. The nuclei of enterocytes were basophilic, contoured, the cytoplasm was intensely neutrophilic. Acidophilic cells differentiated. The lamina propria contained the nuclei of lymphocytes and plasma cells. Lymphocytic infiltration of the lamina propria was observed in individual villi. The submucous base was structured, oxyphilic. The lumen of individual Brunner glands was enlarged, the cytoplasm of mucocytes was weakly oxyphilic and contained a significant number of vacuoles. Cell nuclei were basophilic. The muscle layers were well demarcated (Fig. 4).

In the experimental group II on the 14th day of administration of gadolinium orthovanadate nanoparticles at a dose of 1.0 mg/l of drinking water, it was established that the layers were well demarcated. At the tops of individual villi, peeling of the epithelium was sometimes observed. Goblet cells of villi and crypts were slightly enlarged, vacuoles contained basophilic granules. Acidophilic cells were determined. The number of plasma cells, lymphocytes and fibroblasts of the lamina propria was moderate. The muscle plate was intact. Elastic fibers of the submucous base were structured, integral, oxyphilic. The circular muscle layer was slightly thickened, the staining was uneven, the oxyphilicity of the cytoplasm of myocytes was less pronounced (Fig. 4).

In the experimental group III on the 14th day of administration of gadolinium orthovanadate nanoparticles at a dose of 2.0 mg/l of drinking water, it was established that the separation of layers was good. The villi had signs of necrosis – the internal structure was lost, the stained tissue is neutrophilic. In the case of preservation of the own plate, the latter was infiltrated by lymphocytes. The crypts were enlarged, the nuclei of enterocytes were basophilic, tightly adjacent to each other. Goblet cells were also enlarged. Acidophilic cells differentiated poorly. The reticular fibers of the submucosal base were weakly basophilic and

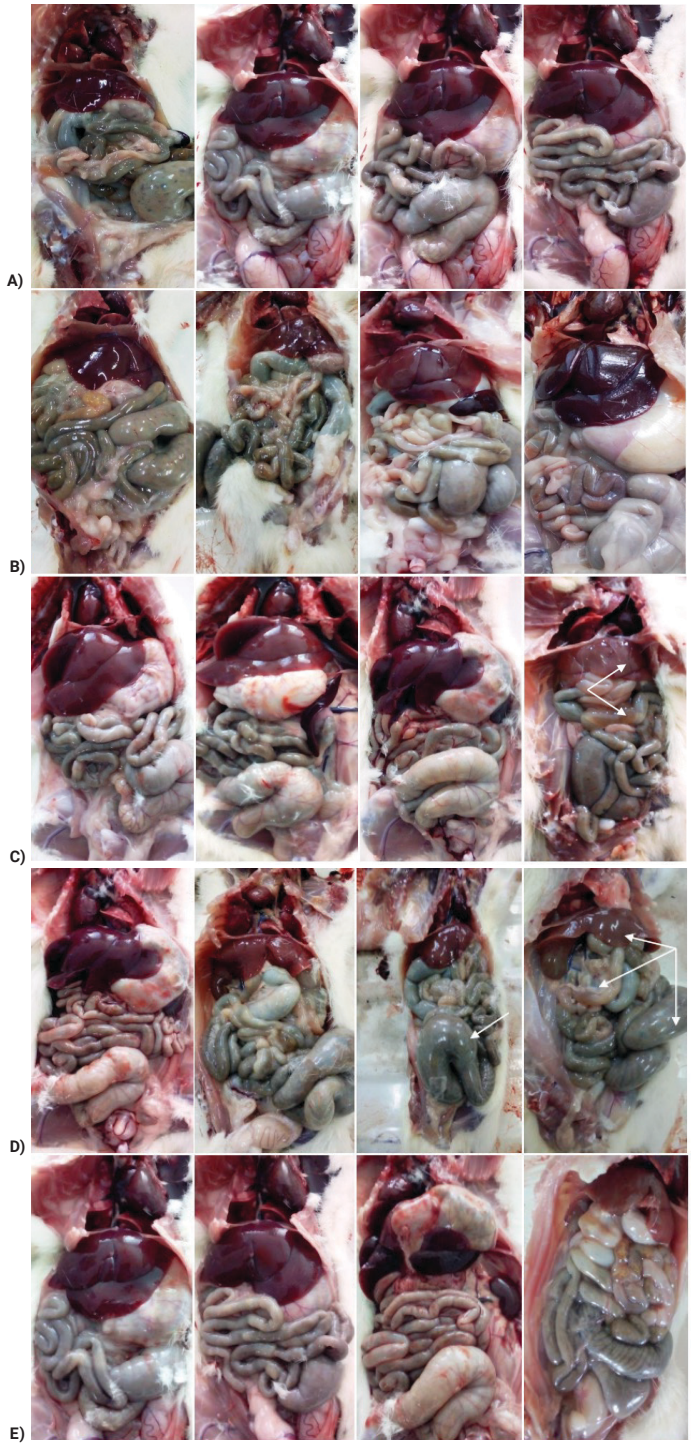

Figure 3: Patho-anatomical picture of internal organs of rats: A) on the 14th day of theexperiment; B) on the 28th day of the experiment; C) on the 42nd day of the experiment; D) onthe 56th day of the experiment; E) 14 days after stopping the administration of the nanoparticle solution

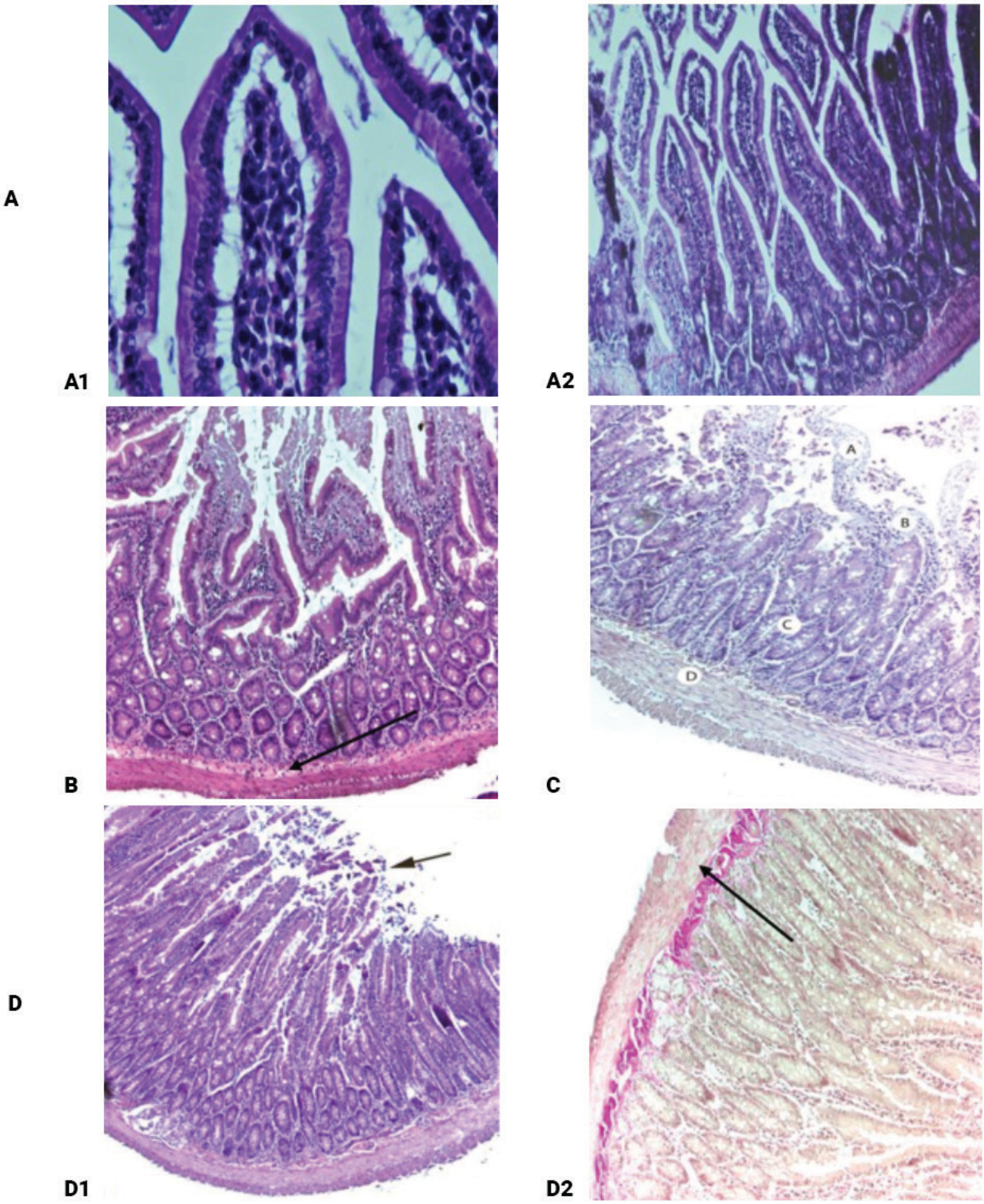

Figure 4: The structure of the duodenum of rats on the 14th day of the experiment: A) control group: A1) Villus of the proximal part, longitudinal section. Hematoxylin and eosin, ×400; A2) Proximal part. Hematoxylin and eosin, ×100; B) I experimental group (NP $GdVO_4$:Eu^{3+} 0,2 mg/l drink water). Lymphocytic infiltration of the lamina propria Hematoxylin and eosin, ×100; D) II experimental group (NP $GdVO_4$:Eu^{3+} 1,0 mg/l drink water). D1) Desquamation of the epithelium of the villi, ×50; D2) Thickening of the circular muscle layer. Van Gieson, ×100; C) III experimental group (NP $GdVO_4$:Eu^{3+} 2,0 mg/l drink water). Dystrophy and necrosis of the villous epithelium (A). Lymphoid infiltration of the lamina propria (B), crypt hyperplasia (C). Edema of the muscle layer (D). Hematoxylin and eosin, ×100

fragmented. The circular muscle layer was thickened, swollen, weakly oxyphilic (Fig. 4).

On the 28th day of the experiment, histological studies of the duodenum fragments of the control group of rats showed that the layers were well demarcated. Villi were whole, evenly covered with a layer of epithelium. The nuclei of enterocytes were basophilic, contoured, the cytoplasm was neutrophilic. Goblet cells were well defined, vacuoles were transparent.

Acidophilic cells differentiated. The nuclei of lymphocytes and plasma cells of the lamina propria were contoured and basophilic. The vessels of the submucosal base were moderately filled with blood. The connective tissue of the submucosal base was oxyphilic and structured. The muscle layers were well demarcated (Fig. 5).

In the experimental group I on the 28th day of administration of gadolinium orthovanadate nanoparticles at a dose of 0.2 mg/l of drinking water, it was established that the layers were demarcated. Sometimes, the tips of the villi were destructured, the epithelial layer was fragmented or peeled off. In some places, nuclei and cell boundaries werenot defined. Slight destructuring of the own plate of the tip of the villi. The basal part of the villi and the crypts were preserved. The main plate was somewhat filled with lymphocytes and plasma cells. The nuclei of enterocytes were basophilic, contoured, the cytoplasm was neutrophilic. Goblet cells were well defined, some of them were enlarged. Acidophilic cells differentiated. The submucous base was structured. Fibers were oxyphilic, cell nuclei were basophilic, contoured. The muscle layers were painted evenly (Fig. 5).

In the experimental group II on the 28th day of administration of gadolinium orthovanadate nanoparticles at a dose of 1.0 mg/l of drinking water, it was established that the demarcation of layers was good. Villi were whole, evenly covered with a layer of epithelium. The nuclei of enterocytes were basophilic, contoured, the cytoplasm was intensely neutrophilic. Goblet cells contained transparent vacuoles. Acidophilic cells differentiated. The lamina propria contained the nuclei of lymphocytes and plasma cells. Lymphocytic infiltration of the lamina propria was observed in some villi. The submucosal base was structured, oxyphilic (Fig. 5).

In the experimental group III on the 28th day of administration of gadolinium orthovanadate nanoparticles at a dose of 2.0 mg/l of drinking water, it was established that the layers were demarcated. The villi had signs of apical destruction: the epithelial layer was fragmented or absent, the enterocytes of the apices were pyknomorphic, the lamina propria was homogenized, neutrophilic and infiltrated by lymphocytes. In some cases, the villi were completely destroyed. Acidophilic cells were determined. Goblet cells were slightly enlarged.

Crypts were enlarged and elongated. The epithelium of the crypts had signs of hyperplasia – the nuclei were hyperchromic, densely located. The vessels of the submucosal base were dilated, filled with blood cells. Reticular fibers were acidophilic, structured. The muscle layers were well demarcated. There was a lot of mucus in the intestinal lumen (Fig. 5).

On the 42nd day of the experiment, histological studies of the fragments of the duodenum of the control group of rats established that the demarcation of the layers was well defined, the villi were intact, and the epithelium covered the surface evenly. Nuclei of enterocytes were moderately basophilic, rounded, equal in size, located at the basal pole of the cells. goblet cells were contoured, vacuoles were transparent, rounded. Acidophilic cells were well defined.

The crypt lumen was free. Lymphocytes, plasma cells and fibroblasts of the lamina propria were evenly distributed and had a contoured, basophilic core. Lacteal lumen was moderate. The muscle plate was intact, the cytoplasm of the cells was oxyphilic, the nuclei were contoured, basophilic. The vessels of the submucosal base were moderately filled with blood. Reticular fibers were oxyphilic, evenly stained. The number of fibrocytes and lymphocytes in the submucosal base was moderate. The muscle layers were intact, structured, the cell nuclei were well contoured, basophilic, the cytoplasm was oxyphilic, and the layer between the fibers was defined. Enterocytes of the crypts were hyperchromic, the nuclei were densely located. Acidophilic cells differentiated. The vessels of the submucosal base were dilated, the connective tissue was oxyphilic and structured. The muscle layers were well demarcated and structured. The nuclei of epithelial cells, lymphocytes, and fibroblasts were stained brown-black, the intercellular substance was light brown (Fig. 6).

In the experimental group I, on the 42nd day of administration of gadolinium orthovanadate nanoparticles at a dose of 0.2 mg/l of drinking water, it was established that the demarcation of the layers of the wall of the small intestine was good. Villi were thickened. Sometimes, the epithelial layer was unevenly distributed. The lamina propria was focally infiltrated with lymphocytes. Enterocytes of the crypts were hyperchromic, nuclei were densely arranged, acidophilic cells were differentiated. Some goblet cells were hypertrophied. In the submucosal layer, there was defibrillation of the structures, the fibers were oxyphilic. The muscle layers were well demarcated, the cytoplasm of the cells was oxyphilic (Fig. 6).

In the experimental group II on the 42nd day of administration of gadolinium orthovanadate nanoparticles at a dose of 1.0 mg/l of drinking water, it was established that the demarcation of the layers of the wall of the small intestine was good. The tips of some villi were with signs of necrosis of the epithelium and lamina propria. Enterocyte cells were weakly stained, some nuclei were missing, and the

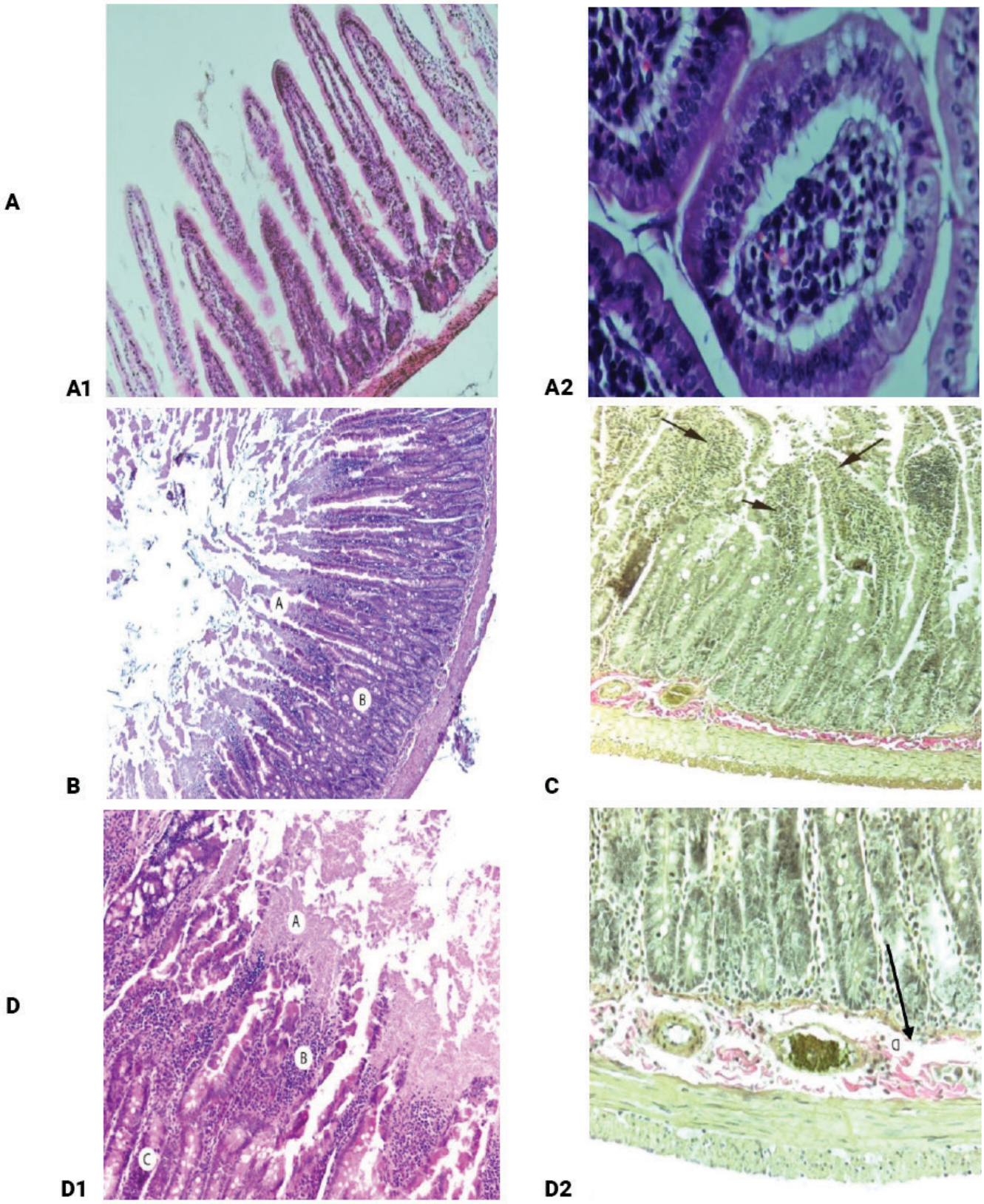

Figure 5: The structure of the duodenum of rats on the 28th day of the experiment.: A) control group: A1) Rat duodenum. Hematoxylin and eosin, ×100; A2) Villus of the proximal part, transverse section. Hematoxylin and eosin, ×400; B) I experimental group (NP $GdVO_4$:Eu^{3+} 0,2 mg/l of drinking water). Necrosis of the tips of the villi (A). Hypertrophy of goblet cells (B). Hematoxylin and eosin, ×50; C) II experimental group (NP $GdVO_4$:Eu^{3+} 1,0 mg/l of drinking water). Lymphocytic infiltration of individual villi. Van Gieson, ×100; D) III experimental group (NP $GdVO_4$:Eu^{3+} 2,0 mg/l drinking water): D1) Dystrophy and necrosis of the villous epithelium (A). Lymphoid infiltration of the main plate (B). Hyperplasia of the crypt epithelium (C). Hematoxylin and eosin, ×100; D2) Edema of the submucosal base. Van Gieson, ×200.

cytoplasm had a fragmented structure. The lamina propria was infiltrated with lymphocytes. In most villi, the structure was preserved, enterocytes had basophilic contoured nuclei. Goblet cells were well defined and had transparent vacuoles. Acidophilic cells differentiated. The muscular plate was intact, the submucous base was oxyphilic and structured. The muscle layers were well demarcated (Fig. 6).

In the experimental group III on the 42nd day of administration of gadolinium orthovanadate nanoparticles at a dose of 2.0 mg/l of drinking water, it was established that the demarcation of the layers of the wall of the small intestine was good. Infiltration of the lamina propria by lymphocytes was observed. At the tips of the villi, the epithelium was exfoliated in many cases, the tips of the villi were thickened due to lymphoid infiltration. Fragments of villi tissues were observed in the intestinal lumen. In some cases, only the shells of the basal membrane and vessel walls remained from the villi, while atrophy of the mucous layer as a whole was observed. Goblet cells were well contoured, their vacuoles were transparent. Enterocytes of crypts were hyperchromic, acidophilic cells differentiated in individual crypts. The connective tissue of the submucosal base was oxyphilic, with signs of defibrillation. The muscle layers were structured, oxyphilic, and evenly stained (Fig. 6).

On the 56th day of the experiment, histological studies of duodenum fragments of rats in the control group established that the demarcation of the layers was well defined, the villi were intact, and the epithelium covered the surface evenly. Nuclei of enterocytes were moderately basophilic, rounded, equal in size, located at the basal pole of the cells. Goblet cells were contoured, vacuoles were transparent, rounded. Acidophilic cells were well defined. The crypt lumen was free. Lymphocytes, plasma cells and fibroblasts of the lamina propria were evenly distributed and had a contoured, basophilic nucleus. Lacteal lumen was moderate. The muscle plate was intact, the cytoplasm of the cells was oxyphilic, the nuclei were contoured, basophilic. The vessels of the submucosal base were moderately filled with blood. Reticular fibers were oxyphilic, evenly stained. The number of fibrocytes and lymphocytes in the submucosal base was moderate. The muscle layers were intact, structured, the cell nuclei were well contoured, basophilic, the cytoplasm was oxyphilic, and the layer between the fibers was defined. The color of the drug was uniform. Slight fuchsinophilia was observed in the structures of the submucosal base and muscle layers. The nuclei of epithelial cells, lymphocytes, and fibroblasts were stained brown-black, the intercellular substance was light brown. Connective tissue structures were stained in red (Fig. 7).

In the experimental group I on the 56th day of administration of gadolinium orthovanadate nanoparticles at a dose of 0.2 mg/l of drinking water, it was established that the demarcation of layers was good. Desquamation of the epithelial layer, loss of its structure, was sometimes observed on the tips of the villi. The central part of the villi was preserved. The epithelial layer was structured, the nuclei of endotheliocytes were basophilic, the cytoplasm was neutrophilic, weakly basophilic. In the lamina propria, nuclei of lymphocytes, plasma cells, and blood vessels were observed. Goblet cells were contoured, alveoli were transparent. In some crypts, goblet cells were enlarged in size (Fig. 7).

In the experimental group II on the 56th day of administration of gadolinium orthovanadate nanoparticles at a dose of 1.0 mg/l of drinking water, it was established that the demarcation of the layers of the wall of the small intestine was good. The tips of the villi had signs of epithelium desquamation and necrosis of the lamina propria. The tissue had neutrophilic staining and was homogenized. The middle part of the villi was better preserved: a layer of enterocytes was defined. Cell nuclei were basophilic, contoured. The cytoplasm was neutrophilic or weakly basophilic. Nuclei of lymphocyte, plasmocytes, and vascular structures were observed in the lamina propria. Goblet cells were well defined, their vacuoles were transparent.

Enterocytes of the crypts were intensely basophilic, acidophilic cells were weakly differentiated.

The muscular plate was intact, the tissue of the submucous base had a fibrous structure and oxyphilic coloration. On some preparations, the layers between the fibers were enlarged. The circular muscle layer was slightly thickened (Fig. 7).

In the experimental group III on the 56th day of administration of gadolinium orthovanadate nanoparticles at a dose of 2.0 mg/l of drinking water, it was established that the demarcation of the layers of the wall of the small intestine was good. There was thickening of the tips of the villi, homogenization of the structures of the lamina propria, and desquamation of the epithelium. Villous enterocytes had a contoured basophilic nucleus and neutrophilic cytoplasm. The number of goblet cells of villi was reduced. Lymphocytic infiltration was observed at the base of the villi, in some areas. Enterocytes of individual crypts were hyperchromic, their nuclei were quite densely arranged. The goblet cells of the crypts were slightly enlarged. Acidophilic cells differentiated. The muscle plate was intact. The submucous base was structured, oxyphilic. The vessels of the submucosal base had collapsed. The muscle layers were well demarcated and structured (Fig. 7).

14 days after stopping the administration of nanoparticle preparations, histological studies of the fragments of rat duodenum in the control group revealed that the demarcation of the layers was good, the villi were intact, and the epithelium covered the surface evenly. The nuclei of enterocytes were moderately basophilic, rounded, of the same size, located at the basal pole of the cells. Goblet cells were contoured, vacuoles were transparent, rounded. Acidophilic cells were well defined. The crypt lumen was free. Lymphocytes, plasma cells and fibroblasts of the lamina

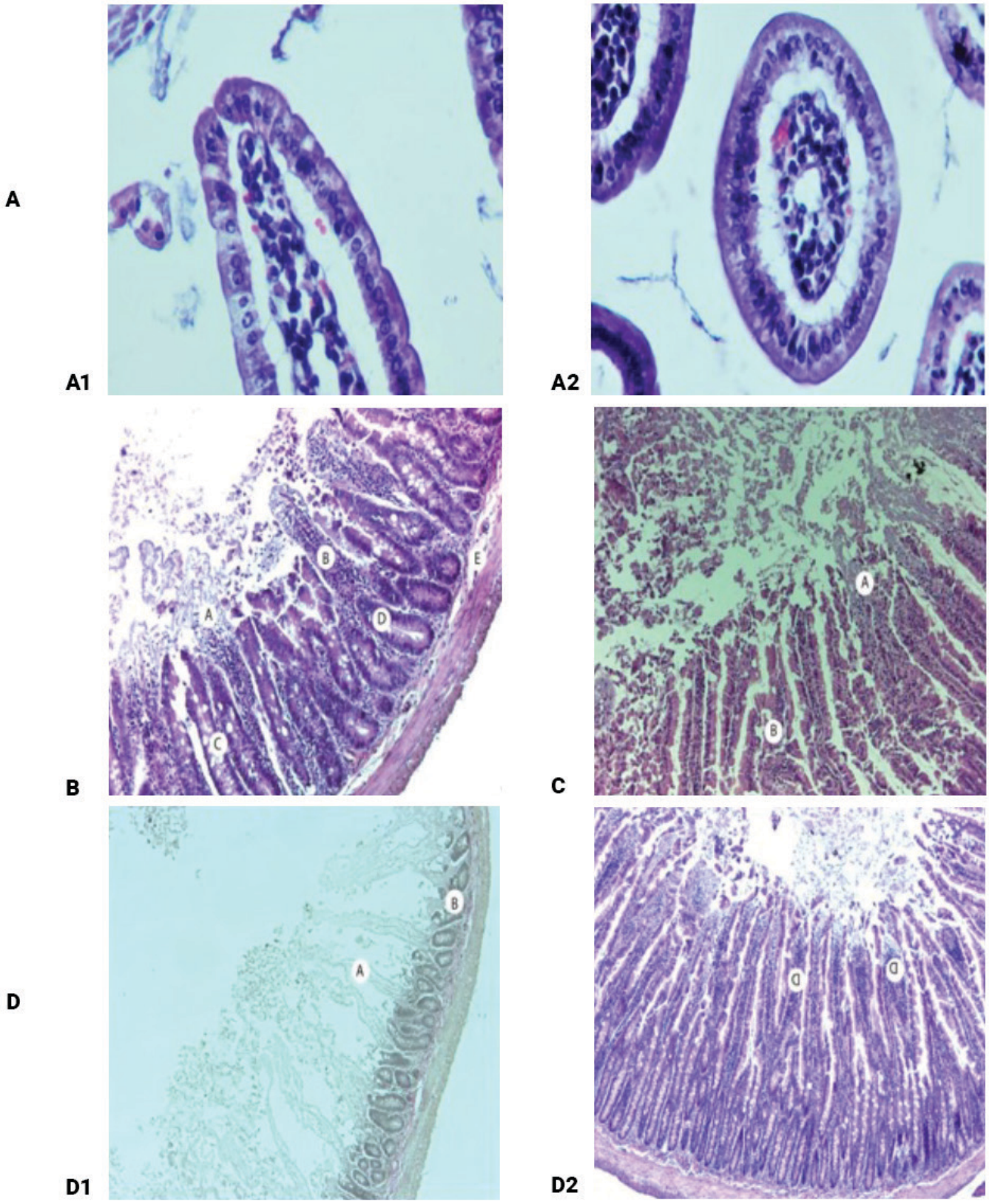

Figure 6: The structure of the duodenum of rats on the 42nd day of the experiment: A) control group: A1) The tip of the villi, longitudinal section. Hematoxylin and eosin, ×400; A2) The tip of the villi, cross section. Hematoxylin and eosin, ×400; B) I experimental group (NP $GdVO_4$:Eu^{3+} 0,2 mg/l of drinking water). Destruction of the epithelium and own plate of villi (A). Lymphocytic infiltration of the lamina propria (B), hypertrophy of goblet cells (C) and hyperplasia of crypt enterocytes (D). Edema of the submucosal base (E). Hematoxylin and eosin, ×100; C) II experimental group (NP $GdVO_4$:Eu^{3+} 1,0 mg/l of drinking water). Necrosis and desquamation of the epithelium of the tips of some villi (A). Lymphoid infiltration of the lamina propria of some villi (B). Hematoxylin and eosin. ×100. D) III experimental group (NP $GdVO_4$:Eu^{3+} 2,0 mg/l of drinking water): D1) Necrosis of the villi (A) and mucosal atrophy (B). Van Gieson, ×50; D2) Lymphoid infiltration of the lamina propria (D). Hematoxylin and eosin, ×50.

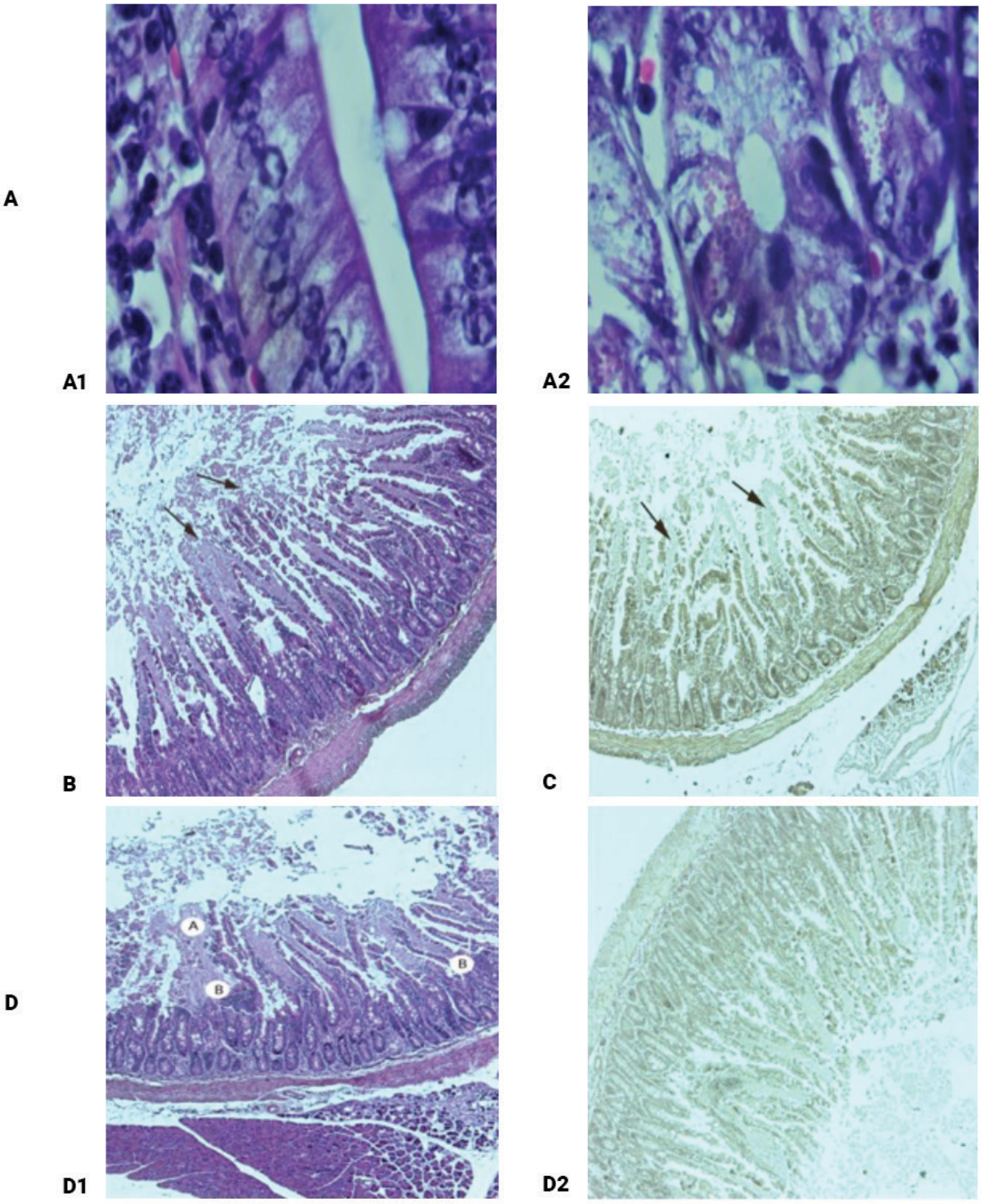

Figure 7: The structure of the duodenum of rats on the 56th day of the experiment: A) controlgroup: A1) Acidophilic cells of the crypt. Hematoxylin and eosin, ×1000; A2) Enterocytes of villi. Hematoxylin and eosin, ×1000; B) I experimental group (NP $GdVO_4$:Eu^{3+} 0,2 mg/l of drinking water). Desquamation of the epithelium of the villi. Hematoxylin and eosin, ×50; C) II experimental group (NP $GdVO_4$:Eu^{3+} 1,0 mg/l of drinking water). Desquamation of the epithelium and necrosis of the lamina propria of the tips of the villi. Van Gieson, ×50; D) III experimental group (NP $GdVO_4$:Eu^{3+} 2,0 mg/l of drinking water): D1) Desquamation of the epithelium, necrosis of the tips of the villi (A) and lymphocytic infiltration of the lamina propria (B).

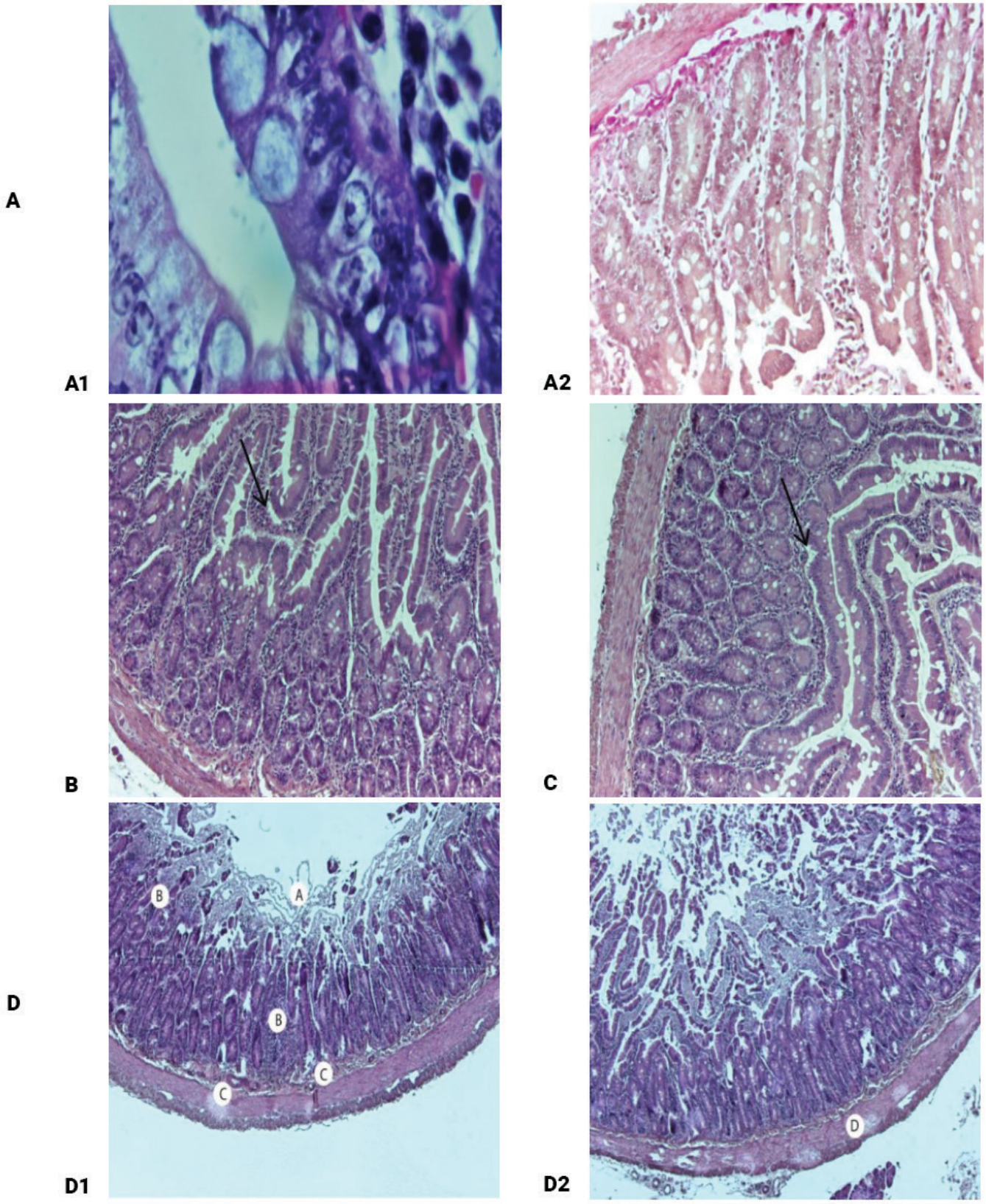

Figure 8: The structure of the duodenum of rats 14 days after stopping the administration of nanoparticle preparations: A) control group: A1) Goblet cells. Hematoxylin and eosin, ×1000; A2) Rat duodenum. Van Gieson, ×200; B) I experimental group (NP $GdVO_4$:Eu^{3+} 0,2 mg/l of drinking water). Slight infiltration of the lamina propria. Hematoxylin and eosin, ×100; C) II experimental group (NP $GdVO_4$:Eu^{3+} 1,0 mg/l of drinking water). Rat duodenum. Lymphocytic infiltration of the lamina propria. Hematoxylin and eosin, ×100; D) III experimental group (NP $GdVO_4$:Eu^{3+} 2,0 mg/l of drinking water): D1) Necrosis of mucosal villi (A) and lymphoid infiltration of the lamina propria (B). Edema of the submucosal base (C). Hematoxylin and eosin, ×50; D2) Edema and infiltration of the circular muscle layer (D). Hematoxylin and eosin, ×50

propria were evenly distributed and had a contoured, basophilic nucleus. Lacteal lumen was moderate. The muscle plate was intact, the cytoplasm of the cells was oxyphilic, the nuclei were contoured, basophilic. The vessels of the submucosal base had collapsed, there were blood cells in the lumen of some of them. Reticular fibers were oxyphilic, evenly stained. The number of fibrocytes and lymphocytes in the submucosal base was moderate. The muscle layers were intact, structured, the cell nuclei were well contoured, basophilic, the cytoplasm was oxyphilic, and the interlayer between the fibers was defined (Fig. 8).

In the experimental group I, 14 days after stopping the administration of gadolinium orthovanadate nanoparticles at a dose of 0.2 mg/l of drinking water, it was established that the layers of the wall of the small intestine were well demarcated. Villi were whole, evenly covered with a layer of epithelium. The nuclei of enterocytes were basophilic, contoured, the cytoplasm was neutrophilic. Goblet cells were well defined, vacuoles were transparent. Acidophilic cells differentiated. The nuclei of lymphocytes and plasma cells of the lamina propria were contoured and basophilic. Slight infiltration of the lamina propria was noted. The vessels of the submucosal base were moderately filled with blood. The connective tissue of the submucosal base was oxyphilic and structured. The muscle layers were well demarcated (Fig. 8).

In the experimental group II, 14 days after stopping the administration of gadolinium orthovanadate nanoparticles at a dose of 1.0 mg/l of drinking water, it was established that the layers of the wall of the small intestine were well demarcated. Villi werewhole, evenly covered with a layer of epithelium. Individual villi were thickened due to an increase in lymphocytes and plasma cells of the main plate. The goblet cells of the crypts were enlarged. Enterocytes of individual crypts had signs of hyperplasia: the nuclei were hyperchromic, closely adjacent to each other, and their number was significantly increased. The lacteals were narrowed. The nuclei of enterocytes were basophilic, contoured, the cytoplasm was intensely neutrophilic. Acidophilic cells differentiated. The lamina propria contained the nuclei of lymphocytes and plasma cells. Lymphocytic infiltration of the lamina propria was observed in some villi. The submucous base was structured, oxyphilic. The lumen of individual Brunner glands was enlarged, the cytoplasm of mucocytes was weakly oxyphilic and contained a significant number of vacuoles. Cell nuclei were basophilic. The muscle layers were well demarcated (Fig. 8).

In the experimental group III, 14 days after stopping of administration of gadolinium orthovanadate nanoparticles at a dose of 2.0 mg/l of drinking water, it was established that the demarcation of the layers of the wall of the small intestine was good. Necrosis of the lamina propria was observed in almost all villi of the mucous membrane, while separate fragments of the epithelial cover and basement membrane were preserved. The crypts were elongated, the cells were hyperchromic, the lumen of the glands was insignificant. Goblet cells were contoured. Areas of lymphoid infiltration were observed between the crypts. The muscle plate was fragmented. The submucous base was weakly oxyphilic or neutrophilic. The vessels of the submucosal base had collapsed. The circular muscle layer was thickened, oxyphilicity was reduced, the color was uneven (Fig. 8).

Discussion

At the beginning of the discussion, we would like to note that this research is the first regarding this type of nanoparticles, the terms and conditions of their administration (young animals and the presence of a stress factor). First of all, we would like to focus on the control group of animals, because a logical question arises: why did food stress not cause significant pathological changes in the duodenum of rats compared to the use of nanoparticles?

Let's recall the structure of the intestinal mucosa of animals, which includes several protective barriers. This is quite well reflected in the scheme proposed by Chinese researchers (33). They distinguish four barriers: the first is microbiological (the so-called "good" microflora), the second is chemical (includes neutral and acidic mucin), the third is a mechanical barrier (intestinal epithelial cells are tightly connected by proteins), and the fourth is immunological (includes macrophages and cytokines) (Fig. 9).

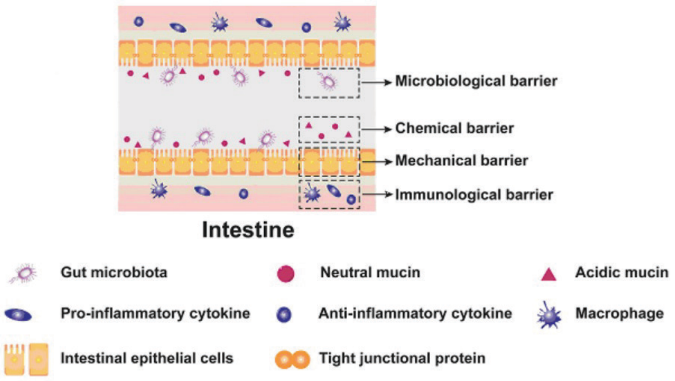

Figure 9: Schematic structure of the mucous membrane of the small intestine of animals (33)

In our opinion and based on the available literature data (34, 35, 36), the absence of pathological changes in the control group is associated with the presence of adaptive reactions of the intestinal wall to excessive fiber, which caused subchronic mechanical irritation, namely: by increasing the synthesis and secretion of mucin, which neutralized inflammatory processes. This mechanism can be roughly depicted as follows (Fig. 10): due to mechanical action, the fiber peels off the microbiological chemical barrier and interacts with the epithelium of the mucous membrane, stimulating the formation of mucin, which in turn has anti-inflammatory properties (37) and increasing its quantity prevents further

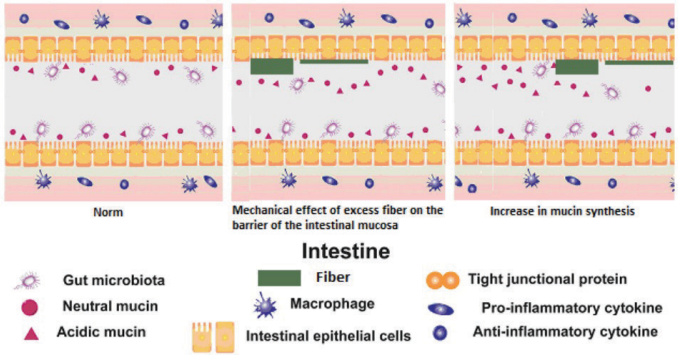

Figure 10: The mechanism of action of excess fiber on the intestinal mucosa

destruction of the mechanical barrier. Besides, some authors have observed no or only minor apparent effects on small and large intestinal morphology in response to high fiber feeding in pigs and rats (38, 39, 40, 41).

The introduction of nanoparticles slightly changes the mechanism of adaptation of the intestinal wall, depending on the dose and time of introduction: the fiber peels off the microbiological chemical barrier, which allows the nanoparticles to come into direct contact with the epithelium of the mucous membrane, resulting in the activation of both villus cells and the immunological barrier. In the future, due to the increase in mucin secretion, part of the nanoparticles probably binds to its components, part interacts with bacteria, and part enters the general bloodstream, which causes a general effect on the body (Fig. 11).

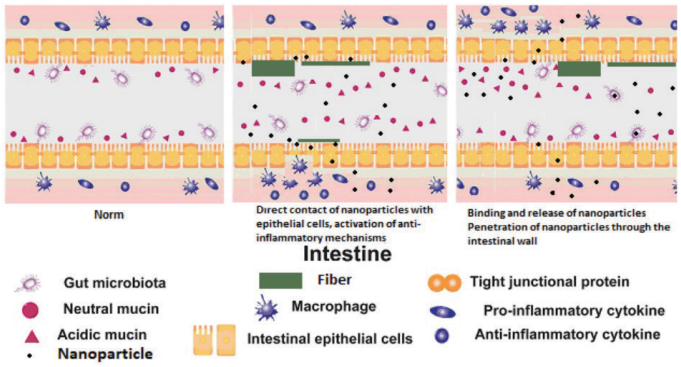

Figure 11: The mechanism of action of excess fiber together with nanoparticles on the intestinal mucosa

With a 5-fold increase in the dose of gadolinium orthovanadate nanoparticles to 1.0 mg/l of drinking water (≈0.15 mg/kg of body weight), the processes of activation of the mechanical barrier continue up to the 42nd day of administration, which is manifested by an increase in goblet cells of villi and crypts, and the processes of activation of the immunological barrier – during the entire period of administration by the presence of lymphocytic infiltration of the lamina propria. From the 42nd to the 56th day of administration, there is a certain exhaustion of adaptation processes in the cells of the epithelium of the intestinal mucosa of rats, which is indicated by the presence of signs of necrosis of the epithelium of some villi tips, fragmentation of the cytoplasm, desquamation of the epithelium and necrosis of the lamina propria.

It should be noted that these changes were also reversible, since the 14th day after the cessation of the administration of nanoparticles, the restoration of the integrity of the villi was observed, but some villi still remained thickened due to the increase in lymphocytes and plasma cells of the main plate. Also, the goblet cells of the crypts remained enlarged, and the enterocytes of individual crypts had signs of hyperplasia. So, we can also assert the adaptogenic effect of NP $GdVO_4$:Eu^{3+} at a dose of ≈0.15 mg/kg of body weight (1.0 mg/l of drinking water), but it is limited in time –28 days.

When NP $GdVO_4$:Eu^{3+} was administered to rats at a dose of ≈0.3 mg/kg of body weight (2.0 mg/l of drinking water), the processes of exhaustion of the adaptive capabilities of the intestinal mucosa and excessive activation of the immunological barrier were observed, which were manifested by dystrophic changes starting from the 14th day of administration: necrosis and loss of the internal structure of villi, increase of crypts, thickening and swelling of the circular muscle layer, excessive lymphocytic infiltration of the lamina propria. As a result of nanoparticles administration for 28 days, dystrophic processes progressed: the villi had signs of tip destruction (in some cases they were completely destroyed), homogenization of the lamina propria, increase of goblet cells and elongation of crypts, hyperplasia of the epithelium, which caused excessive mucus formation and general clinical manifestation in the form of liquefaction of feces on the 42nd and 56th days of administration, respectively. Accordingly, at the given period of the experiment, significant signs of destruction of the intestinal mucosa of rats were also noted: fragments of villi tissue were noted in the lumen of the intestine, in some cases only the shells of the basement membrane and vessel walls remained from the villi, atrophy of the mucous layer as a whole was observed. Significant infiltration of mucosal elements by lymphocytes was also noted, that is, existing inflammation. It should be noted that 14 days after the stopping of administration, only partial signs of restoration of the mucous membrane structure were observed: some fragments of the epithelial cover and basement membrane were preserved, there were areas of lymphoid infiltration between the crypts, and in general, lamina propria necrosis occurred in almost all villi of the mucous membrane. Based on the above, it is possible to assert the toxic effect of NP $GdVO_4$:Eu^{3+} at a dose of ≈0.3 mg/kg of body weight (2.0 mg/l of drinking water) under the conditions of feed stress.

In addition to the dose and external factors (increase or decrease in direct access to cells), the toxicity of nanoparticles depends on their properties. So, for example, gold nanoparticles smaller than 6 nm effectively penetrated the cell nucleus, while large NPs (10-16 nm) penetrated only through the cell membrane and were located only in the

cytoplasm. This suggests that NPs smaller than 10 nm may exhibit more toxic effects than those larger than 10 nm (42). The dependence of toxicity on their size was also established using the example of gold nanoparticles: 15 nm NPs were 60 times less toxic than 1.4 nm NPs for fibroblasts, epithelial cells, and macrophages (43). NPs smaller than 5 nm usually cross cell barriers nonspecifically, for example, by translocation, while larger particles enter cells by phagocytosis; a NP size of around 25 nm is thought to be optimal for pinocytosis (44). That is, the investigated gadolinium orthovanadate nanoparticles are quite accessible to cells (size 8×25 nm), and theoretically can have a negative effect on cells.

Another likely factor in the toxicity of the investigated nanoparticles in a larger dose is their shape (spindle-shaped). For example, a comparison of the effects of hydroxyapatite NPs of different shapes (acicular, lamellar, rod-like, and spherical) on cultured BEAS-2B cells showed that rod-shaped and acicular NPs cause more cell death than spherical and rod-shaped NPs (45). The cytotoxic potential of rod-like (65 ± 15 nm) ZnO nanoparticles was greater than that of spherical (60 ± 20 nm) ZnO nanoparticles when applied to human peripheral blood mononuclear cell culture and was limited to proliferative lymphocytes. At the same time, rod-shaped ZnO NPs produced more more active forms of oxygen compared to spherical ones and caused significant DNA damage in the above cell culture (46). However, the most destructive effects in the body are caused by spindle-shaped nanoparticles. Also, when affecting the body, the dose-effect relationship is clearly visible (47, 48).

Conclusions

Based on the conducted subchronic toxicological experiment on white rats under conditions of feed stress, taking into account the results of clinical and pathohistological studies, a safe and effective range of doses for further use in farm animals can be considered a concentration of gadolinium orthovanadate nanoparticles of 0.2-1.0 mg/dm^3 of drinking water (≈ 0.03-0.15 mg/kg of body weight), and the administration period – 42-28 days, respectively.

Nanoparticles of gadolinium orthovanadate under certain conditions (food stress, young animals) have a rather small range of therapeutic effect, since when the dose was increased to 2.0 mg/dm^3 of drinking water (≈0.3 mg/kg of body weight), destructive processes occurred in the intestines of rats .

References

1. Goodenough KM, Schilling J, Jonsson E, et al. Europe's rare earth element resource potential: an overview of REE metallogenetic provinces and their geodynamic setting. Ore Geol Rev 2016; 72: 838–56. doi:10.1016/j.oregeorev.2015.09.0
2. Balaram V. Rare earth elements: a review of applications, occurrence, exploration, analysis, recycling, and environmental impact. Geosci Front 2019; 10(4): 1285–303.
3. Cheisson T, Schelter EJ. Rare earth elements: Mendeleev's bane, modern marvels. Science 2019; 363(6426): 489–93.
4. Runowski M, Ekner-Grzyb A, Mrówczyńska L, et al. Synthesis and organic surface modification of luminescent, lanthanide-doped Core/Shell nanomaterials (LnF3@100SiO2@NH2@organic acid) for potential bioapplications: spectroscopic, structural, and in vitro cytotoxicity evaluation. Langmuir 2014; 30(31): 9533–43.
5. Jaiswal VV, Bishnoi S, Swati G, et al. Luminescence properties of yttrium gadolinium orthovanadate nanophosphors and efficient energy transfer from VO4 3− to Sm 3+ via Gd 3+ ions. Arab J Chem 2017; 13(1): 474–80.
6. Toro-González M, Dame AN, Mirzadeh S, Rojas JV. Gadolinium vanadate nanocrystals as carriers of α-emitters (225Ac, 227Th) and contrast agents. J Appl Phys 2019; 125(21): e214901. doi:10.1063/1.5096880
7. Maksimchuk PO, Hubenko KO, Seminko VV, et al. High antioxidant activity of gadoliniumyttrium orthovanadate nanoparticles in cell-free and biological milieu. Nanotechnology 2021; 33(5): e055701. doi:10.1088/1361-6528/ac3
8. Maksimchuk PO, Yefimova SL, Omielaieva VV, et al. X-ray induced hydroxyl radical generation by GdYVO4:Eu3+ nanoparticles in aqueous solution: main mechanisms. Crystals 2020; 10(5): e370. doi:10.3390/cryst1005037
9. Karpenko NA, Malukin YuV, Koreneva EM, et al. The effects of chronic intake of nanoparticles of cerium dioxide or gadolinium ortovanadate into aging male rats. Proc Int Conf NanoMat: Appl Prop 2013; 2(1): e01001 https://nap.sumdu.edu.ua/index.php/nap/nap2013/paper/view/1289/488
10. Koreneva EM, Karpenko NA, Smolenko NP, et al. The influence of gadolinium ortovanadate and cerium dioxide nanoparticles on spermogram of adult male rats with neonatal induced disorders of reproductive function. Probl Endocr Pathol 2016; 55(1): 48–55.
11. Belkina IO. Gonadotoxicity of gadolinium ortovanadate nanoparticles under their chronic exposure. Probl Endocr Pathol 2017; 61(3): 78–85.
12. Belkina IO, Smolenko NP, Klochkov VK, et al. The assessment of gadolinium orthovanadate nanoparticles value for neonatally-induced reproductive disease in male rats. Int J Physiol Pathophysiol 2017; 8(4): 299–307.
13. Chistyakova EYe, Smolenko NP, Belkina IO, Korenyeva YeM, Karpenko NO. Effect of the different doses of nanoparticles gadolinium ortovanadat on the reproductive function of male rats. Bull Probl Biol Med 2017: 3,2(138): 127–30. https://vpbm.com.ua/ua/kopiya-vyipusk-3-tom-2-(138),/9025
14. Bölükbaş SC, Al-Sagan AA, Ürüşan H, Erhan MK, Durmuş O, Kurt N. Effects of cerium oxide supplementation to laying hen diets on performance, egg quality, some antioxidant enzymesin serum and lipid oxidation in egg yolk. J Anim Physiol Anim Nutr (Berl) 2016; 100: 686–93.
15. Reka D, Thavasiappan V, Selvaraj P, Arivuchelvan A. Effect of dietary REE supplementation on blood biochemical parameters in layer chicken. Int J Curr Microbiol Appl Sci 2018; 7(1): 181–5.
16. Tommasi F, Thomas PJ, Pagano G, et al. Review of rare earth elements as fertilizers and feed additives: a knowledge gap analysis. Arch Environ Contam Toxicol 2021; 81(4): 531–40.

17. Rossander L, Sandberg AS, Sandström B. The influence of dietary fibre on mineral absorption and utilisation. In: Schweizer TF, Edwards CA, eds. Dietary fibre - a component of food. London: Springer, 1992: 197–216.

18. Hennigar SR, Kelley AM, McClung JP. Metallothionein and zinc transporter expression in circulating human blood cells as biomarkers of zinc status: a systematic review. Adv Nutr 2016; 7(4): 735–46.

19. Goff JP. Invited review: mineral absorption mechanisms, mineral interactions that affect acid–base and antioxidant status, and diet considerations to improve mineral status. J Dairy Sci 2018; 101(4): 2763–813.

20. Blaxter KL. Nutrition and climatic stress in farm animals. Proc Nutr Soc 1958; 17(2): 191–97.

21. Poroshyns'ka OA, Shmajun SS, Nishhemenko MP, Stovbec'ka LS, Jemel'janenko AA, Kozij VI. Influence of stress factors on adaptive and behavioral responses in sows and piglets. Sci J Vet Med 2020; 2: 110–21.

22. Shevchuk MO, Stoyanovskyy VG, Kolomiiets IA. Technological stress in poultry. Scientific Messenger of LNU of Veterinary Medicine and Biotechnologies. Series: Veterinary sciences 2018; 20(88): 63–8.

23. Tkachenko A, Pogozhykh D, Onishchenko A, et al. Gadolinium orthovanadate $GdVO_4$:Eu^{3+} nanoparticles ameliorate carrageenan-Induced intestinal inflammation. J Pharm Nutr Sci 2021; 11: 40–8.

24. Fan MZ, Adeola O, Asem EK, King D. Postnatal ontogeny of kinetics of porcine jejunal brush border membrane-bound alkaline phosphatase, aminopeptidase N and sucrase activities. Comp Biochem Physiol Part A Mol Integr Physiol 2002; 132(3): 599–607.

25. Dahiya JP, Hoehler D, Van Kessel AG, Drew MD. Effect of different dietary methionine sources on intestinal microbial populations in broiler chickens. Poult Sci 2007; 86(11): 2358–66.

26. Sachuk R, Stravsky YA. Zhyhalyuk S, Katsaraba O, Mandyhra Yu. Quality and safety of feeds for cows in the dry period and the parturition in the obstetrics dispensation system. Sci Horiz 2019; 12(85): 39–47.

27. Melnyk AYu, Sakara VS, Vovkotrub NV, Kharchenko AV, Bilyk BP. Metabolic disorders in poultry (review). Scientific Messenger of LNU of Veterinary Medicine and Biotechnologies. Series: Veterinary sciences 2021; 23(103): 125–35.

28. Klochkov VK, Grigorova AV, Sedyh OO, Malyukin YuV. Characteristics of nLnVO4 : Eu3+(Ln = La, Gd, Y, Sm) sols with nanoparticles of different shapes and sizes. J Appl Spectrosc 2012; 79(5): 726–30. doi:10.1007/s10812-012-9662-7

29. Klochkov VK, Malyshenko AI, Sedykh OO, Malyukin YuV. Wet chemical synthesis and characterization of luminescent colloidal nanoparticles: $ReVO_4$: $Eu3^+$(Re = La, Gd, Y) with rodlike and spindlelike shape. Funct Mater 2011; 18(1):111–5.

30. Malyukin YuV. New luminescent nanomaterials: fundamental properties, biomedical and technical applications. Visn Nac Acad Nauk Ukr 2017; 12: 28–34. doi:10.15407/visn2017.12.028

31. Diet. Meat Free Rat and Mouse Diet (SF00-100) 2015: https://www.specialtyfeeds.com/new/wp-content/uploads/2022/06/meat_free_rm.pdf

32. Kotsyumbas IYa. Preclinical studies of veterinary medicinal products: scientific edition. Lviv: Triada Plus, 2006: 360. [in Ukrainian] ne najdem podatkov!!

33. Hao W, Cha R, Wang M, Zhang P, Jiang X. Impact of nanomaterials on the intestinal mucosal barrier and its application in treating intestinal diseases. Nanoscale Horiz 2022; 7: 6–30. doi:10.1039/d1nh00315a

34. Montagne L, Pluske J, Hampson D. A review of interactions between dietary fibre and the intestinal mucosa, and their consequences on digestive health in young non-ruminant animals. Anim Feed Sci Technol 2003; 108(1/4): 95–117. doi:10.1016/s0377-8401(03)00163-9

35. Maswanganye GMT, Liu B, Che D, Han R. Review: effects of dietary fiber levels and composition on the intestinal health of finishing pigs. Open J Anim Sci 2021; 11: 384–98. doi:10.4236/ojas.2021.113028

36. Sekh N, Karki D. Dietary fiber in poultry nutrition in the light of past, present, and future research perspective: a review. Open J Anim Sci 2022; 12: 662–87. doi:10.4236/ojas.2022.124046

37. Grondin JA, Kwon YH, Far PM, Haq S, Khan WI. Mucins in intestinal mucosal defense and inflammation: learning from clinical and experimental studies. Front Immunol 2020; 11: 2054. doi:10.3389/fimmu.2020.02054

38. Anugwa FOI, Varel VH, Dickson JS, Pond WG, Krook LP. Effects of dietary fiber and protein concentration on growth, feed efficiency, visceral organ weights and large intestine microbial populations of swine. J Nutr 1989; 119(6): 879–86. doi:10.1093/jn/119.6.879

39. Sugano M, Ikeda I, Imaizumi K, Lu Y-F. Dietary fiber and lipid absorption. In: Kritchevsky D, Bonifield C, eds. Dietary fiber: Boston: Springer, 1990: 137–56. doi:10.1007/978-1-4613-0519-4_9

40. McCracken BA, Gaskins HR, Ruwe-Kaiser PJ, Klasing KC, Jewell DE. Diet-dependant and diet-independant metabolic responses underlie growth stasis of pigs at weaning. J Nutr 1995; 125(11): 2838–45. doi:10.1093/jn/125.11.2838

41. McRorie JW, McKeown NM. Understanding the physics of functional fibers in the gastrointestinal tract: an evidence-based approach to resolving enduring misconceptions about insoluble and soluble fiber. J Acad Nutr Diet 2017; 117(2): 251–64.

42. Huo S, Jin S, Ma X, et al. Ultrasmall gold nanoparticles as carriers for nucleus-based Gene therapy due to size-dependent nuclear entry. ACS Nano 2014; 8(6): 5852–62. doi:10.1021/nn5008572

43. Pan Y, Neuss S, Leifert A, et al. Size-dependent cytotoxicity of gold nanoparticles. Small 2007; 3(11): 1941–9. doi:10.1002/smll.200700378

44. Zhang S, Gao H, Bao G. Physical principles of nanoparticle cellular endocytosis. ACS Nano 2015; 9(9): 8655–71. doi:10.1021/acsnano.5b03184

45. Sukhanova A, Bozrova S, Sokolov P, Berestovoy M, Karaulov A, Nabiev I. Dependence of nanoparticle toxicity on their physical and chemical properties. Nanoscale Res Lett 2018; 13(1): e 44 doi:10.1186/s11671-018-2457-x

46. Bhattacharya D, Santra CR, Ghosh AN, Karmakar P. Differential toxicity of rod and spherical zinc oxide nanoparticles on human peripheral blood mononuclear cells. J Biomed Nanotechnol 2014; 10(4): 707–16. doi:10.1166/jbn.2014.1744

47. Misra SK, Nuseibeh S, Dybowska A, Berhanu D, Tetley TD, Valsami-Jones E. Comparative study using spheres, rods and spindle-shaped nanoplatelets on dispersion stability, dissolution and toxicity of CuO nanomaterials. Nanotoxicology 2013; 8(4): 422–32. doi:10.3109/17435390.2013.796017

48. Bandas IA, Krynytska I Ya, Kulitska MI, Korda MM. Nanoparticles: importance today, classification, use in medicine, toxicity. Med Clin Chem 2015; 17(3): 123–9. doi:10.11603/mcch.2410-681X.2015.v17.i3.5066

Patomorfološke spremembe v dvanajstniku podgan ob subkroničnem peroralnem dajanju nanodelcev gadolinijevega ortovanadata ob prehranskem stresu

A. Masliuk, O. Lozhkina, O. Orobchenko, V. Klochkov, S. Yefimova, N. Kavok

Izvleček: V naši raziskavi nas je zanimala dejanska prisotnost prilagoditvenih ali negativnih reakcij v steni tankega črevesa belih podgan pod vplivom nanodelcev gadolinijevega ortovanadata v razponu odmerkov (≈ 0,03–0,3 mg/kg telesne teže) v pogojih prehranskega stresa (zaradi presežka vlaknin in pomanjkanja beljakovin v prehrani) in njihova stopnja izražanja, saj se tovrstna nesorazmernost obrokov v Ukrajini pogosto pojavlja. Nanodelci gadolinijevega ortovanadata imajo pomemben potencial za uporabo v živinoreji in perutninarstvu, saj v območju odmerkov 0,03–0,15 mg/kg telesne teže preprečujejo negativne učinke na črevesno sluznico tudi pri stresu zaradi krme. Ugotovljeno je bilo, da dajanje nanodelcev gadolinijevega ortovanadata v odmerkih 0,03 in 0,15 mg/kg telesne teže belim podganam s pitno vodo 56 oziroma 28 dni povzroči aktivacijo mehanske in imunološke pregrade sluznice, kar se kaže v povečanju števila čašastih celic, hiperplaziji enterocitov nekaterih kript, zadebelitvi resic in infiltraciji limfocitov, ki 14 dni po prenehanju dajanja dosežejo kontrolno raven. Vendar pa povečanje odmerka nanodelcev gadolinijevega ortovanadata na 0,3 mg/kg telesne teže pri prehranskem stresu povzroči izčrpavanje prilagoditvenih sposobnosti črevesne sluznice in pretirano aktivacijo imunološke pregrade, kar se je od 14. dneva dajanja pokazalo z distrofičnimi spremembami, ki so se poglobile do 56. dne in se po 14 dneh po prenehanju dajanja niso izravnale.

Ključne besede: redke zemeljske kovine; nanodelci gadolinijevega ortovanadata; patomorfološke spremembe, dvanajstnik; bele podgane; krmni stres

DOI 10.26873/SVR-1716-2023
UDC 636.1:616.936:57.083.33(620)
Pages: 95–103

Original Research Article

Equine Leptospirosis in Egypt: Seroprevalence and Risk Factors

Key words

Leptospirosis;
seroprevalence;
risk factors;
horse;
Egypt

Mohamed Marzok[1,2]*, Abdelrahman M. Hereba[3,4], Abdelfattah Selim[5]*

[1]Department of Clinical Sciences, College of Veterinary Medicine, King Faisal University, Al-Hofuf, 31982, Saudi Arabia, [2]Department of Surgery, Faculty of Veterinary Medicine, Kafr El Sheikh University, Kafr El Sheikh, Egypt, [3]Department of Biomedical Physics, Medical Research Institute, Alexandria University, Egypt, [4]Department of Microbiology, College of Veterinary Medicine, King Faisal University, Al-Ahsa 31982, Saudi Arabia, [5]Department of Animal Medicine (Infectious Diseases), Faculty of Veterinary Medicine, Benha University, Toukh 13736, Egypt

***Corresponding authors:** abdelfattah.selim@fvtm.bu.edu.eg, mmarzok@kfu.edu.sa

Abstract: Most leptospiral infections in horses are asymptomatic; however, acute disease manifestations as well as reproductive failure and recurrent uveitis have been reported. Horses are considered accidental hosts. The data about equine leptospirosis in Egypt are scarce. Hence, the present study aimed to investigate presence of antibodies against *Leptospira* sp. in horse in four Egyptian governorates and determine the associated risk factors for the infection. To determine the seroprevalence in 305 serum samples, the microscopic agglutination test (MAT) was carried using eight Leptospira serovars antigens. The results revealed 104 animals were positive for at least one of the serovars (34.1%; 95%CI: 29.01-39.59). The most common reaction was reported to Icterohaemorrhagiae serovar (15.14%), followed by Canicola (14.75%), Bratislava (11.47%), Copenhageni (8.19%), Pomona (7.86%), and Hardjo (6.88%). The most prevalent was observed among females, older horses raising in pasture or in contact with ruminants or dogs and lack of rodents control. The significant seroprevalence suggests that Egyptian horses living in the studied area are at high risk of infection or exposure by *Leptospira* sp. Thus, the establishment of emergency surveillance and control program is very crucial for this zoonotic pathogen.

Received: 2 March 2023
Accepted: 18 May 2023

Introduction

Leptospirosis is one of the most common zoonoses in the world and is caused by gram-negative spirochetes from *Leptospira* genus (*Leptospiraceae* family, order *Spirochaetales*) (1, 2). It affects both human and animals, mainly in tropical regions where the organism thrives in optimal temperature and humidity circumstances (3). Infections in horses are most occurred through direct contact with urine or placenta secretions of diseased animals, or indirectly through a contaminated surroundings (4).

Leptospira sp. infection is predominantly subclinical in equines and is thought to be a significant cause for abortion, stillbirth, delivery weak foals, and neonatal mortality (5, 6). However, the main symptoms in horses are anorexia, moderate fever, jaundice and recurrent uveitis (7). Moreover, pulmonary hemorrhage and deaths due to interstitial nephritis may be occurred (8).

Leptospirosis infection in horses is one of the leading causes of significant economic loss in the equine agribusiness sector due to the numerous consequences of the disease, including the cost of treating diseases animals, the interruption of training, a decline in performance, and the exclusion of affected animals from auctions and competitions (9, 10). Moreover, the infected animals in either acute or chronic phases are thought of as reservoirs and play a significant part in the transmission of disease that poses a risk to public health (11).

Leptospirosis has traditionally been diagnosed in a laboratory using serological tests. The standard serological test

is the microscopic agglutination test (MAT), where a single detection of a high antibody titer associated with clinical symptoms and a four-fold or more shift in antibody titers in paired acute and convalescent samples are considered diagnostic. It is preferable to isolate the spirochete, however this is a challenging and time-consuming (12). Moreover, the polymerase chain reaction (PCR) have been used as a specific test for detection of *Leptospira* DNA in tissue of premature born foals (13, 14) and in the vitreous fluid of horses with recurrent uveitis. (15).

Leptospiral infection in horses is frequently detected using serology. The most common reported serovars are *L. interrogans* sv. Bratislava, *L. interrogans* sv. Pomona, *L. kirschneri* sv. Grippotyphosa and *L. interrogans* sv. Icterohaemorrhagiae (16).

In Egypt, most of previous studies on leptospirosis were focused on human or pets like dogs, cats (17) and few studies in cattle (18). Nonetheless, there is no epidemiological data about the *Leptospira* infection in horse particularly in Nile Delta of Egypt.

Therefore, the objective of the current study was to assess the prevalence of leptospirosis among horses in the four governorates of northern Egypt as well as potential risk factors for leptospiral infection.

Materials and methods

Ethical statement

The study protocol was approved by ethical committee of the Faculty of Veterinary Medicine, Benha University, Egypt, which complies with all applicable Egyptian regulations on research and publication. The Committee's Animal Ethical Rules and Guidelines were followed in the collection and handling of serum samples.

Study location

A serological survey was conducted from January 2020 to April 2021 in the northern Egyptian governorates of Cairo, Giza, Kafr ElSheikh, and Qalyubia, which situated geographically at 30°2'40"N 31°14'9"E, 29.9870°N 31.2118°E, 31.3°N 30.93°E and 30.41°N 31.21°E, Figure 1.

According to Köppen, the climate of Giza is similar to an arid, hot desert. Because of its proximity to Cairo, it has a similar climate to Cairo. The average temperature is 25 °C and highest temperature reported in August, while the rain is rare in this area with average rainfall of 100-200 mm annually. In addition, the weather in Kafr ElSheikh and Qalyubia governorates is hot, muggy, arid summers and chilly, dry, windy, mainly clear winters. The temperature falls between 15 to 30 °C throughout the year.

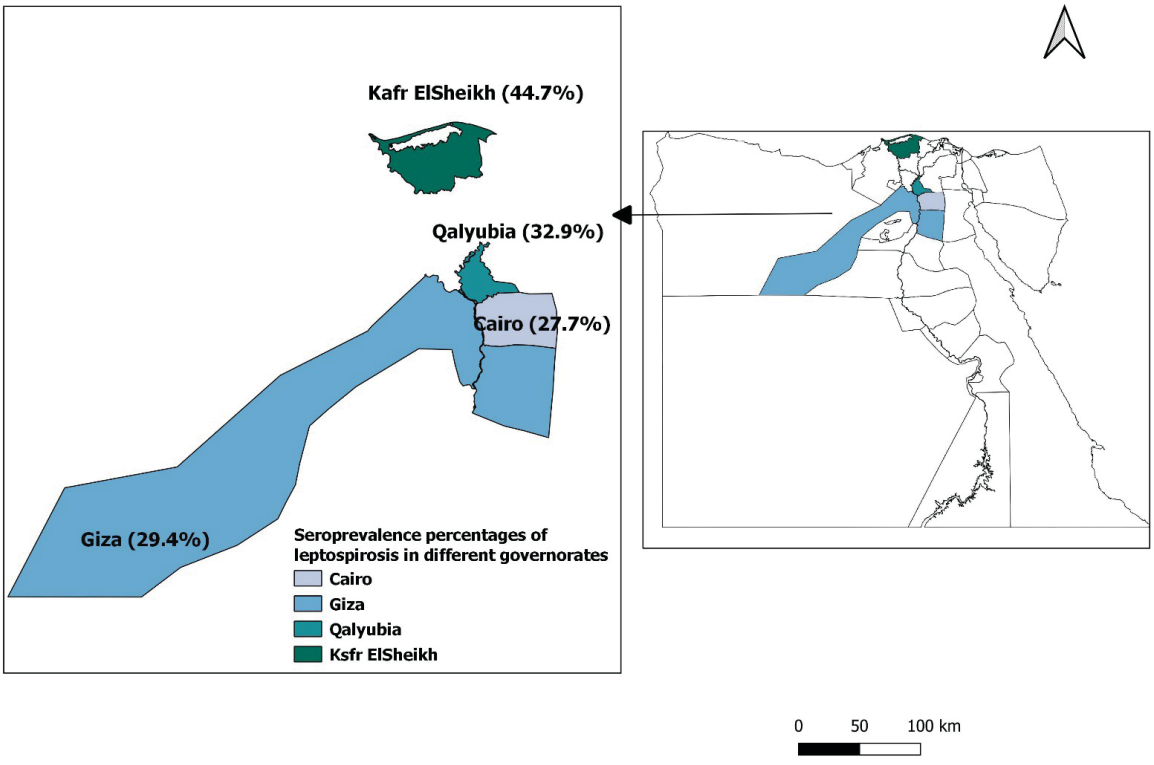

Figure 1: MAP demonstrate studied governorates and seropositivity percentages to *Leptospira* sp.

Sampling and epidemiological data

Win Epi 2.0 was used to estimate the sample size, which was 305 horses, with a predicted prevalence of 50%, a 95% confidence range, and an accepted error of 5%. Because there haven't been any epidemiological study that describe the state of horse leptospirosis in the examined region, the predicted prevalence of 50% was chosen. The examined horses had not specific signs for the disease and have not been vaccinated against leptospirosis. In the present study, no exclusion criteria or repeat sampling of the same horses were applied. The blood samples were taken after obtaining the farmer's informed consent from horse by puncturing the jugular vein with vacuum tubes without an anticoagulant. The samples were centrifuged at 3000 xg for 10 min to separate the serum, which kept at -20 °C until serological analysis.

In order to determine risk variables related with seropositive horses, a questionnaire was made accessible to the owners of the study's horses. Questionnaire was set to collect the data associated with the potential risk factors for leptospira infection. The questionnaire included the data about sex (male or female), age (<6 years, 6-10 years, and >10 years), season (winter, autumn, summer, and spring), the presence of ruminants (yes/no), the presence of dogs (yes/no), the type of housing (Stable, pasture, mixed), and control of rodents (yes/no).

Serological testing

The microscopic agglutination test (MAT) was used to screen serum samples for *Leptospira* antibodies. A variety of *Leptospira* serovars were used as antigens in the microscopic agglutination reaction, including serogroup Icterohaemorrhagiae, serovar Copenhageni and Icterohaemorrhagiae; serogroup Canicola, serovar Canicola; serogroup Grippotyphosa, serovar Grippotyphosa; serogroup Pomona, serovar Pomona; serogroup Sejroe, serovar Hardjo; serogroup Tarassovi, serovar Tarassovi and serogroup interrogans serovar Bratislava. The serum samples were tested at 1:100 dilution by mixing of 25 µL of diluted serum 1:14 in sterile saline with 150 µL of the diluted *Leptospira* suspensions. Sera that produced a positive reaction were titrated further in a series of two-fold dilutions, commencing at 1:125 and continuing until the titer endpoint. Antibody titers were calculated as the reciprocal of the highest serum dilution that resulted in a 50% or more reduction in the amount of free leptospires in the suspension when compared to a sterile saline-based negative control. A titer of ≤100 was considered positive, meaning it indicated exposure to or infection with *Leptospira*.

Statistical analysis

Data were organized and statistically analyzed using SPSS software version 24 (IBM, Chicago, USA). Chi-square test was used to evaluate the relationship between the results of the serology (positive and negative) and the factors. Findings with *P*-value less than 0.05 were regarded as statistically significant. First, the univariate binary logistic regression analysis was performed to identify important risk factors linked to *Leptospira* seropositivity. Then, all variables with $P<0.05$ in univariate regression model were passed to multivariant logistic regression model. The odds ratios (ORs) and 95% confidence intervals were calculated to evaluate the degree of risk. The model's fit was evaluated using the Hosmer and Lemeshow goodness test.

Results

At a serum dilution of 1:100, 104 horses (34.1%, 95%CI: 29.01-39.59) from four governorates showed positive MAT titers to one or more *Leptospira* serovars. The majority of

Table 1: MAT antibody titer distribution for different *Leptospira* serovars

Serovar	Number of positive horses in each titer						No of positive animals (%)
	125	250	500	1000	2000	4000	
Icterohaemorrhagiae	15	12	7	8	6	5	53/305 (15.14%)
Canicola	14	11	8	4	3	5	45/305 (14.75%)
Bratislava	13	10	6	3	1	2	35/305 (11.47%)
Copenhageni	11	9	5	0	0	0	25/305 (8.19%)
Pomona	11	8	3	1	1	0	24/305 (7.86%)
Hardjo	9	6	5	0	1	0	21/305 (6.88%)
Grippotyphosa	0	0	0	0	0	0	0/305 (0)
Tarassovi	0	0	0	0	0	0	0/305 (0)

Table 2: Number of seropositive animals to single and multiple serovars

No of serovar	Number of animals reacted positive (%)
1	59/104 (56.7%)
2	22/104 (21.1%)
3	18/104 (17.3%)
4	5/104 (4.8)
5	0/104 (0)

horses tested positive for Icterohaemorrhagiae serovar, followed by Canicola, Bratislava, Copenhageni, Pomona, and Hardjo, but no animals tested positive for Grippotyphosa or Tarassovi serovars, Table 1. The seropositive horses reacted with single serovar were 59/104 (56.7%), while 43.3% (45/104) of the seropositive horses tested positive to numerous serovars, Table 2.

In this study, it was discovered that 104 animals possessed *Leptospira* antibodies, representing a seroprevalence of 34.1%. Horses from Kafr ElSheikh had the greatest prevalence rate (44.7%), followed by those from Qalyubia (32.9%), while animals from the Giza governorate had the lowest prevalence (27.7%), as indicated in Table 3.

Considering sex as a potential risk factor among the tested animals, gelding horses and male vs female horses showed a significant difference ($P< 0.05$). Significantly, the infection rate among females was the greatest (39%), while the prevalence rate among male animals was the lowest (24.3%). In addition, age was associated with a greater seroprevalence that was statistically significant ($P=0.001$). In comparison to horses in the age groups < 6 and 6 to 10 years old, all horses over 10 years old had greater prevalence rates (49.1%), table 3. The highest prevalence rates were seen in the autumn (50.6%) and spring (33.3%), with a significant seasonal difference in *Leptospira* seropositivity ($P<0.05$). According to the findings, horses raised in close proximity to ruminants or dogs had higher seropositivity rates, which were 39.9% and 38.5%, respectively. Also, the findings show that, in comparison to horses living in stables or mixing houses, horses roaming freely in pastures had the highest prevalence rate (42%). It's interesting to note that rodent control has a substantial effect on the prevalence of *Leptospira* in horses, where the prevalence rate significantly rose in the presence of rodent control, Table 3.

The result of multivariate logistic regression analysis summarized in table 4 and showed that sex, age, season, housing, contact with ruminants or dogs and control of rodents were identified as risk factor for *Leptospira* infection. Females (OR= 1.27, 95%CI: 0.49-5.70) within age group more than 10 years old (OR=3.25, 95%CI: 1.31-8.11) was found to be a greater risk than gelding and other age groups. Moreover, horses raised in contact with ruminants (OR=2.43, 95%CI: 1.35-4.36) or dogs (OR=1.36, 95%CI: 0.66-2.78) and living freely in pasture (OR=2.30, 95%CI: 1.16-4.52) had high risk of infection than other animals. Also, autumn season (OR=2.66, 95%CI: 1.21-5.83) and presence of rodents control (OR=3.26, 95%CI: 1.55-6.85) increased risk of infection, Table 4.

Discussion

Horses are not frequently thought as a potential source of leptospirosis spread unlike other domestic and wild animals. Nevertheless, horses may have *Leptospira* in their kidneys, making them carriers and transmit the bacterium in the environment (5). In horses, the disease varies geographically in terms of prevalence and serovars involved, and its effects are still unknown (8, 19). The current study used the MAT to determine the prevalence of antibodies against eight different Leptospira serovars and related risk variables in horses living in the four Egyptian governorates.

The findings of present study revealed that 34.1% of horses had positive MAT titers for at least one *Leptospira* serovar, while 53.3% of seropositive horses had antibodies for several serovars. Several infections or cross-reactions may cause seropositivity to multiple serovars. Additionally, because none of the horses were immunized against leptospirosis, we concluded that the presence of antibodies indicated *Leptospira* exposure or illness.

The *Leptospira* sp. seroprevalence in Egyptian horses was lower than that reported in Europe. In Switzerland, Italy and the Netherlands, seroprevalences were determined to be 58.5% 67.2% and 79%, respectively (20-22). On the other hand, the seroprevalence rate in the current study was higher than those reported in Italy, which were 11.4% and 1.5%, respectively (23, 24). Additionally, in a Brazilian studies, the seropositivity rates were 71.4% (25), 28.75% (26), 45.9%, (27) and 8% (28). Furthermore, according to a recent study conducted in various States of the American Midwest, healthy horses have a 77% seroprevalence rate (29). The findings of present investigation were attributed to the type of environment (30-34). The studied horses were kept under good care conditions and in regions with little stagnant water (35).

The present fndings revealed that the most prevalent serovar was Icterohaemorrhagiae (15.14%), followed by Canicola (14.75%). These findings are consistent with earlier serological studies conducted on Brazilian horses (21, 27, 36). It's interesting that no animals tested positive for the Grippotyphosa serovar. Although this serovar very seldom affects horses, it is thought to be the one most frequently linked to equine recurrent uveitis (ERU) in Europe (20). The obtained findings were consistent with those reported by several authors, where most of seropositive or infected horses have no symptoms (7, 8).

Table 3: The risk factors associated with *Leptospira* spp. seropositivity in horse

Variable	Total tested horses	No of positive	No of negative	% of positive	95% CI	Statistic
locality						
Giza	85	25	60	29.4	20.78-39.82	x^2=6.322 df=3 *P*=0.097
Cairo	65	18	47	27.7	18.29-39.58	
Kafr ElSheikh	85	38	47	44.7	34.6-55.28	
Qalyubia	70	23	47	32.9	23-44.5	
Sex						
Male	74	18	56	24.3	15.97-35.2	x^2=7.552 df=2 *P*=0.023*
Female	210	82	128	39.0	32.7-45.79	
Gelding	21	4	17	19.0	7.67-40	
Age						
<6 years	64	11	53	17.2	9.88-28.22	x^2=13.805 df=2 *P*=0.001*
6-10	186	66	120	35.5	28.96-42.59	
>10	55	27	28	49.1	36.38-61.92	
Season						
Winter	73	17	56	23.3	15.08-34.17	x^2=15.067 df=3 *P*=0.002*
Spring	75	25	50	33.3	23.71-44.58	
Summer	76	21	55	27.6	18.84-38.57	
Autumn	81	41	40	50.6	39.95-61.23	
Contact with ruminants						
Yes	198	79	119	39.9	33.33-46.85	x^2=8.451 df=1 *P*=0.004*
No	107	25	82	23.4	16.35-32.21	
Contact with dogs						
Yes	231	89	142	38.5	32.49-44.94	x^2=7.968 df=1 *P*=0.005*
No	74	15	59	20.3	12.87-31.18	
Housing						
Stable	81	17	64	21.0	13.54-31.07	x^2=12.599 df=2 *P*=0.002*
Pasture	181	76	105	42.0	35.04-49.27	
Mixed	43	11	32	25.6	14.93-40.24	
Control of rodents						
No	76	12	64	15.8	9.27-25.6	x^2=15.100 df=1 *P*<0.0001*
Yes	229	92	137	40.2	34.03-46.63	
Total	305	104	201	34.1	29.01-39.59	

*The result is significant at $P < 0.05$

Table 4: Multivariate logistic regression analysis for variables associated with horse leptospirosis

Factors	B	S.E.	OR	95% CI for OR		P value
				Lower	Upper	
Sex						
Male	0.240	0.662	1.27	0.35	4.65	0.717
Female	0.518	0.624	1.68	0.49	5.70	0.407
Age						
6-10	0.749	0.401	2.11	0.96	4.64	0.062
>10	1.180	0.466	3.25	1.31	8.11	0.011
Season						
Spring	0.300	0.410	1.35	0.60	3.02	0.464
Summer	0.068	0.416	1.07	0.47	2.42	0.870
autumn	0.978	0.400	2.66	1.21	5.83	0.015
Contacts with ruminants						
Yes	0.886	0.299	2.43	1.35	4.36	0.003
Contacts with dogs						
Yes	0.306	0.366	1.36	0.66	2.78	0.403
Housing						
Pasture	0.831	0.346	2.30	1.16	4.52	0.016
Mixed	0.373	0.489	1.45	0.56	3.79	0.446
Control of rodents						
Yes	1.182	0.379	3.26	1.55	6.85	0.002

B: Logistic regression coefficient, SE: Standard error, OR: Odds ratio, CI: Confidence interval

According to our data, older horses are significantly more likely than young horses to be seropositive to *Leptospira* sp. This finding is consistent with results from previous studies (9, 37) and could be explained by the fact that exposure to *Leptospira* is more likely as horse get older and that seropositivity can last for a very long time. Nevertheless, other researchers did not observe significant relationship between age and seropositivity (27, 38).

The present findings are consistent with previous studies showing that females more susceptible to get *Leptospira* infection than males (27, 28). These findings confirm that females are more vulnerable than males since they are allowed to roam more freely on pasture on stud farms and are often included in batches of the most animals (39-47).

According to our findings, the seroprevalence rate of *Leptospira* was highest during autumn in comparison with other seasons, which come in accordance with findings of Trimble and colleagues (29). Since leptospires may survive and spread infection for a longer period of time in warm and humid climates. Thus, spring and fall have higher seroprevalences.

The study's findings confirmed the necessity of sanitary management when different species cohabit, with the presence of animals such as sheep, goats, or cows on nearby farms serving as risk factors for exposure to *Leptospira* sp. in study participants' animals (9). *Leptospira* infections in ovine and caprine are frequent, and these species, like bovines, can serve as significant reservoirs of the disease and

have epidemiological implications (39, 48-52). Moreover, according to findings reported by Chiareli and colleagues (53), equines that coexist with other species share communal drinking and pasture, have direct or indirect contact with contaminants of aborted materials, graze on pasture contaminated with infected urine, and have contact with animals on neighbouring properties are more likely to be exposed to *Leptospira* spp.

In the horses' indoor habitat, rats are probably the most common species of animals, and *Leptospira interrogans* prevalence was positively correlated with the density of the rat population (54). The possibility of the *Leptospira* spreading to horses was greatly decreased by the existence of pest control methods. Rodent control is seen as a key element in prevention (55) despite the fact that it can occasionally be challenging to assess the role that rodents play in the transmission of leptospiral serovars (56).

In agreement with findings of Pinna and colleagues (57), appropriate management, such as the availability of veterinary support on the property, control measures for presence of rodents, and quarantine of recently arriving animals, suggested probable circumstances of less exposure to leptospirosis. In contrast, Batista and colleagues (58), observed no significant associateion between presence of rodents and livestock farming and seropositivity for *Leptospira* sp. and they attributed this to inaccurate data, a non- conclusive epidemiological questionnaire, the presence of confounding variables, and unmeasured environmental variables.

Conclusion

The present study confirms presence of antibodies against *Leptospira* sp. among Egyptian horses and horses living in studied areas high risk exposure to pathogenic leptospires. Age, sex, season, the presence of ruminants or dogs, and the absence of rodent controls were the risk factors targeted in this investigation for the occurrence of horse leptospirosis. Thus, control of roddent is important factor to reduce the spreading of infcetion among horses and consequently for human.

Acknowledgements

The authors would like to acknowledge the Deanship of Scientific Research, Vice Presidency for Graduate Studies and Scientific Research, King Faisal University, Saudi Arabia for the financial support of this research through the Grant Number 3413.

Authors' contributions. Conceptualization, methodology, formal analysis, investigation, resources, data curation, writing-original draft preparation, A.S., A.M.H. and M.M.; writing-review and editing, A.S. and M.M.; project administration, M.M.; funding acquisition, A.S., A.M.H. and M.M. All authors have read and agreed to the published version of the manuscript.

Ethics approval and consent to participate. The study protocol was approved by ethical committee of the Faculty of Veterinary Medicine, Benha University, Egypt, which complies with all applicable Egyptian regulations on research and publication. The Committee's Animal Ethical Rules and Guidelines were followed in the collection and handling of serum samples.

Consent for publication not applicable.

Availability of data and materials. All data generated or analysed during this study are included in this published article

Competing interests. There are no conflicts of interest declared by the authors.

Funding. This work was supported through the Annual Funding track by the Deanship of Scientific Research, Vice Presidency for Graduate Studies and Scientific Research, King Faisal University, Saudi Arabia (Grant Number 3413).

References

1. Pappas G, Papadimitriou P, Siozopoulou V, Christou L, Akritidis N . The globalization of leptospirosis: worldwide incidence trends. Int J Infect Dis 2008; 12(4): 351–7.
2. Vijayachari P, Sugunan AP, Shriram AN. Leptospirosis: an emerging global public health problem. J Biosci 2008; 33(4): 557–69.
3. Bharti AR, Nally JE, Ricaldi JN, et al. Leptospirosis: a zoonotic disease of global importance. Lancet Infect Dis 2003; 3(12): 757–1.
4. Hamond C, Martins G, Lawson-Ferreira R, Medeiros MA, Lilenbaum W. The role of horses in the transmission of leptospirosis in an urban tropical area. Epidemiol Infect 2013; 141(1): 33–5.
5. Hamond C, Pinna A, Martins G, Lilenbaum W. The role of leptospirosis in reproductive disorders in horses. Trop Anim Health Prod 2014; 46(1): 1–10.
6. Whitwell K, Blunden A, Miller J, Errington J. Two cases of equine pregnancy loss associated with Leptospira infection in England. Vet Rec 2009; 165(13): 377–8.
7. Divers T, Chang YF, Irby N, Smith JL , Carter CN. Leptospirosis: an important infectious disease in North American horses. Equine Vet J 2019; 51(3): 287–92.
8. Verma A, Stevenson B, Adler B. Leptospirosis in horses. Vet Microbiol 2013; 167(1/2): 61–6.
9. Båverud V, Gunnarsson A, Engvall EO, Franzén P, Egenvall A. Leptospira seroprevalence and associations between seropositivity, clinical disease and host factors in horses. Acta Vet Scand 2009; 51(1): 1–10.
10. Pinto PS, Libonati H, Lilenbaum W. A systematic review of leptospirosis on dogs, pigs, and horses in Latin America. Trop Anim Health Prod 2017; 49(2): 231–8.
11. Daher EDF, Abreu KLS, Silva Junior GB. Insuficiência renal aguda associada à leptospirose. Braz J Nephrol 2010; 32(4): 408–15.
12. OIE. Leptospirosis. In: Manual of diagnostic tests and vaccines for terrestrial animals. 8th ed. Paris: OIE, 2018; 503–16.

13. Vemulapalli R, Langohr IM, Sanchez A, et al. Molecular detection of Leptospira kirschneri in tissues of a prematurely born foal. J Vet Diagn Invest 2005; 17(1): 67–71.

14. Selim AM, Elhaig MM, Gaede W. Development of multiplex real-time PCR assay for the detection of Brucella spp., Leptospira spp. and Campylobacter foetus. Vet Ital 2014; 50(4): 269–75.

15. Brandes K, Wollanke B, Niedermaier G, Brem S, Gerhards H. Recurrent uveitis in horses: vitreal examinations with ultrastructural detection of leptospires. J Vet Med A Physiol Pathol Clin Med 2007; 54(5): 270–5.

16. Hashimoto VY, Gonçalves DD, Silva FGd, et al. Occurrence of antibodies against Leptospira spp. in horses of the urban area of Londrina, Paraná, Brazil. Rev Inst Med Trop São Paulo 2007; 49(5): 327–30.

17. Samir A, Soliman R, El-Hariri M, Abdel-Moein K , Hatem ME . Leptospirosis in animals and human contacts in Egypt: broad range surveillance. Rev Soc Bras Med Trop 2015; 48(3): 272–7.

18. Ibrahim NA, Alrashdi BM, Elnaker YF, et al. Serological investigation and epidemiological analysis of bovine leptospirosis in Egypt. Trop Med Infect Dis 2022; 7(9): 208.

19. Martinez F. Leptospirosis in horses: a European perspective. Equine Vet J 2019; 51(3): 285–6.

20. Vera E, Taddei S, Cavirani S, et al. Leptospira Seroprevalence in bardigiano horses in northern Italy. Animals 2019; 10(1): e 23. doi: 10.3390/ani10010023

21. Houwers DJ, Goris MGA, Abdoel T, et al. Agglutinating antibodies against pathogenic Leptospira in healthy dogs and horses indicate common exposure and regular occurrence of subclinical infections. Vet Microbiol 2011; 148(2/4): 449–51.

22. Blatti S, Overesch G, Gerber V, Frey J, Hüssy D. Seroprevalence of Leptospira spp. in clinically healthy horses in Switzerland. Schweiz Arch Tierheilkd 2011; 153(10): 449–56.

23. Cerri D, Ebani V, Fratini F, Pinzauti P, Andreani E . Epidemiology of leptospirosis: observations on serological data obtained by a" diagnostic laboratory for leptospirosis" from 1995 to 2001. New Microbiol 2003; 26(4): 383–9.

24. Ebani VV, Bertelloni F, Pinzauti P, Cerri D . Seroprevalence of Leptospira spp. and Borrelia burgdorferi sensu lato in Italian horses. Ann Agric Environ Med 2012; 19(2): 237–40.

25. Hamond C, Martins G, Lilenbaum W. Subclinical leptospirosis may impair athletic performance in racing horses. Trop Anim Health Prod 2012; 44(8): 1927–30.

26. Dewes C, Fortes TP, Machado GB, et al. Prevalence and risk factors associated with equine leptospirosis in an endemic urban area in Southern Brazil. Braz J Dev 2020; 6(8): 58380–90.

27. Da Silva AS, Jaguezeski AM, Laber IF, et al. Leptospira spp. in horses in southern Brazil: seroprevalence, infection risk factors, and influence on reproduction. Comp Immunol Microbiol Infect Dis 2020; 73: e101552. doi:10.1016/j.cimid.2020.101552

28. Siqueira CC, Fraga DBM, Chagas-Junior AD, et al. Seroprevalence and risk factors associated with equine leptospirosis in the metropolitan region of Salvador and Recôncavo Baiano region, Bahia state (NE Brazil). Trop Anim Health Prod 2020; 52(1): 31–9.

29. Trimble AC, Blevins CA, Beard LA, Deforno AR, Davis EG . Seroprevalence, frequency of leptospiuria, and associated risk factors in horses in Kansas, Missouri, and Nebraska from 2016-2017. PLoS One 2018; 13(10): e0206639. doi:10.1371/journal.pone.0206639

30. Selim A, El-Haig M, Galila ES, Gaede W. Direct detection of Mycobacterium avium subsp. paratuberculosis in bovine milk by multiplex Real-time PCR. Anim Sci Pap Rep 2013; 31(4): 291–302.

31. Elhaig MM, Selim A, Mandour AS, Schulz C, Hoffmann B. Prevalence and molecular characterization of peste des petits ruminants virus from Ismailia and Suez, Northeastern Egypt, 2014–2016. Small Ruminant Res 2018; 169: 94–8.

32. Selim A, Ali A-F, Ramadan E. Prevalence and molecular epidemiology of Johne's disease in Egyptian cattle. Acta Trop 2019; 195: 1–5.

33. Abdallah M-C, Kamel M, Karima B, et al . First report of Toxoplasma gondii infection and associated risk factors in the dromedary camel (Camelus dromedarius) population in south east Algeria. Vet Parasitol Reg Stud Rep 2020; 22: e100475. doi:10.1016/j.vprsr.2020.100475

34. Selim A, Abdelhady A. The first detection of anti-West Nile virus antibody in domestic ruminants in Egypt. Trop Anim Health Prod 2020; 52(6): 3147–51.

35. Raghavan R, Brenner K, Higgins J, Shawn Hutchinson JM , Harkin KR . Evaluations of hydrologic risk factors for canine leptospirosis: 94 cases (2002–2009). Prev Vet Med 2012; 107(1/2): 105–9.

36. Coiro CJ, Langoni H, da Silva RC. Epidemiological aspects in the Leptospira spp. and Toxoplasma gondii infection in horses from Botucatu, São Paulo, Brazil. J Equine Vet Sci 2012; 32(10): 620–3.

37. Rocha T, Ellis W, Montgomery J, Gilmore C, Regalla J, Brem S. Microbiological and serological study of leptospirosis in horses at slaughter: first isolations. Res Vet Sci 2004; 76(3): 199–202.

38. Wangdi C, Picard J, Tan R, Dowling B, Gummow B . Equine leptospirosis in tropical Northern Queensland. Aust Vet J 2013; 91(5): 190–7.

39. Langoni H, Da Silva A, Pezerico S, Lima VY. . Anti-leptospirose agglutinins in equine sera, from São Paulo, Goiás, and Mato Grosso do Sul, Brazil, 1996-2001. J Venom Anim Toxins Incl Trop Dis 2004; 10(3): 207–18.

40. Selim A, Abdelhady A. Neosporosis among Egyptian camels and its associated risk factors. Trop Anim Health Prod 2020; 52(6): 3381–5.

41. Selim A, Ali A-F. Seroprevalence and risk factors for C. burentii infection in camels in Egypt. Comp Immunol Microbiol Infect Dis 2020; 68: e101402 .doi:10.1016/j.cimid.2019.101402

42. Selim A, Marawan MA, Ali A-F, Manaa E , AbouelGhaut HA . Seroprevalence of bovine leukemia virus in cattle, buffalo, and camel in Egypt. Trop Anim Health Prod 2020; 52(3): 1207–10.

43. Selim A, Megahed AA, Kandeel S, Abdelhady A. Risk factor analysis of bovine leukemia virus infection in dairy cattle in Egypt. Comp Immunol Microbiol Infect Dis 2020; 72: e101517. doi:10.1016/j.cimid.2020.101517

44. Selim A, Radwan A. Seroprevalence and molecular characterization of West Nile Virus in Egypt. Comp Immunol Microbiol Infect Dis 2020; 71: e101473. doi: 10.1016/j.cimid.2020.101473

45. Selim A, Radwan A, Arnaout F, Khater H. The recent update of the situation of West Nile fever among equids in Egypt after three decades of missing information. Pak Vet J 2020; 40(3): 390–3.

46. Marawan MA, Alouffi A, El Tokhy S, et al. Bovine Leukaemia Virus: current epidemiological circumstance and future prospective. Viruses 2021; 13(11): e2167. doi: 10.3390/v13112167

47. Selim A, Almohammed H, Abdelhady A, Alouffi A, Alshammari FA . Molecular detection and risk factors for Anaplasma platys infection in dogs from Egypt. Parasites Vector 2021; 14(1): e429. doi: 10.1186/s13071-021-04943-8

48. Martins G, Lilenbaum W. The panorama of animal leptospirosis in Rio de Janeiro, Brazil, regarding the seroepidemiology of the infection in tropical regions. BMC Vet Res 2013; 9: e237. doi:10.1186/1746-6148-9-237

49. Selim A, Manaa E, Khater H. Molecular characterization and phylogenetic analysis of lumpy skin disease in Egypt. Comp Immunol Microbiol Infect Dis 2021; 79: e101699 . doi:10.1016/j.cimid.2021.101699

50. Selim A, Manaa E, Khater H. Seroprevalence and risk factors for lumpy skin disease in cattle in Northern Egypt. Trop Anim Health Prod 2021; 53(3): e350. doi:10.1007/s11250-021-02786-0

51. Selim A, Manaa EA, Alanazi AD, Alyousif MS. Seroprevalence, risk factors and molecular identification of bovine leukemia virus in Egyptian cattle. Animals 2021; 11(2): e319. doi:10.3390/ani11020319

52. Selim A, Megahed A, Kandeel S, Alouffi A, Almutairi MA. West Nile virus seroprevalence and associated risk factors among horses in Egypt. Sci Rep 2021; 11: e20932. doi:10.1038/s41598-021-00449-6

53. Chiareli D, Moreira E, Gutiérrez H, et al. Freqüência de aglutininas anti-Leptospira interrogans em eqüídeos, em Minas Gerais, 2003 a 2004. Arq Brasil Med Vet Zootec 2008; 60(6): 1576–9.

54. Barwick RS, Mohammed HO, McDonough PL, White ME. Epidemiologic features of equine Leptospira interrogans of human significance. Prev Vet Med 1998; 36(2): 153–65.

55. Tsegay K, Potts A, Aklilu N, Lötter C, Gummow B. Circulating serovars of Leptospira in cart horses of central and southern Ethiopia and associated risk factors. Prev Vet Med 2016; 125: 106–15.

56. Simbizi V, Saulez MN, Potts A, Lötter C, Gummow B. A study of leptospirosis in South African horses and associated risk factors. Prev Vet Med 2016; 134: 6–15.

57. Pinna MH, Varges R, Lilenbaum W. Aplicação de um programa integrado de controle da leptospirose em eqüinos no Rio de Janeiro, Brasil. Rev Brasil Ciência Vet 2008; 15(2): 63–6.

58. Batista CdSA, Alves CJ, Azevedo SSd, et al. Soroprevalência e fatores de risco para a leptospirose em cães de Campina Grande, Paraíba. Arq Brasil Med Vet Zootec 2005; 57(suppl. 2): 179–85.

Leptospiroza konj v Egiptu: seroprevalenca in dejavniki tveganja

Mohamed Marzok, Abdelrahman M. Hereba, Abdelfattah Selim

Izvleček: Večina leptospiroz pri konjih je asimptomatskih, vendar obstajajo poročanja o akutnih bolezenskih znakih, reprodukcijskih motnjah in ponavljajočih se uveitisih. Konji veljajo za naključne gostitelje. Podatki o leptospirozi konj v Egiptu so pomanjkljivi. Zato je bil namen te študije raziskati prisotnost protiteles proti bakteriji *Leptospira* sp. pri konjih v štirih egiptovskih pokrajinah in določiti z njimi povezane dejavnike tveganja za okužbo. Za določitev seroprevalence v 305 vzorcih seruma je bil opravljen mikroskopski aglutinacijski test (MAT) z osmimi antigeni serovara *Leptospira*. Rezultati so pokazali, da so bile 104 živali pozitivne na vsaj enega od serovarov (34,1 %; 95-odstotni indeks: 29,01–39,59). Najpogostejša reakcija je bila na serovar Icterohaemorrhagiae (15,14 %), sledili so Canicola (14,75 %), Bratislava (11,47 %), Copenhageni (8,19 %), Pomona (7,86 %) in Hardjo (6,88 %). Najpogostejše so bile pri kobilah, starejših konjih, konjih, ki se redijo na pašnikih ali so v stiku s prežvekovalci ali psi in pri pomanjkanju nadzora nad glodavci. Velika seroprevalenca kaže, da so egiptovski konji, ki živijo na proučevanem območju, izpostavljeni velikemu tveganju za okužbo z bakterijo *Leptospira* sp. Zato je za ta zoonotski patogen zelo pomembna vzpostavitev programa nujnega nadzora in obvladovanja.

Ključne besede: Leptospirosis; seroprevalence; risk factors; horse; Egypt

DOI 10.26873/SVR-1734-2023
UDC 598.1:591.567:618.36:611.018
Pages: 105–14

Case Report

Viviparity in Snakes – Histological Study of the Relationship Between Fetus, Fetal Membranes and Oviduct in Emerald Tree boa (*Corallus caninus*)

Key words

viviparity;
snakes;
placenta;
histology;
immunohistochemistry;
Corallus caninus

Pia Cigler[1+], Tanja Švara[2+], Valentina Kubale[3*]

[1]Institute for Fish and Wildlife Health, University of Bern, Längasstrasse 122, 3012 Bern, Switzerland, [2]Instutute of Pathology, Wild Animals, Fish and Bees, 3Institute of Preclinical Sciences, Veterinary Faculty University of Ljubljana, Ljubljana, Gerbičeva 60, 1000 Ljubljana, Slovenia

[+]Authors have equally contributed to the study and are listed by the alphabetical order

***Corresponding author:** valentina.kubale@vf.uni-lj.si

Abstract: Viviparity is an important reproductive mode in reptiles from an evolutionary perspective. Viviparous reproduction is associated with certain physiological changes, probably in response to inadequate environmental conditions for egg development. Unlike in oviparous species, embryos remain and develop in the oviduct until birth. In order for the developing embryo to exchange respiratory gasses, water, and food, a placenta is required, which consists of fetal membranes that interact with the maternal oviduct. About 20% of squamates (snakes and lizards) are viviparous, but the morphology of the snake placenta has been studied only in the subfamilies Thamnophiinae and Hydrophiinae. Our objective was to study the structure of the placental layers and fetus *in situ* in the maternal oviduct of a 6-year-old emerald tree boa (*Corallus caninus*). Five fertilized and three unfertilized slugs were found in the uterus during *post mortem* examination. The average mass of the slug with the fetus (48 mm length x 26 width) was 55–65 g and that of the unfertilized slug was 15–35 g. The fetal membranes and two fetuses were examined by light microscopy. Multiple projections of the tissue samples were made and cut into 5 µm thick paraffin tissue sections, which were stained with Haematoxylin-eosin, Toluidine blue, Goldner's Trichrome and assessed immunohistochemically with monoclonal antibodies for cytokeratin. The morphology of the fetal membranes was described and found to have an anatomy similar to that of most squamates: a type I allantoplacenta. The structure of the oviduct and of the fertilized and unfertilized slug was described. This case report provides a better understanding of placental morphology in boids and expands the spectrum of viviparous squamate species described.

Received: 25 March 2023
Accepted: 24 May 2023

Introduction

Reptiles have evolved numerous modes of reproduction to ensure the survivability of their offspring in the habitats they inhabit. Most reproduce by egg-laying, known as oviparity, in which the eggshell and membranes protect the developing embryo from environmental influences outside the mother's body. However, about 20% of squamate species (snakes and lizards) have evolved to retain the embryo in the oviduct until development is complete and give birth to live, fully functional young. This form of parity, termed viviparity, probably evolved from egg-laying species because climatic conditions were insufficient for egg development (1, 2).

The structure of the placenta in viviparous species, as well as nutrient uptake, varies according to the feeding mode of the fetus. These can be divided into lecithotrophy in which nutrients for embryonic development come primarily from the yolk, and matrotrophy, in which the female provides nutrients through the placenta or a functionally homologous trait (3).

In both cases, the placenta is required for the uptake of nutrients from the yolk and for gas exchange (4, 5). The extraembryonic membranes that contribute to placentation are complex. The placenta is formed by the attachment of extraembryonic membranes (chorioallantois) and tissues of the maternal fallopian tube (oviduct, uterus). The chorioallantois surrounds most of the embryo, while the omphallantois forms the ventral wall, which consists of a bilaminar omphalopleure and an omphalallantois membrane (6), aligned with the chorioviteline membrane (7). The chorioallantois is the only vascular membrane thought to be involved in gas exchange. It is connected to the uterus and forms the allantoplacenta. The types of allantoplacenta in squamates are classified according to differently organized morphotypes defined by i) the degree of folding between uterine and chorionic tissues and ii) differences at the maternal-fetal interface. Type I allantoplacenta is known to be the simplest and most common form. It is dependent on nutrient uptake from the yolk, the so-called "leicitotrophic viviparity". The maternal-fetal interface consists of a vascularized chorioallantois with squamous epithelium (in some species also remnants of the shell membrane) and uterine tissue. In the allantoplacenta type II, in which the shell is lost earlier, the luminal surface of the uterus is elevated in shallow ridges and consists of capillaries and a very thin layer of uterine epithelium. The chorionic epithelium is more cuboidal. The type III allantoplacenta is described as a placentoma in which an elliptical area of folded maternal and fetal tissue is located at the mesometrial pole of the uterus ventral to the great uterine vessels. The IV type allantoplacenta is also described as a placentoma located below the uterine artery and vein. Distinct villous folds of the uterine endometrium radiate outward and project deeply into an invagination of the chorioallantois, making separation of these tissues difficult (7, 8).

Viviparous (life-bearing) snakes are an important alternative to traditional mammalian models for studying placental structure, function, and development. Understanding of placental morphology in snakes is based on a handful of publications covering only a small fraction of viviparous species. More data on placental morphology are available from lizard species (6, 9). However, the independent evolutionary origin limits the comparability of the two groups. Although there are some similarities, there are also numerous differences, particularly in the chorioallantoic portion of the placenta, that warrant further investigation of placentation in snakes.

In the present study we examined the histological characteristics of the placental membranes of gravid emerald tree boa (*Corallus caninus*), as well as the oviduct and yolk characteristics. Our aim was to identify the type of placenta and describe its histological characteristics using various histological, histochemical and immunohistochemical stains.

Materials and methods

Material and sample processing

The samples of a 6-year-old emerald tree boa (*Corallus caninus*) for gross and histological examination were obtained *post mortem* from Golob d.o.o., Clinic for small, wild, and exotic animals, Muta Slovenia, under permit number U34443-6/2917/2, as animal by-products according to Regulation (EC) No. 1069/2009. Two deceased embryos with their surrounding fetal membranes and one slug were fixed in 10% buffered formalin, and routinely embedded in paraffin using a Leica TP1020 automated tissue processor (Leica Biosystems, Buffalo Grove, USA). The tissue samples were then cut into 5 µm thick tissue sections at 50-µm intervals using a Leica SM 2000R microtome (Leica Biosystems, Nußloch, Germany).

Histological and immunohistochemical preparation

After deparaffinization, sections were stained with Haematoxylin-eosin (HE), Toluidine blue, Goldner's Trichrome as well as immunohistochemically stained with anti-human cytokeratin and examined under a light microscope.

Briefly, samples were deparaffinized (2 x 5 minutes) in xylene substitute (Neo-Clear™ Xylene Substitute, Merck Millipore) and rehydrated in decreasing concentrations of ethanol (100% 2 x 5 minutes, 96% 5 minutes, 75% 5 minutes) and distilled water (2 x 5 minutes). Subsequently, samples were either stained with haematoxylin (Merck) (2 minutes), washed under running water (20 minutes), stained with eosin (1–2 minutes) and washed in distilled water (5 minutes), or stained with Toluidine blue solution (7 minutes) and washed three times in distilled water (5 minutes).

The samples were also stained with Goldner's Trichrome stain (Masson-Goldner staining kit, Merck, Darmstadt, Germany) according to the standard procedure. Briefly, after initial deparaffinization and rehydration, nuclei were stained with Weigert's iron haematoxylin for 2 minutes. Samples were washed under tap water for 10 minutes then rinsed in 1% acetic acid for 30 seconds, stained in azophloxin solution for 10 minutes, and subsequently rinsed in 1% acetic acid for 30 seconds. Samples were then incubated in tungstophosphoric acid orange G solution for 1 minute, rinsed with 1% acetic acid for 30 seconds, incubated in light green SF solution for 2 minutes, and finally rinsed in 1% acetic acid for 30 seconds.

After dehydration with increasing concentration of ethanol (75% about 5 minutes, 96% 1 x about 5 minutes, 100% of 2 x 5 minutes) clearing of the samples was performed in xylene substitute (Neo-Clear™ Xylene Substitute, Merck Millipore) (3 x 5 minutes). Finally, a drop of Neo-Mount medium™ -anhydrous mounting medium (Merck Millipore) was added to each tissue sample and the sample was covered with a cover slide. The samples were then air dried for approximately 30 minutes. The samples were stored in the dark prior to analysis.

In addition, paraffin-embedded tissue sections were stained by immunohistochemical procedure using an anti-human cytokeratin antibody (1: 100, CK MNF 116, Dako, Glostrup, Denmark) for immunolabelling of epithelial cells. For immunohistochemistry, deparaffinized and rehydrated tissue sections were unmasked by boiling the slides in citrate buffer (pH 6.0) for 20 minutes in a microwave oven (for immunolabeling of cytokeratin). Incubation with the primary antibodies lasted for one hour at room temperature in a humid chamber. The rest of the immunohistochemical procedure was performed according to a previously described protocol (10). A Nikon Microphot-FXA microscope equipped with a DS-Fi1 camera and NIS Elements imaging software (NIS Elements D.32; Nikon Instruments Europe B.V., Badhoevedorp, The Netherlands) was used for histological examination.

Results and discussion

In our case, five embryos and three unfertilized slugs were collected from an adult female emerald tree boa (*Corallus caninus*). Figure 1A shows the species in a very typical loop position on the branch. The average size of the embryo with surrounding membranes and yolk was 48 x 26 mm and the mass was 55–65 g. The unfertilized eggs were lighter, and their mass was 15–35 g. Female emerald tree boas reach sexual maturity at about 4–5 years of age. Their gestation lasts about 7 months, and they give birth to 7–10 live, fully developed young (11). In our study, embryos were

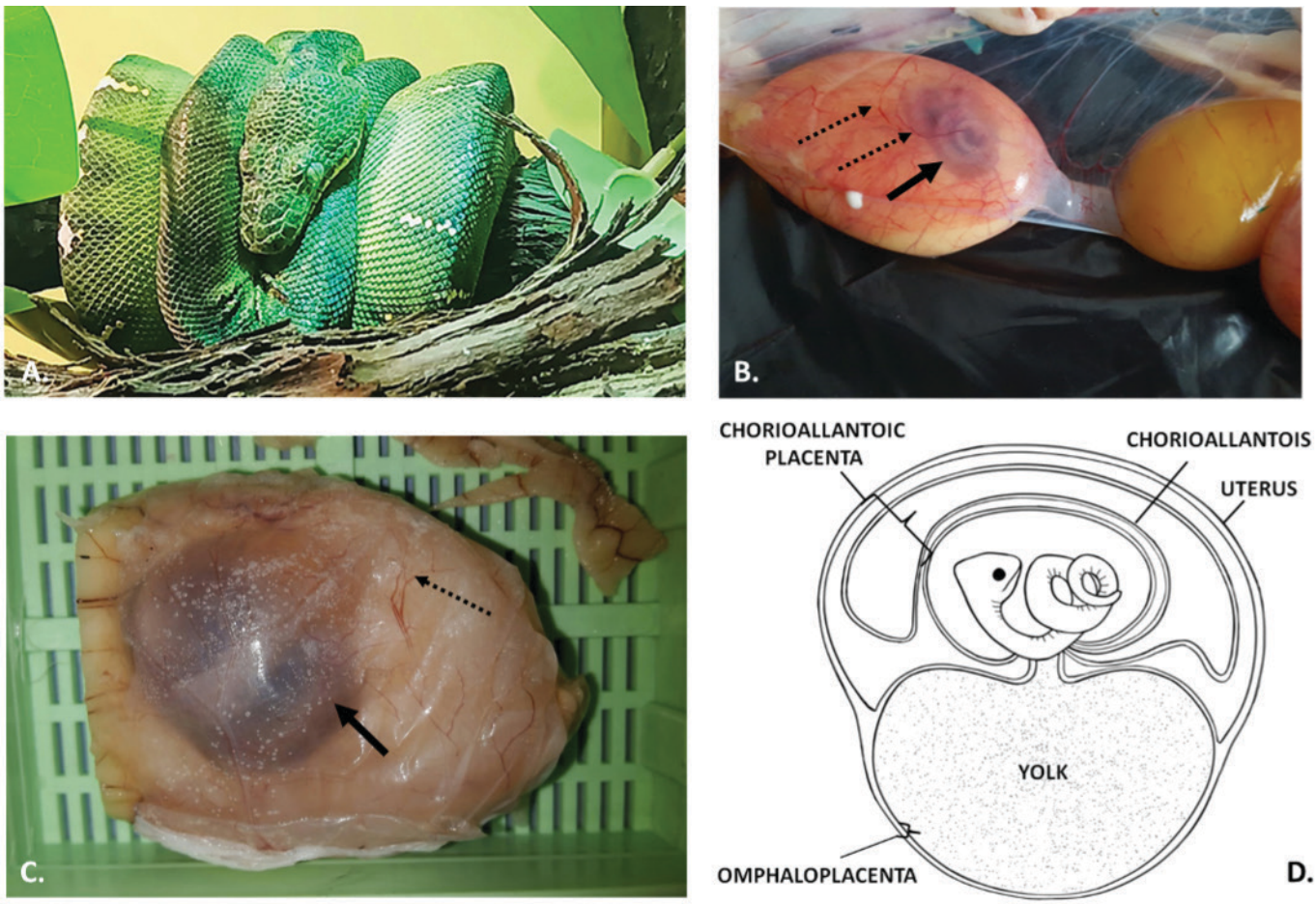

Figure 1: Adult specimen and fetuses of *Corallus caninus*

A. Adult female emerald tree boa (*Corralus caninus*) in a coiled loop on a branch (Photo: Freja Katarina Dvojmoč). B. Developing embryo (bold arrow) of *Corallus caninus* in the oviduct, vascularization (dotted arrow) (Photo: Zlatko Golob). D. A whole formalin-fixed and paraffin-embedded *Corallus caninus* embryo (bold arrow) with preserved fetal membranes and well seen vascularization (dotted arrows) in Tissue-Tek Mega-Cassette system (size 40 x 25 x 10 mm) (Photo: Valentina Kubale). D. The position of the snake embryo in the uterus and the two types of placental contact; chorioallantoic and omphaloallantoic placenta (designed by Pia Cigler, adapted from Blackbourn DG (4) and Bavdek SV et. al. (12).

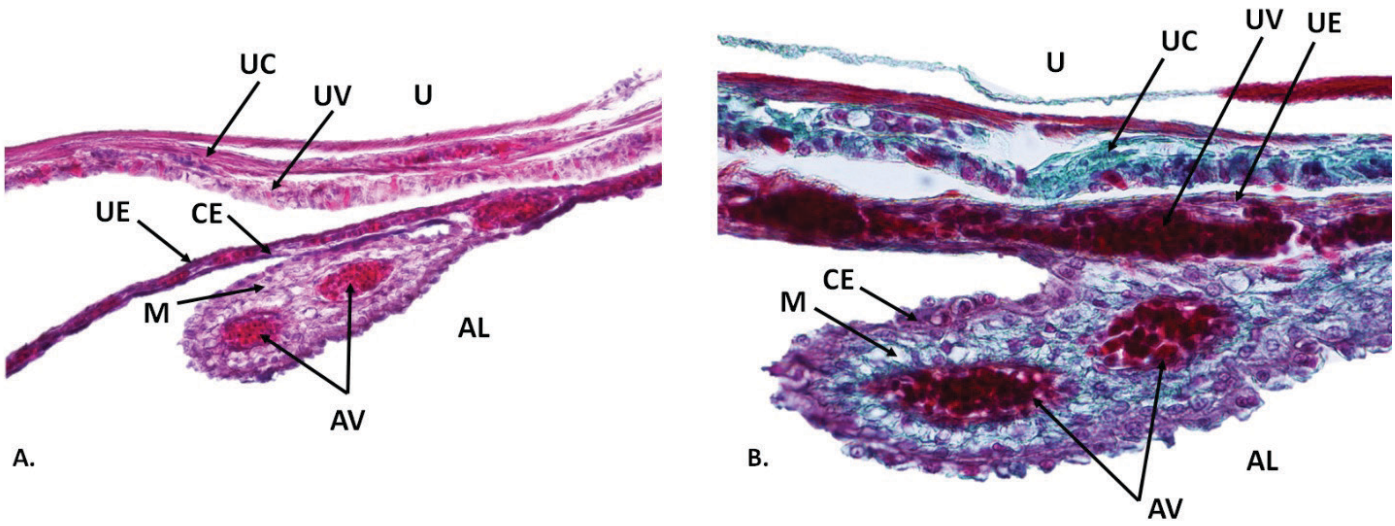

Figure 2: Representative histological characteristics of chorioallantoic placenta

The chorioallantois was observed as thin vascularized membrane, next to uterus. AL, allantoic lumen, AV, allantoic blood vessel, M, mesenchyme, CE, chorionic epithelium, U, uterus, UE, uterine epithelium, UV, uterine vessel, UC, uterine connective tissue (A. 200× magnification, Haematoxylin-eosin; B. 400× magnification, Goldner's Trichrome).

observed on the upper surface of the yolk sac in a coiled position, with a highly vascularized chorioallantois (Figure 1B). Because the embryo was preserved in its original position, it was difficult to estimate the length of the embryo. However, we were able to estimate the diameter of the embryo in the coiled form, which was approximately 1 cm (Figure 1C). The embryos described in this case were at an early stage of development. The position of the snake embryo in the uterus and the type of placental contact (chorioallantoic and omphalloalantoic placenta) are shown in Figure 1D.

Light microscopic examination of the fetal membranes in the region of the chorioallantoic placenta revealed that the chorionic epithelium consists of thin unilaminar squamous epithelium (Figure 2A, B). In the following layer of the trophectoderm, a highly vascularized area with an extensive network of allantois capillaries was observed, located near the uterus in the mesoderm and stained green with Goldner's Trichrome (Figure 2B). No lamina propria or allantois connective tissue was identified. The chorionic epithelium interacted with the uterine epithelium, a very thin, unilaminar squamous epithelium comparable to the chorionic epithelium (Figure 2A, B). The chorioallantois formed multiple folds in the numerous areas above the fetus, most likely important for enhanced gas exchange through enlarged areas of mesenchymal tissue with blood vessels in the allantois (Figure 3). In addition to Haematoxylin-eosin staining and Goldner's Trichrome, an immunohistochemical approach showed that the epithelial cells of the chorioallantois folds strongly expressed cytokeratin MNF116 (Fig. 3B). The broad-spectrum cytokeratin marker which was used recognizes the basic and some acidic keratins. Schematic representations of the chorioallantois are shown in Figure 3D. No shell membrane was observed between the highly vascularized fetal and maternal epithelia.

The omphaloplacenta consisted of an omphalopleure with a layer of thin squamous epithelium and a layer of simple cuboidal epithelium, and a yolk splanchnopleure. The yolk splanchnopleure consisted of squamous epithelium and a highly vascularized area. The omphalopleure and yolk splanchnopleure formed the lining of the yolk cleft. The yolk splanchnopleure surrounded the yolk with numerous yolk vesicles (Figure 4 and 5). Immediately adjacent to it, the embryo was surrounded by the amnion (Figure 4) and further superficially by the allantois. The yolk splanchnopleure and the allantois formed a yolk sac cleft. The morphology of placenta examined was consistent with a type I allantoplacenta.

The oviduct is divided into four distinct regions in snakes, namely infundibulum, uterine tube, uterus and vagina. In our study we examined the infundibulum, uterine tube, and uterus. In the infundibulum, we observed finger-like irregular folds of the mucosal layer that protruded anteriorly. The epithelium was a cuboidal epithelium that was cilliated in some places and was not cilliated toward the uterine tube. The wall of the infundibulum was thin. The uterine tube area was similar to the infundibulum. However, the wall, which consisted of lamina propria, tunica muscularis, and partially visible tunica serosa, was much thicker (Figure 6). The uterus consisted of three histological layers: the luminal epithelium, the subepithelial lamina propria, and the uterine muscularis. The luminal epithelium consisted of cuboidal to slightly columnar, non-cilliated cells that strongly expressed cytokeratin by immunohistochemistry. The underlying lamina propria of the uterus consisted of dense, irregular tissue composed of fibroblasts in a matrix of irregularly arranged

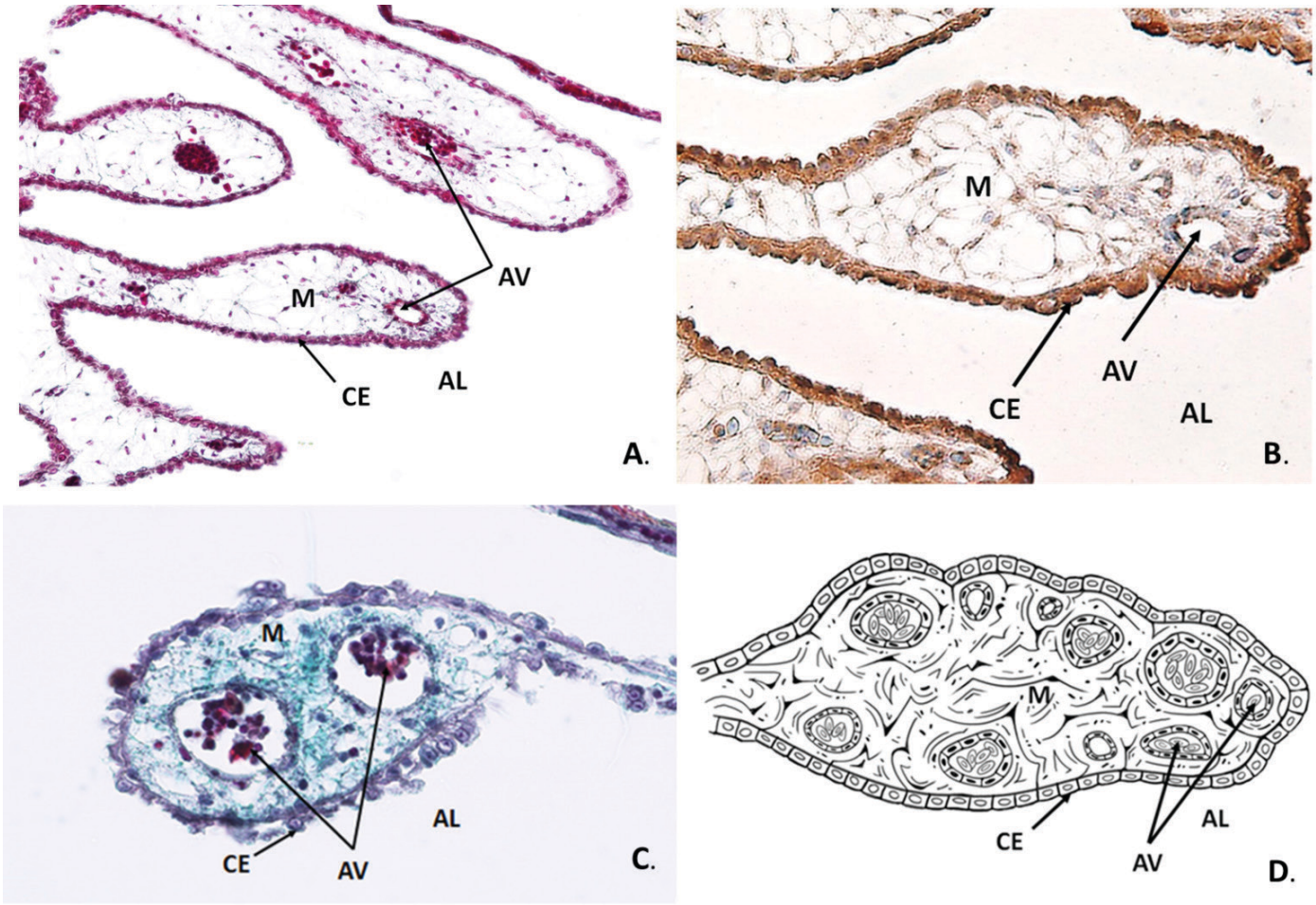

Figure 3: Histological characteristics of chorioallantoic placenta, enlargement of the surface of the fetal membranes

Several folds of chorioallantois were observed in the numerous parts above the fetus, having important role in improved gas exchange through enlarged areas of mesenchymal tissue with blood vessels in the allantois. AL, allantois lumen, AV, allantois blood vessel, M, mesenchyme, CE, chorionic epithelium. A. 200× magnification, Haematoxylin-eosin, B. Cytokeratin immunohistochemistry for cytokeratin labelled epithelial cells and confirmed their origin. 400× magnification, mouse monoclonal anti-cytokeratin MNF 116 antibody, horseradish peroxidase-labelled polymer (EnVision + Kit), counterstained with Mayer's haematoxylin; C. 400× magnification, Goldner's Trichrome, D. Schematic representation of chorioallantois, designed by Pia Cigler).

collagen fibers, with vessels of various sizes (ranging from capillaries to other small vessels) scattered among them. Vascularity was modest, typical of early to mid-gestation. This layer also contained tubular shell glands with a simple cuboidal epithelium surrounding a small central lumen. The glands in the lamina propria were stained blue with Toluidine blue, indicating their activity, but did not express cytokeratins. They were not numerous and did not appear to be very active. The tunica muscularis was organized into 2 layers: an inner circular layer and an outer longitudinal layer of smooth muscle cells. The simple squamous cells of the visceral peritoneum are located outside the tunica muscularis (Figure 7).

Furthermore, as fertilized and unfertilized slugs were harvested, we have examined both microscopically (Figure 8). The Haematoxylin-eosin and Goldner's Trichrome stainings showed distinguishing yolk structures between fertilized and unfertilized yolk. Both yolks were distinctive already at low magnification. In the fertilized eggs, they were partly surrounded by a light eosinophilic fibrous shell membrane. The yolk supporting developing embryos was less densely packed and had small to medium sized spherical yolk granules that are strongly stained with eosinophilic stain and a moderate amount of amorphous substance. The unfertilized yolk contained round spaces, that resembled lipid vesicles, were the same size as yolk granules and contained dense, darker eosinophilic amorphous material. Individual yolk droplets were rarely seen, and eosinophilic compounds were absent. In fertilized slug, stained with Goldner's Trichrome, the amorphous material was stained green (Figure 8B).

Lecitotrophy is the predominant form of viviparity described in reptiles. There are numerous morphological differences between histotrophic and lecitotrophic species, but placental changes are not the only indicator of the degree of nutrient transfer between mother and embryo. Boids are also snakes, known for their viviparity, but the placental anatomy of boids has not been described in detail. Emerald tree boa embryos, like those of most snakes, are known to develop by lecitotrophy. Similar placental anatomy has been

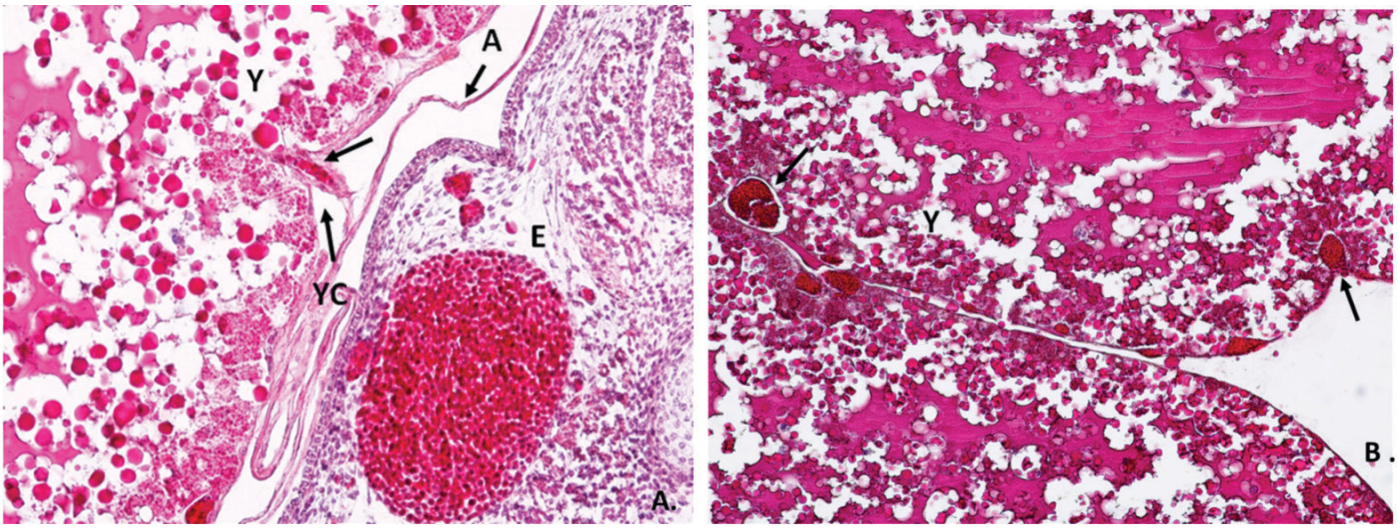

Figure 4: Representative histological characteristics of amnion

The embryo was surrounded by the amnion and superficially by the allantois, next to which was the yolk splanchnopleure. Between embryo and egg yolk is a yolk cleft. (Y, yolk vesicle, YC, yolk cleft, A, amnion, E, embryo, egg yolk vessels are indicated by arrows (100× magnification, Haematoxylin-eosin).

described in other snake species including numerous thamnophine snakes such as Da Kay´s brown snake (*Storeria dekayi*) (13) and the common garter snake (*Thamnophis sirtalis*) (Hoffman, 1970), as well as the rough earth snake (*Virginia striatula*) (9) and *Dieurostus dussumierii* (14).

Much of the research on viviparity in squamates has focused on lizards, particularly those in the family Scincaidae (6, 15). Although comparisons can be made between them and snakes, the difference in evolutionary origin limits direct comparability. A type I allantoplacenta has been described in most lizard species with lecitotrophic viviparity (16).

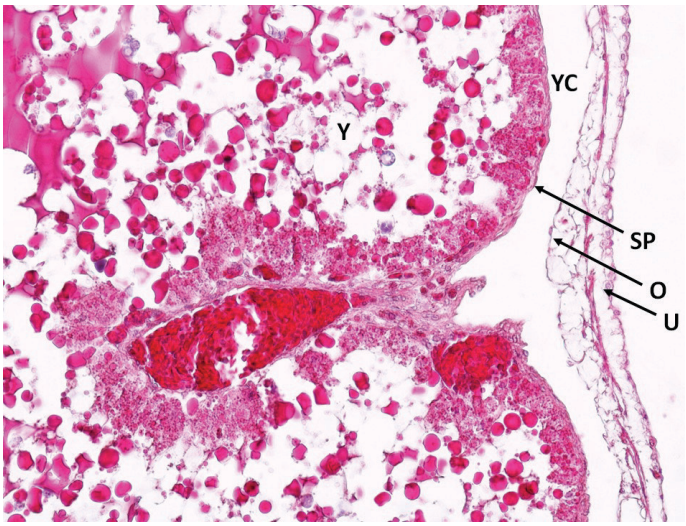

Figure 5: Representative histological characteristics of omphaloplacenta

The omphaloplacenta consisted of an omphalopleure with a layer of thin squamous epithelium, a layer of simple cuboidal epithelium and a yolk splanchnopleure. The yolk splanchnopleure consisted of squamous epithelium and a highly vascularized area. The omphalopleure and yolk splanchnopleure formed the lining of the yolk cleft. The yolk splanchnopleure surrounded the yolk with numerous yolk vesicles. U, uterus, O, omphalopleure, SP, yolk sac splanchnopleure, Y, yolk vesicle, YC, yolk cleft (100× magnification, Haematoxylin-eosin).

The placenta of viviparous snakes, as in lizards, is a temporary organ that develops during pregnancy to facilitate gas and nutrient exchange between the mother and her developing offspring. It is composed of the chorionic layer and the allantoic layer. The chorionic layer is the outer layer and is connected to the mother's uterine wall. It is composed of cells that secrete a variety of hormones and proteins that facilitate gas and nutrient exchange and protect the embryo from the mother's immune system. The allantoic layer is the inner layer that is directly connected to the developing offspring. This layer consists of a highly vascularized network of blood vessels that facilitate the exchange of oxygen and nutrients from the mother to the developing offspring (3).

The developmental morphology of chorioallantoic membranes has been studied in only two species of Galloanserae (17, 18). Some similarities were noted, but more of these species are oviparous than viviparous, so the structure was usually described and associated with the eggshell, which was not observed in our case. It is known that the chorioallantoic membrane of egg-laying reptiles forms a vascular interface with the eggshell. The eggshell of the oviparous species contains calcium, mainly in the form of calcium carbonate. The calcium is extracted from the chorioallantoic membrane and mobilized to contribute to the nutrition of the embryo (19). Eggshell calcium is thought to have been a source of embryonic nutrition in the early developmental stage of Sauropsida. It is known that there are calcium-transporting cells in the chorioallantoic membrane of corn snakes (19). This specialization of the chorioallantoic membrane to calcium uptake was not observed in our case, nor was the eggshell. The chorioallantoic membrane plays an important role in mobilizing calcium from the eggshell

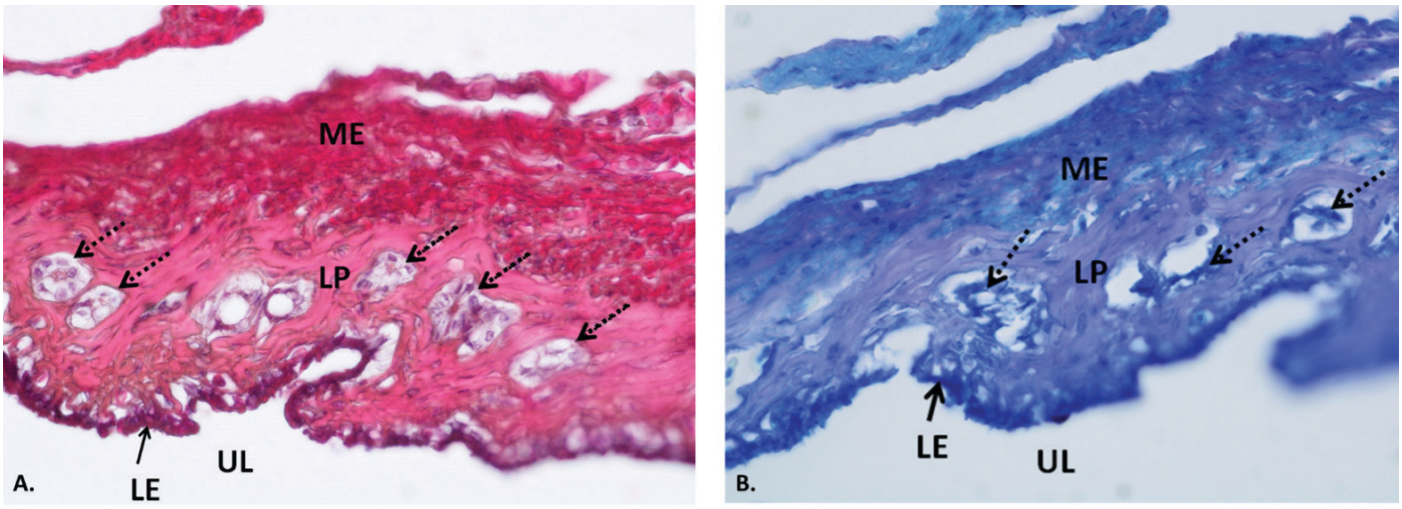

Figure 6: Representative histological characteristics of maternal component – oviduct (uterine tube)

A. 200× magnification, Haematoxylin-eosin. B. 400× magnification, Toluidine blue staining. UL, uterine lumen, LE, lamina epithelialis, LP, lamina propria, ME, muscularis externa, glands (dotted arrowheads).

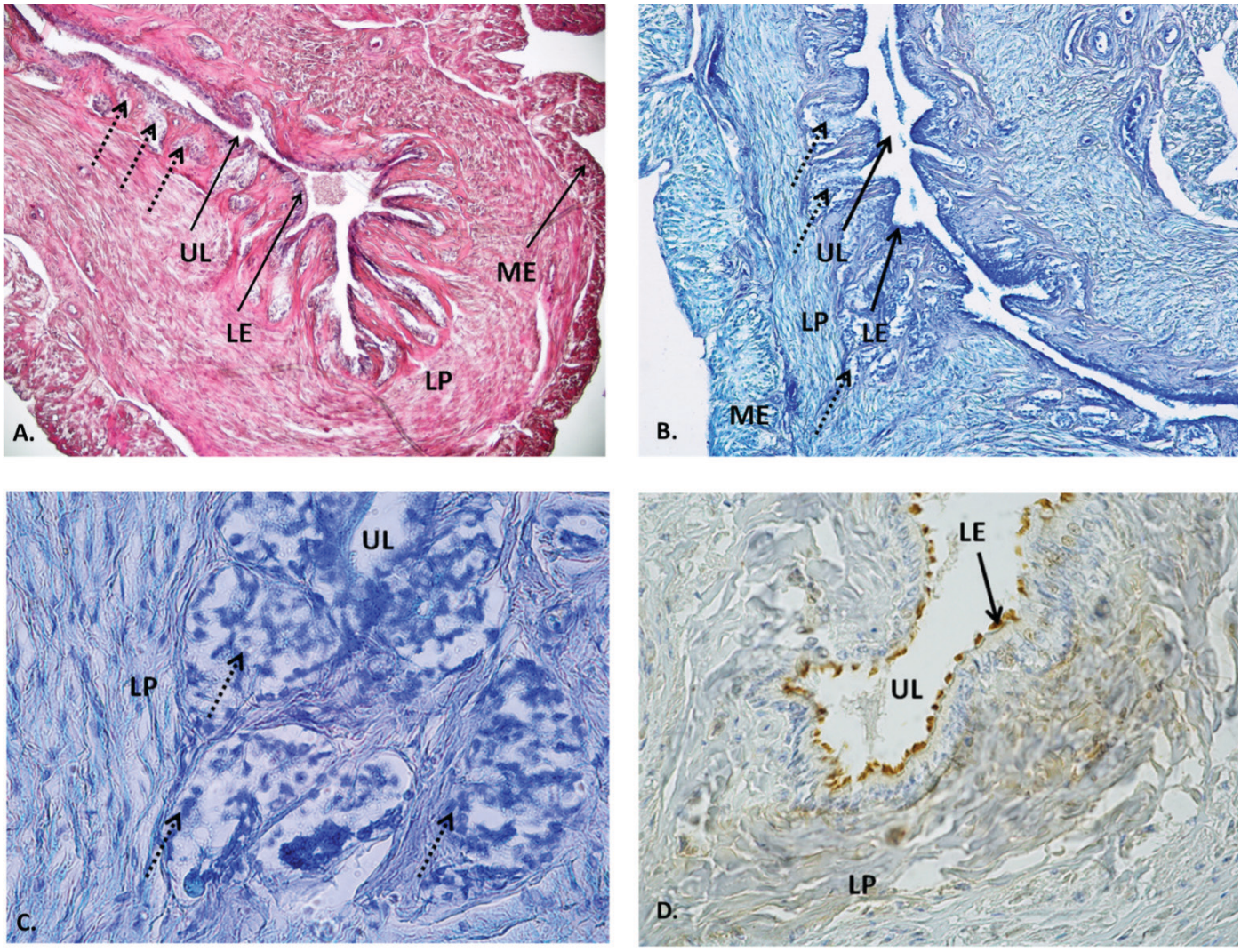

Figure 7: Representative and histological characteristics of maternal component – oviduct (uterus)

UL, uterine lumen, LE, lamina epithelialis, LP, lamina propria, ME, muscularis externa, glands (dotted arrows). A. 100× magnification, haematoxylin eosin; B. 100× magnification, Toluidine blue staining; C. 200× magnification, Toluidine blue staining; D. Immunohistochemistry for cytokeratin shows strong expression of cystokeratins in luminal epithelium. 200× magnification, mouse monoclonal anti-cytokeratin MNF 116 antibody, horseradish peroxidase-labelled polymer (EnVision + Kit), counterstained with Mayer's haematoxylin.

of egg-laying species or directly, as in our case, from the uterus, as known from other viviparous species (20–22). Some studies compare the structure of the chorioallantoic membrane to that of birds, but not much is known about the morphology and function of the chorioallantoic membrane in turtles, crocodiles, and tuatara.

In most viviparous reptiles, the first part of the oviduct (infundibulum and uterine tube) consists of a thinner wall with ciliary to non-ciliary epithelium and finger-like irregular folds in the mucosal layer. These irregular folds probably allow the infundibulum to expand as the eggs pass through (6). Uterine wall consists of three layers: an outer layer of longitudinal muscle fibers, a middle layer of circular muscle fibers, and an inner layer of simple columnar epithelium. This epithelial layer is particularly important because it facilitates the exchange of nutrients, hormones, and waste products between the mother and her developing embryos.

The uterine wall of viviparous reptiles also contains glands that produce secretions that contribute to the nutrition of the embryos and provide them with hormones. The glands are located in the lamina propria of the uterine wall and are surrounded by a thin layer of connective tissue. The secretions produced by these glands are then distributed throughout the uterus by contractions of the muscle fibers in the middle layer of the uterine wall. The epithelial layer of the uterine wall is also responsible for the formation of the chorion in viviparous reptiles. These glands are more present in active in oviparous species and contain secretory granules (23).

Comparing the structure of the uterus with other described species, many similarities can be observed, but also differences that depend on the type of placenta (13, 24, 25).

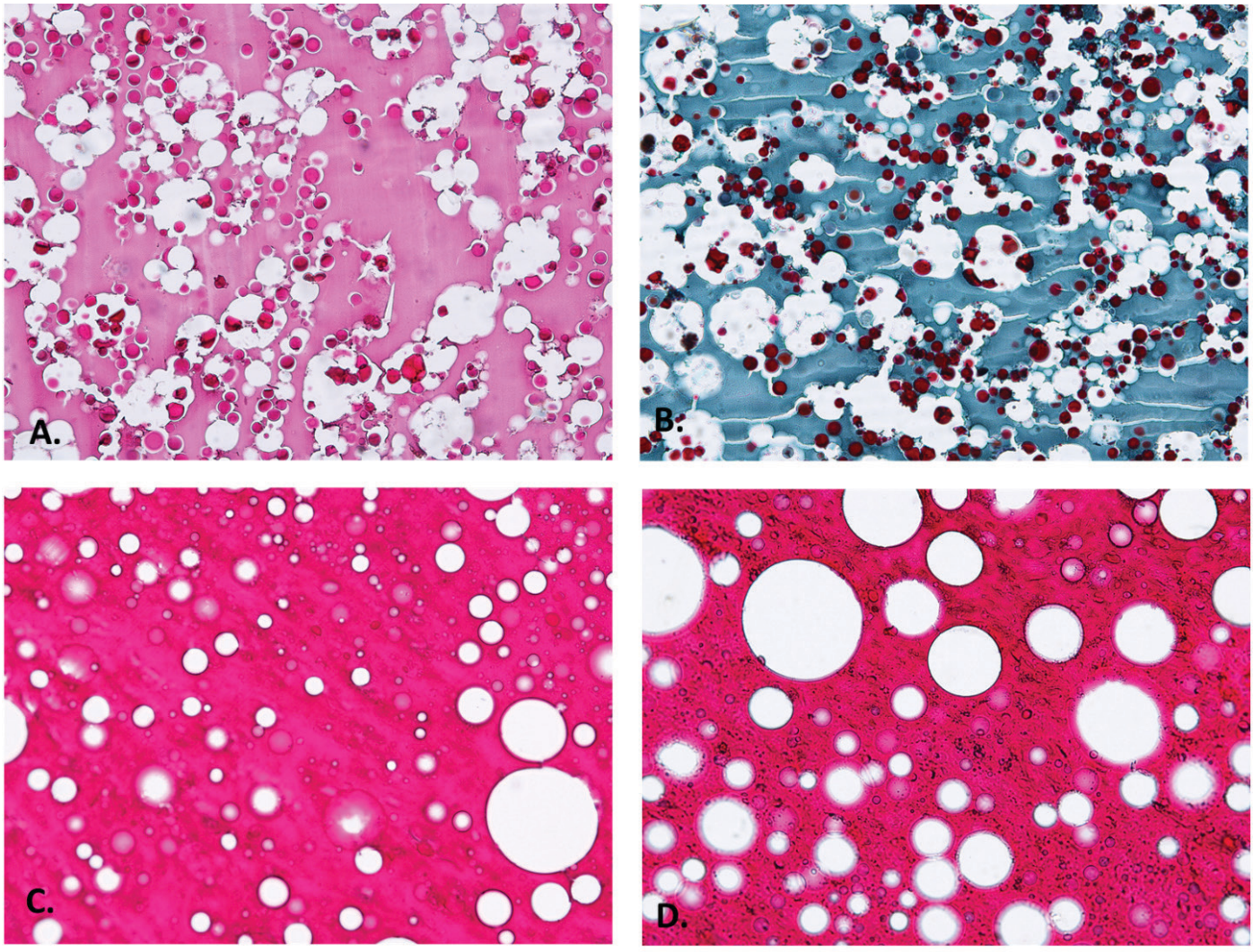

Figure 8: Histological characteristics of fertilized and non-fertilized yolk vesicles

Microscopic examination of the slugs revealed differences in yolk droplet structures between fertilized and non-fertilized yolk. The yolk supporting developing embryos was less densely packed, light eosinophilic and amorphous, while the unfertilized yolk was dark eosinophilic and contained many lipid vesicles. A. Fertilized yolk vesicle, 200× magnification, haematoxylin eosin. B. Fertilized yolk vesicle, 200× magnification, Goldner's Trichrome. C. and D. Non-fertilized yolk vesicle, 200× and 400× magnification, Haematoxylin-eosin.

Structures called "yolk sacs" are responsible for nourishing the developing embryo. The yolk sacs are located in the uterus and are connected to the embryo by a yolk stalk. The yolk stalk consists of a network of blood vessels that transports nutrients from the yolk sac to the embryo. The yolk stalk is composed of a network of blood vessels, that transports the nutrients from the yolk sac to the embryo. The embryo also receives oxygen and other substances from the mother's bloodstream through the placenta. The yolk sac also plays an important role in the development of the embryo's organs, including the liver and intestines (26). The yolk sac structure in viviparous reptiles is unique among vertebrates. It is the only reproductive system in which the embryo is nourished and developed internally, rather than externally. It is believed that this structure evolved to protect the embryo from the harsh environment of the outside world. As a result, viviparous reptiles have a better chance of survival and more successful reproduction than their egg-laying counterparts. Egg development is nonsynchronous, so intact eggs can be observed without signs of fertilization. Unfertilized slugs are known to be reabsorbed in the oviduct, which is beneficial in viviparous snakes and lizards to adapt reproduction to environmental conditions in this manner while minimizing the physical stress and loss of nutrients that these eggs represent (25, 27). Reabsorption is thought to occur through digestion and phagocytosis, but we have not yet observed higher numbers of phagocytes in our case report. In our case, the unfertilized eggs showed no signs of thinning or rupture at the mesometrial pole.

In conclusion, the placenta of viviparous snakes plays an important role in the development of the offspring. It helps to provide the developing offspring with the nutrients and gasses necessary for growth and development and protects them from harmful environmental factors. Emerald tree boa embryos develop by lecitotrophic viviparity using a type I allantoplacenta. However, because only embryos at early stages of development were available for study, further investigation is needed to better understand the dynamics of uterine and placental structure in emerald tree boas and boids in general throughout gestation.

Acknowledgements

The authors would like to thank and acknowledge Zlatko Golob, PhD, DVM for material, photographic material and information, Prof. Emeritus Srdjan V. Bavdek, DVM (*in memoriam*) for long discussions and Jasna Šporar, as well as Benjamin Cerk for excellent technical support. The authors gratefully acknowledge financial support from the Slovenian Research Agency (P4-0053 and P4-0092) and Creative path to knowledge projects 150_PKP5 Sloexo and 150_PKP_Sloexo2.

The authors declare no conflict of interest.

References

1. Lode T. Oviparity or viviparity? That is the question. Reprod Biol 2012; 12: 259–64.
2. Braz HB, Scartozzoni RR, Almeida-Santos SM. Reproductive modes of the South American water snakes: a study system for the evolution of viviparity in squamate reptiles. Zool Anz 2016; 263: 33–44.
3. Blackburn DG. Viviparous placentotrophy in reptiles and the parent–offspring conflict. J Exp Zool B Mol Dev Evol 2015; 324: 532–48.
4. Blackbourne DG. Chorioallantoic placentation in squamate reptiles: structure, function, development and evolution. J Exp Zoo 1993; 266: 414–30.
5. Dunson WA. The biology of sea snake. Baltimore: University Park Press, 1975.
6. Adams SM, Biazik J, Stewart RL, Murphy CR, Thompson MB. Fundamentals of viviparity: comparison of seasonal changes in the uterine epithelium of oviparous and viviparous *Lerista bougainvillii* (Squamata: Scincidae). J Morphol 2007; 268: 624–35.
7. Weekes HC. A review of placentation among reptiles with particular regard to the function of the placenta. Proc Zool Soc 1935; 2: 625–45.
8. Blackburn DG. Structure, function, and evolution of the oviducts of squamate reptiles, with special reference to viviparity and placentation. J Exp Zool 1998; 282: 560–617.
9. Stewart RJ, Brasch KR. Ultrastructure of the placentae of the natricine snake *Virginia striatula* (Reptilia: Squamata). J Morphol 2003; 255: 177–201.
10. Cociancich V, Gombač M, Švara T, Pogačnik M. Malignant mesenchymoma of the aortic valve in a dog. Slov Vet Res 2013; 50: 83–8.
11. Riel CAP. Reproduction of *Corallus caninus* (Linnaeus, 1758) in captivity. Litteratura Serpentium 1984; 4: 173–81.
12. Bavdek SV, Golob Z, Janžekovič F, Kubale V, Skok J. Osnove primerjalne anatomije vretenčarjev. Ljubljana: Veterinarska fakulteta, 2015.
13. Blackburn DG, Anderson KE, Johnson AR, Knight SR, Gavelis GS. Histology and ultrastructure of the placental membranes of the viviparous brown snake, *Storeria dekayi* (Colubridae: Natricinae). J Morphol 2009; 270: 1137–54.
14. Parameswaran K. The foetal membranes and placentation of *Enhydris dussumieri* (Smith). Proc Indian Acad Sci 1962; 56: 302–27.
15. Vitt LJ, Blackbourn D. Reproduction in the lizard *Mabuya heathi* (Scincidae): a commentary on viviparity in new world *Mabuya*. Can J Zool 1983; 61: 2798–806.
16. Griffith OW, Brandley MC, Belov K, Thompson MB. Reptile pregnancy is underpinned by complex changes in uterine gene expression: a comparative analysis of the uterine transcriptome in viviparous and oviparous lizards. Genom Biol Evol 2016; 8: 3226–39.
17. Fancsi T, Feher G. Ultrastructural studies of chicken embryo chorioallantoic membrane during incubation. Anat Histol Embryol 1979; 8: 151–9.
18. Lusimbo WS, Leighton FA, Wobeser GA. Histology and ultrastructure of the chorioallantoic membrane of the mallard duck (*Anas platyrhynchos*). Anat Rec 2000: 259: 25–34.
19. Ecay TW, Steward JR, Khambaty M. Functional complexity in the chorioallantoic membrane of an oviparous snake: specializations for calcium uptake from the eggshell. J Exp Zool B Mol Dev Evol 2022; 338: 331–41.
20. Stewart JR, Ecay TW. Patterns of maternal provision and embryonic mobilization of calcium in oviparous and viviparous squamate reptiles. Herpetol Conserv Biol 2010; 5: 341–59.

21. Hernandez-Diaz N, Leal F, Ramirez Pinilla MP. Parallel evolution of placental calcium transfer in the lizard Mabuya and Eutherian mammals.J Exp Biol 2021; 224: jeb237891. doi:10.1242/jeb.237891

22. Stinnett HK, Stewart JR, Ecay TW, Pyles RA, Herbert JF, Thomson MB. Placental development and expression of calcium transporting proteins in the extraembryonic membranes of a placentotrophic lizard. J Morphol 2012; 273: 347–59.

23. Braz HB, Almeida-Santos SM, Murphy CR, Thompson MB. Uterine and eggshell modifications associated with the evolution of viviparity in South American water snakes (*Helicops spp.*). J Exp Zool B Mol Dev Evol 2018; 330: 165–80.

24. Hoffman LH. Placentation in the garter snake, *Thamnophis sirtalis*. J Morphol 1970; 131: 57–87.

25. Thongboon L, Senarat S, Kettratad J et al. Morphology and histology of female reproductive tract of the dog-faced water snake *Cerberus rynchops* (Schneider, 1799). Maejo Int J Sci Technol 2020; 14: 11–26.

26. Elinson RP, Steward JR, Bonneau LJ, Blackburn DG. Amniote yolk sacs: diversity in reptiles and a hypothesis on their origin. Int J Dev Biol 2014; 58: 889–94.

27. Blackburn DG. Evolutionary origins of viviparity in the Reptilia. II. Serpentes, *Amphisbaenia*, and *Ichthyosauria*. Amphib Reptil 1985; 6: 259–91.

Viviparnost pri kačah – histološka povezava plodu, plodovih ovojev in jajcevoda pri pasjeglavem udavu (*Corallus caninus*)

P. Cigler, T. Švara, V. Kubale

Izvleček: Viviparnost (živorodnost) je z evolucijskega vidika pomemben način razmnoževanja pri plazilcih. Takšen način razmnoževanja je povezan z določenimi fiziološkimi spremembami, verjetno kot odziv na neustrezne okolijske razmere za razvoj jajc. Za razliko od oviparih vrst se zarodki do rojstva razvijajo in se zadržijo v jajcevodu. Razvijajoči se zarodek potrebuje način za izmenjavo dihalnih plinov, vode in hrane. Za to potrebuje placento, ki jo sestavljajo plodove membrane in jajcevod matere. Približno 20 odstotkov luskarjev (*Squamata*) (kuščarjev in kač) je živorodnih, morfologijo placente pa so proučevali predvsem pri rodovih Thamnophiinae in Hydrophinae. Namen naše raziskave je bil preučiti strukturo placente in situ v jajcevodu 6-letne samice pasjeglavega udava (*Corallus caninus*). Pri sekciji smo našli 5 oplojenih in 3 neoplojena jajca. Povprečna masa jajca s plodom (48 mm dolžine x 26 širine) je bila 55–65 g, neoplojenega jajca pa 15–35 g. Fetalne membrane in dva ploda pasjeglavega udava smo pregledali s pomočjo svetlobne mikroskopije. Narejenih je bilo več 5 µm debelih parafinskih tkivih rezin, ki so bile obarvane s hematoksilinom in eozinom, toluidinskim modrilom, trikromnim barvanjem po Goldnerju ter s pomočjo imunohistokemičnega barvanja citokeratina in dezmina. Opazovali smo položaj in strukturo plodovih ovojev *in situ*. Morfologija plodovih ovojev je pokazala, da pri pasjeglavem udavu najdemo tip I alantoplacente. Opisali smo tudi strukturo jajcevoda, oplojenega in neoplojenega jajca. Raziskava je omogočila boljše razumevanje morfologije placente pri kačah in razširila spekter opisanih živorodnih vrst luskarjev.

Ključne besede: živorodnost; kače; placenta; histologija; imunohistokemija; *Corallus caninus*

Table of Content